New method to measure dune erosion processes using a mobile, contained environment on a real beach

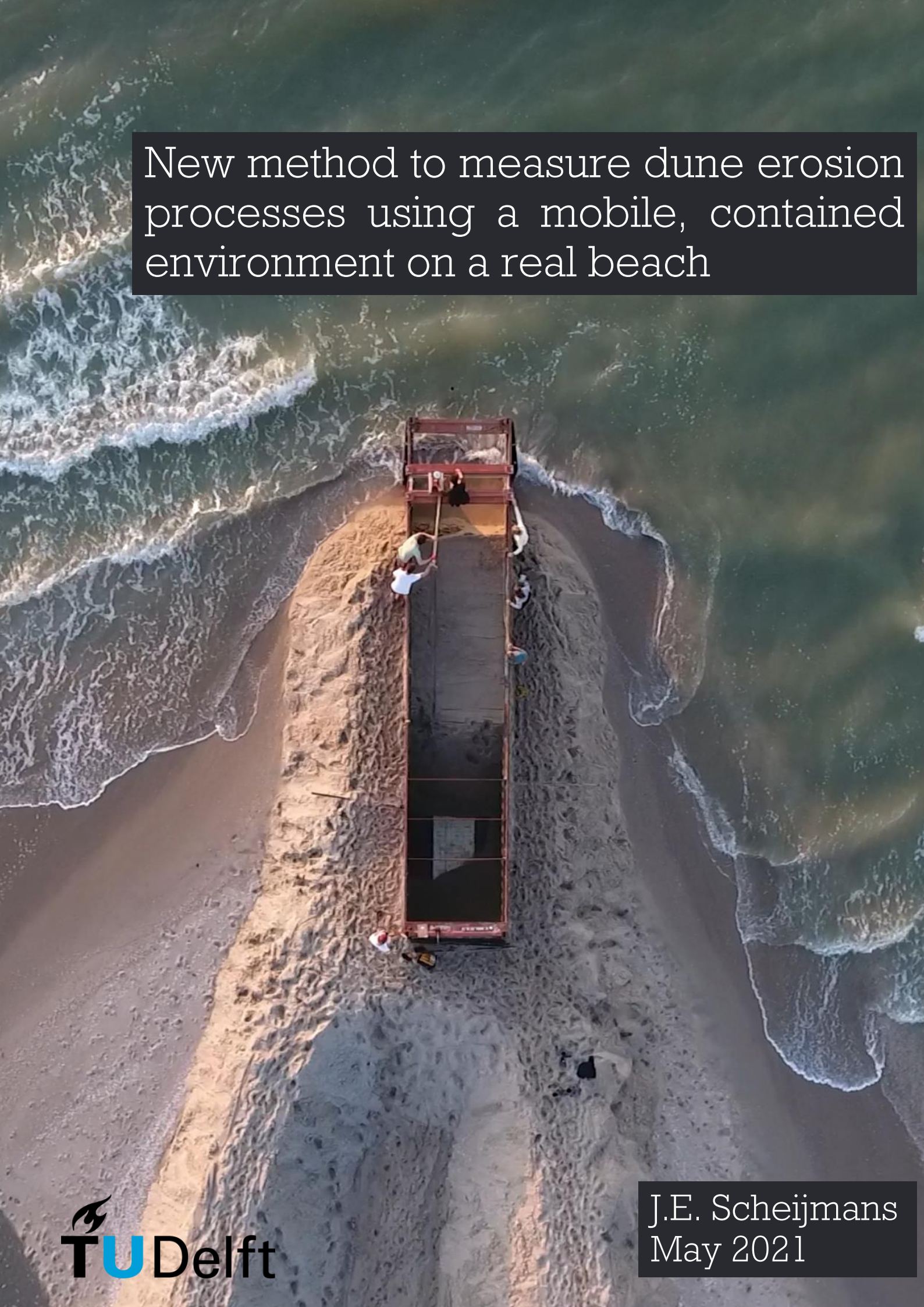

J.E. Scheijmans
May 2021

TU Delft

Master Thesis

New method to measure dune erosion processes using a mobile, contained environment on a real beach

by

J.E. Scheijmans

to obtain the degree of Master of Science
at the Delft University of Technology,

Jasper Scheijmans 4278941

Supervisors:	Prof. dr. ir. S.G.J. (Stefan) Aarninkhof	TU Delft
	Dr. ir. S. (Sierd) de Vries	TU Delft
	Dr. ir. M.F.S. (Marion) Tissier	TU Delft
	Ir. P.P.J. (Paul) van Wiechen	TU Delft

An electronic version of this thesis is available at http://repository.tudelft.nl/.

TU Delft

Abstract

The Netherlands has 254 km of coastline that is covered with sandy dunes. These dunes function as primary flood defences and must therefore meet the strict requirements of the government. These state that the amount of sand that erodes during the normative storm remains within safe margins. In order to predict this storm response, intensive research has been conducted into dune erosion in recent years. This research mainly took place in laboratories, because all boundary conditions could be controlled and measurements could take place very accurately. However, it remains difficult to simulate a natural wave climate in a flume. In addition, there is also the risk of forgetting certain (as yet unknown) natural processes. Partly because of this, the demand for accurate field data and field measurement techniques has increased over the years.

This thesis proposes a new experimental method to investigate dune erosion in the field, in which a 40 feet open-top shipping container is used as an in-field wave flume. Two containers are placed in between the low- and high waterline of the Sand Engine, near Kijkduin. The experimental method is validated by looking at the hydrodynamics within the container and by comparing dune erosion within this container with dune erosion from existing field and laboratory studies. This validation consists of four experiments in which several research hypotheses are tested to see if the wave propagation and erosion processes inside the containers work as expected.

During the experiments, the wave conditions were determined by the use of pressure sensors that were mounted in different configurations during the fieldwork. The dune erosion itself was measured using two GPS devices that made a time series of the shape of the dune while it was eroding. From these time series and the wave data, an evaluation of the dune erosion processes was made.

The first experiment was carried out, to look at the wave propagation and the reflection of the walls inside the container. In the following three experiments, dunes were constructed inside the containers, to investigate the dune erosion processes. As two containers are used simultaneously during the same hydraulic conditions, a comparison between the experiments inside the containers can be made.

In general, it can be concluded that the experiments carried out inside the containers were in good agreement with the tested theories. These theories included that: the avalanching process is present, higher dunes have a bigger eroded volume, the dune toe follows the rising water level and the slope of the foredune remains similar during the erosion process.

As this was the first time this method has been used, some recommendations are made. One of those findings is that the use of the measurement systems should be the same in both containers. A good reason to use this contained erosion method again is for the investigation of the grain size influence in erosion processes.

Preface

This master thesis marks my final work as a student of the Delft University of Technology. It contains the introduction and validation of a new research method for large scale dune erosion in the field. The new method consists of a movable contained environment in the form of a 40-ft open-top sea container. The thesis serves as an exploratory study in order to understand the challenges that are related to this new method.

When I started this project on the 28th of March, the world was facing a new global health issue, the Covid-19 pandemic. Now 11 months later, the end of the pandemic is finally in sight and so is the end of this thesis.

I am extremely grateful that I had the opportunity to do this fieldwork study at the university, especially in combination with the course Hydraulic Fieldwork 2020. I have learned that anything is possible if you really want it to succeed. With a closed university, this fieldwork could still be carried out, with the necessary precautions of course.

This master thesis would not have been possible without the help of a lot of people. First of all I would like to thank my committee: my daily supervisor, Sierd de Vries, for his endless enthusiasm and positivity. I would like to thank my chairman, Stefan Aarninkhof, for his support and belief in this project. I will never forget the Go/no go container meeting. I also want to thank Paul van Wiechen and Marion Tissier, for your enthusiasm and positive feedback.

I want to thank the people that helped me making the fieldwork experiments possible. Matthieu de Schipper for your positivity, your commitment and the adaptation of your course, Hydraulic Fieldwork, in which my experiment could take place. Thank you, Sander de Vree, Jaap van Duin, Chantal Willems, Sander Vos and Arno van Doorn for helping build a car out of a sketch on a napkin and for granting access to the TU while it was essentially closed. Pieter van der Gaag you especially helped me with your quick thinking of small solutions for container problems during the fieldwork. Never stop running. I also want to thank Rijkswaterstaat for giving me the right paperwork and thank you Strukton for the installation of the containers and for helping me making dunes at 4:30 in the morning during a storm. Thank you Hilbrand and Rody the shovel machinist. Last but not least a big thanks to all the students who followed the course Hydraulic Fieldwork and helped me day and night with doing measurements in and around the container: Joep, Michiel, Christian, Vasileios, Carlijn, Charlotte, Fleur, Freek, Gerard, Luka, Michiel, Philipp, Sebastian, Tjerk, Victor, Sam. The tide waits for no one. Also, thank you Roland and Mike, for helping me during the first tests.

Finally, I would like to say a special thanks to all my close friends and family. You have really helped me to maintain a healthy mindset while working from home. Your care has been of much-added value and I really appreciate all of the support you have given me. Last but definitely not least, thank you Liselot, for coping with a dune and container fanatic for 11 months, and for your support through everything.

J.E. Scheijmans
Rotterdam, April 2021

Contents

List of Figures

List of Tables

1

Introduction

Coastal dunes protect low-lying areas from flooding and prevent damage along many sandy coasts around the world. In the Netherlands, 254 km of the 523 km coastline is covered with sandy dunes. 70 percent of the Gross National Product is earned in floodable areas, that are protected by dunes among others (Postma, 2015). Therefore, the safety of these dune rows has to be guaranteed, which makes research of the vulnerability of these dunes important. However, doing research on the strength, form or structure of the dune is not that straightforward.

This thesis is written to investigate a new research method where dunes erosion research can be done in the field, but in a contained format. To understand the necessity of this research, some background information is provided.

1.1. Background

This section provides an introduction in the subject of dune erosion. First, an explanation is given of the essential products, such as an introduction in the dune profile and an explanation of the storm regimes that have an impact on the kind of dune erosion. Secondly, the erosion processes that take place when a wave hits a dune, will be explained. This is followed by an overview of the prediction models on dune erosion, that are made over time. Finally, a section about the current dune erosion research methods in wave flumes will introduce the problem that this thesis addresses.

1.1.1. Dune erosion profile

Sand dunes are found in three types of landscapes: sea coasts and lakeshores, river valleys and arid regions (Maun and Maun, 2009). Coastal dunes are formed along coasts in areas above the high watermark of sandy beaches. They occur all over the world from the northern Arctic to the equator to southern Antarctica. Coastal dunes tend to exist wherever barrier islands or wave-dominated depositional coastal landforms occur, see figure A.1.(Martínez and Psuty, 2004). The shape and the formation of sand dunes is further discussed in Appendix A.

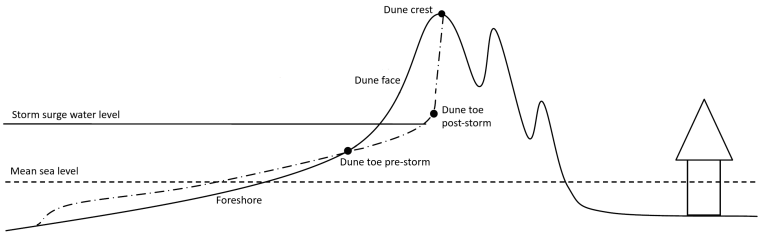

Figure 1.1: Dune erosion profile before and after a storm hits the dune. The dune toe movement up and land inwards due to the storm is visible.

Dune erosion along the southwest North Sea coasts mostly takes place during storm surges. This is when the mean water level increases during a storm and waves can reach the dune face and impact

it. The impact of the waves causes sediment volumes to erode. This eroded sand is then transported offshore by a strong undertow current. The current decreases further seaward and loses the ability to transport sand. This causes suspended sediments to settle and form a new profile that is in equilibrium with the storm surge conditions, as is shown in figure 1.1. The newly developed foreshore is more efficient in dissipating the incoming wave energy, reducing dune erosion rates as a storm progresses.

After a storm surge, the dune width is substantially smaller and the coastal profile is not in equilibrium with the post-storm hydrodynamic conditions. Waves, tide and wind reshape the foreshore and the dunes gain eroded sand back partly. In a situation, without longshore sediment transport gradients, the dunes recover to pre-storm volume. However, the time scale of dune recovery is considerably larger than that of erosion.

1.1.2. Storm regime

During a storm, waves can impact a sandy structure on several scales, damaging the structure in different ways. These levels of impact are divided into different regimes which are based on a combination of the wave forcing (represented by the runup limits) and the resistance as characterised by the geometry of the dune (Sallenger, 2000). Four regimes, representing different levels of impact, are defined. These can be seen in figure 1.2.

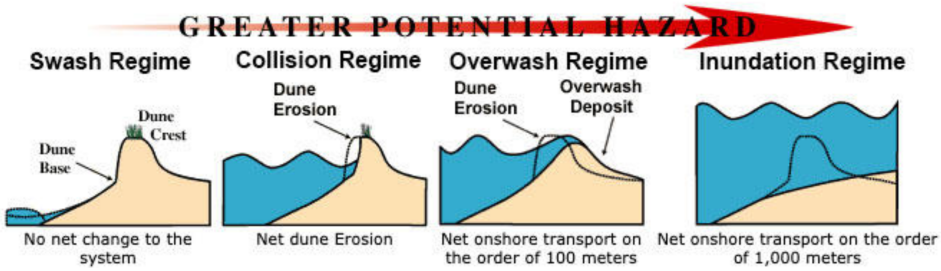

Figure 1.2: Four storm impact regimes defined by Sallenger (2000). From left to right: impact level 1 is the swash regime, impact level 2 is the collision regime, impact level 3 is the overwash regime and impact level 4 is the inundation regime (USGC, 2019).

Impact level 1 is the 'swash' regime, where the maximum runup does not exceed the toe of the dune. The foreshore typically erodes during the storm and recovers following the storm; hence, there is little net change.
Impact level 2 is the 'collision' regime, where the wave runup level is above the dune toe, but below the crest of the dune. In this regime, the foredune is flooded and the sand is redistributed in the cross-shore between the shoreface, beach and the front of the dunes. When the storm has passed, aeolian transport can bring the eroded sediment back to the dune face.
Impact level 3 is the 'overwash' regime, where the runup runs over the dune crest, but the run-down remains below the dune crest. The associated net landward sand transport contributes to the net migration of the barrier landward.
Impact level 4 is the 'inundation' regime, where run-down runs continuously over the dune crest to completely submerge the dune. Sand undergoes net landward transport over the dune (Sallenger, 2000).

In these different regimes, the water level is considered an important factor. During high-energy conditions with breaking waves, the mean water level rises due to tide-induced, wind and wave-induced forces, such as setup (van Rijn, 2009). This rise in water level causes a shift in impact regimes; from the swash to the collision regime, resulting in high energy waves attacking the dune face at high tide.

1.1.3. Erosion processes

When a storm event progresses from the swash regime to the collision regime, nearshore processes cause dune erosion. Dune erosion processes can be categorized into four processes:

- Wave impact

- Low-frequency motions (long waves)
- Turbulence
- Sliding/avalanching of the dune face

Wave impact theory
One process involved in dune erosion is the impact of waves on a steep sandy cliff, which is called a scarp. During the uprush of the waves, water collides with the dune face resulting in a force that is exerted on the dune face. This force is mainly dependent on the profile of the beach in front of the scarp. The steeper the slope, the more intense the wave force (van Rijn, 2009). An assumption in estimating dune erosion rates due to 'wave impact theory' is that there is a linear relationship between the impact (wave force F on the dune due to change in the momentum flux of the bores impacting the dune) and the weight of the sediment volume eroded from the dune (Fisher et al., 1986),(Larson et al., 2004), as is shown in figure 1.3. This linear relationship is also seen on vegetated coastlines such as salt marshes (Leonardi et al., 2016).

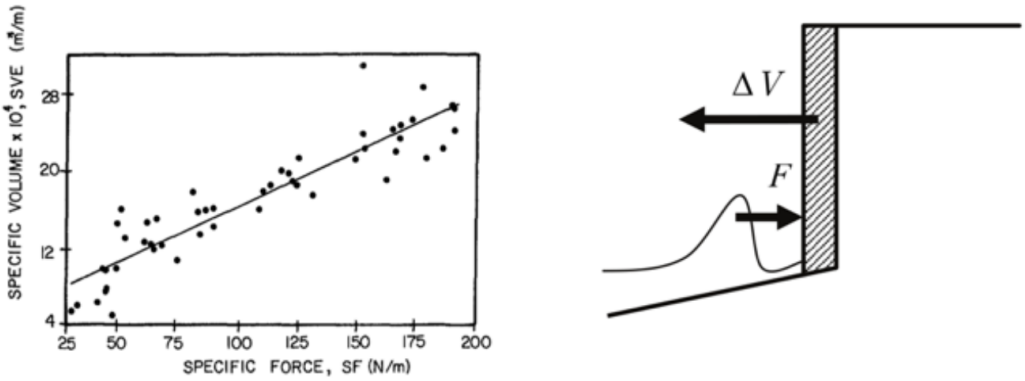

Figure 1.3: Left: Linear correlation of specific force and specific volume eroded for a laboratory dune by Fisher et al. (1986). Right: Visual explanation of a specific wave force (F), that causes erosion of a specific volume of sand (ΔV).

Low frequency motions
Offshore storms produce a wide variety of waves. Short waves that arrive at the shoreline will break, decrease in amplitude and therefore decrease in wave force, making them less important when looking at dune erosion. Low-frequency waves or long waves do not break but grow in amplitude when arriving at the coastline. As a result, the energy of the long waves can be much larger than the short waves (van Thiel de Vries et al., 2008b), (van Thiel de Vries et al., 2008a). Van Gent and van Thiel de Vries discovered that the length of the waves and therefore their period is of big importance when looking at dune erosion.

Turbulence and undertow
As waves break close to the shoreline they cause a disturbance in the flow field. This disturbance is called turbulence and causes sediment to come into suspension. The closer to the shore, the higher the turbulence velocities and the higher the suspended sediment concentrations (van Thiel de Vries et al., 2008a). Van Thiel de Vries did measurements to investigate the flow velocities nearshore and the suspended sediment concentration nearshore. Their data shows a strong return current measured 15 m from the dune front. This is the offshore current compensating for the onshore mass transport by the waves and rollers. These offshore velocities are capable of transporting sediment from the dune face offshore, creating a beach with a milder slope. The result is that sediment is stirred up near the dune face and transported offshore by the undertow. This forms the new profile with a milder slope, that fits the boundary conditions of the storm (van Rijn, 2009).

Avalanching
Another process involved in dune erosion processes is slumping or avalanching. There are two main types of avalanching, the shear-type and the beam-type. Both types of avalanching work on the basic

principle that waves attack the lower part of the dune face which results in a retreat at the top of the dune at locations water has not reached. This retreat happens with 'chunks' of sediment at the time. However, the manner in which the dune face fails can differ.

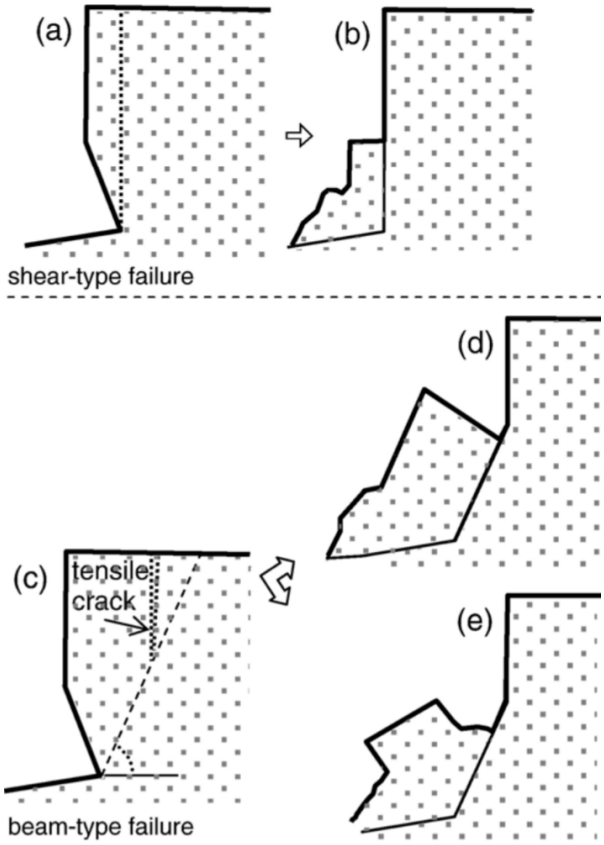

Figure 1.4: Two modes of avalanching were observed by Erikson et al. (2007), and are described as shear- and beamtype failures. The top figure (a-b) represents shear-type failure and the bottom figure (c-e) represents beam-type mass failure.

1) Shear-type failures occur when the weight of the overhang (resulting from notching) exceeds the shear strength of the sediment and slides downward as shown in figure 1.4 a-b.

2) Beam-type failures occur when tension cracks develop some distance landward of the dune face and the pending failure block either rotates or slides downward, shown in figure 1.4 c-e.

Both of these failure types occur when the weight of the overhanging sand is higher than the shear strength. This weight increases due to waves that hit the dune front and make the overhanging 'chunk' wet. Wet sand has a higher density and therefore the mass increases, which makes the 'chunk' more likely to avalanche. Also, the internal friction coefficient of the sand reduces when sand gets wet, causing instability between the wet particles and as a result, the avalanching of the chunks.

The height of the dune face has an influence on the amount of volume that is eroded due to wave impact. Van Thiel De Vries et al. (2011) found that for the same wave forcing a higher dune resulted in a larger eroded volume because more sand will collapse onto the beach. This is also found in experiments, done by de Winter et al. (2015), where a calibration of the XBeach dune erosion model with pre- and post-storm topography measurements of the dune-erosion event in January 2012 at Egmond aan Zee is done.

1.1.4. Dune erosion prediction methods

The safety assessment of Dutch dunes goes back many years and the development of equations and models to predict the amount of erosion under certain boundary condition has developed extensively.

For a long time, the method to predict dune erosion was based on a description of the dune erosion profile after a very severe storm event with a characteristic significant wave height and a still water level. This method was derived by Vellinga (1982). In this method, the location of the dune erosion profile can be obtained by horizontally moving the shape of the dune erosion profile over the initial profile. This is done until the total erosion volume is equal to the total accretion volume, see figure 1.5 (van Gent et al., 2007).

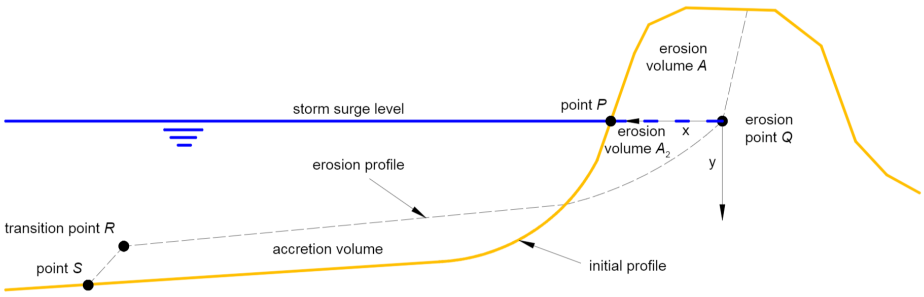

Figure 1.5: Characteristic erosion profile according to van Gent (2008), erosion volumes and (erosion) points in a cross-shore profile. (van Gent, 2008)

This model is thus based on the Bruun principle that the total eroded volume is equal to the accreted volume (Bruun, 1962). The derived equation for the erosion profile is described by Vellinga (1982) and reads:

$$\frac{7.6}{H_{0s}} \cdot y = 0.4714 \left[\left(\frac{7.6}{H_{0s}} \right)^{1.28} \cdot \left(\frac{w}{0.0268} \right)^{0.56} \cdot x + 18 \right]^{0.5} - 2.0 \tag{1.1}$$

and

$$\begin{aligned} x_R &= 250 \cdot \left(\frac{H_{0s}}{7.6} \right)^{1.28} \cdot \left(\frac{0.0268}{w} \right)^{0.56} \\ y_R &= 5.717 \cdot \left(\frac{H_{0s}}{7.6} \right) \end{aligned} \tag{1.2}$$

Here H_{0s} is the significant wave height at a depth of Datum $-20\mathrm{m}; w$is the fall velocity of a grain of sand with diameter $D = D_{50}$ in [m/s] ; y is the depth beneath storm surge level in [m] and x is the horizontal cross-shore distance from point Q positive in seaward direction. Point Q is defined as the maximum storm surge level and forms the origin $(x = 0, y = 0)$. Equation 1.1 describes the erosion profile between point Q and transition point R. In Equation 1.2 the horizontal distance x_R and the vertical distance y_R from the point of origin Q until the transition point R are described by using the wave height H_{0s} and the fall velocity of the sand particles w.

The equations 1.1 and 1.2 were derived on the basis of many experiments including series of large-scale tests for a basic situation with a wave height of $H_{0s} = 7.6\mathrm{m}$ and sediment fall velocity of $w = 0.0268\mathrm{m/s}$, by Vellinga (1982). This basic situation can be clearly recognized as reference values in the equations. Furthermore, the equations were derived for waves with a peak wave period $T_p = 12\mathrm{s}$. According to Vellinga (1982) this method is only valid for situations in which:

- the maximum storm surge level minus $1\ \mathrm{m}$ is exceeded for 5 to 6 hours
- the grain size diameter is $150\mu\mathrm{m} < D_{50} < 400\mu\mathrm{m}$
- the wave steepness is larger than $H_{0s}/L_0 = 0.02$

It is also noted that a post-storm beach profile as measured shortly after the storm will be a little lower than the predicted profile, because of a redistribution of sand after the peak of the storm.

This model was a good base model but it neglected moving water levels, different wave periods (long waves contain more wave energy when arriving at the dune face than short waves) and was only valid under particular circumstances. Therefore, new extensive large-scale dune erosion tests were done to make a model that would predict dune erosion more accurately (van Gent et al., 2006), (van Gent, 2008). This concluded in a wave period depended erosion formula:

$$\frac{7.6}{H_{0s}} \cdot y = 0.4714 \cdot \left[\left(\frac{7.6}{H_{0s}} \right)^{1.28} \cdot \left(\frac{10.9}{T_{m-1,0}} \right)^{0.45} \cdot \left(\frac{w}{0.0268} \right)^{0.56} \cdot x + 18 \right]^{0.5} - 2.0 \tag{1.3}$$

and

$$\begin{aligned} x_R &= 250 \cdot \left(\tfrac{H_{0s}}{7.6} \right)^{1.28} \cdot \left(\tfrac{0.0268}{w} \right)^{0.56} \\ y_R &= \left(\tfrac{H_{0s}}{7.6} \right) \cdot \left[0.4714 \cdot \left(250 \cdot \left(\tfrac{10.9}{T_{m-1,0}} \right)^{0.45} + 18 \right)^{0.5} - 2 \right] \end{aligned} \tag{1.4}$$

In these equations, the peak wave period T_p is added and then replaced by the wave period $T_{m-1,0}$, because the influence of wave spectra on dune erosion is then taken into account more appropriately. (van Gent et al., 2007)

The fall velocity w_s of non-spherical sediment particles can be determined from the following formulas (van Rijn, 1993):

$$\begin{aligned} w_s &= \tfrac{(s-1)gd^2}{18\nu} && 1 < d \leq 100\mu m \\ w_s &= \tfrac{10\nu}{d} \left[\left(1 + \tfrac{0.01*(s-1)gd^3}{\nu^2} \right)^{0.5} - 1 \right] && 100 < d < 1000\mu m \\ w_s &= 1.1[(s-1)gd]^{0.5} && d \geq 1000\mu m \end{aligned} \tag{1.5}$$

Here, the fall velocity w_s is dependent on the sieve size d, the kinematic velocity coefficient $\nu = 1 * 10^{-6}$ and the specific gravity $s = 2.65$.

DUROS and DUROS+

The equations of Vellinga (1982) are used as a model to predict dune erosion. This model is called DUROS. The equations derived by van Gent et al. (2007), are used to improve the existing dune erosion prediction model DUROS. The improved model is called DUROS+ and contains formulas where the wave period $T_{m-1,0}$ is included. A serious drawback of this model is that the development of the storm profile with time is unknown. Effects of varying water levels and varying wave characteristics during the storm surge cannot be accounted for (van de Graaff; Job Dronkers, 2021).

Analytical model

A relatively simple analytic model was developed by Larson et al. (2004, 2016), for the estimation of dune erosion in time. This model is based on the assumption that the eroded dune volume ΔV in a time interval Δt is proportional to the force F exerted by swash waves hitting the dune foot. The following equation was obtained for the loss rate $\frac{dV}{dt}$ of dune volume:

$$\frac{dV}{dt} = -4C_s \frac{(R - z_D)^2}{T}, \text{ where } C_s = 1.3410^{-3} \exp\left(\frac{-3.1910^{-4} H_{rms}}{d_{50}} \right) \tag{1.6}$$

Here the C_s is an empirical value that is site-dependent. According to this equation, the rate of dune erosion $\frac{dV}{dt}$ is a function of the wave height H_{rms}, the wave period T, the grain size d_{50}, the wave runup R, the dune toe height z_D and the foreshore slope β. Equation 1.6 shows that the dune erosion strongly depends on the height z_D of the dune toe, and therefore on the foreshore steepness. This is consistent with observations at Narrabeen-Collaroy Beach, which showed that variability in dune erosion was strongly correlated with variability in dune toe height z_D (Splinter et al., 2018). This equation also

assumes that the beach slope β remains constant during dune erosion (van de Graaff; Job Dronkers, 2021),(Larson et al., 2004). This is similar to the findings presented in Bonte and Levoy (2015), but their described upward migration of the scarp toe cannot always be expected. During slowly rising tide, a beach scarp might form relatively low in the cross-shore profile, just below the maximum wave runup at high tide.

DUROSTA
A serious drawback of the DUROS model was the fact that the model was not time-dependent. Steetzel (1993) made a more advanced model, based on theoretical work and laboratory experiments, DurosTA. DurosTA is a 1D process-based model, that solves sediment transport computations using time average flow- and concentration formulas. This model is based on gradients in the computed sediment fluxes. Therefore, the cross-shore profile is updated at each time step in this model. The DUROSTA model, consequentially, provides estimates of the time evolution of the dune and beach profiles during a storm surge. The results of the model compared well with large scale model tests in the Delta Flume of Delft Hydraulics (van de Graaff; Job Dronkers, 2021).

XBeach
After the addition of the wave period by van Gent et al. (2007) to the equation of Vellinga (1982), a process-based model was developed named XBeach by Roelvink et al. (2009). XBeach is an open-source numerical model which is originally developed to simulate hydrodynamic and morphodynamic processes and impacts on sandy coasts with a domain size of kilometres and on the time scale of storms (Roelvink et al., 2015). This model solves the underlying physical processes instead of applying an empirical relation. The model includes the hydrodynamic processes of short wave transformation (refraction, shoaling and breaking), longwave (infragravity wave) transformation (generation, propagation and dissipation), wave-induced setup and unsteady currents, as well as overwash and inundation. The morphodynamic processes include bedload and suspended sediment transport, dune face avalanching, bed update and breaching. The model has been validated with a series of analytical, laboratory and field test cases using a standard set of parameter settings. This model is still in development but it gives accurate results for storm impact on dune faces with water level changes due to tidal elevation. The influences of different grain sizes have been implemented in this model, but not yet to the full extend.

These models have all been made by analysing large scale dune erosion test. These tests are mostly done in big wave flumes. Flumes are big gutters that have a wave machine on one side and an experiment on the other side. This way, dunes, dikes, revetments and other sea barriers can be tested on strength. Formulas are derived from these test and models are made from these formulas. Hence, testing the strength of dunes is very important for the safety of the Dutch coastline.

1.1.5. Dune erosion research in flumes
To investigate dune safety, research of erosion speeds, superstorms and dune structure has been done. In labs around the world, big flumes are used to mimic storm waves that hit dune faces. The biggest flume in the world is based in Delft at Deltares and is called the Delta Flume, see figure 1.6.

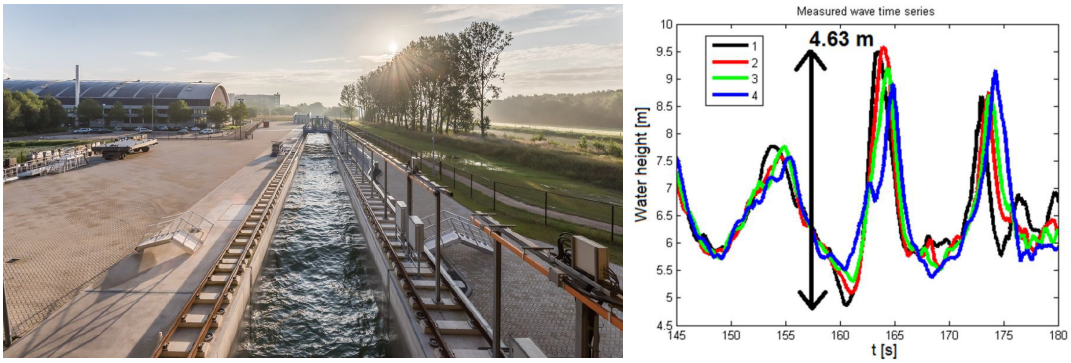

Figure 1.6: An overview of the Deltaflume at Deltares, Delft, is shown left. Right, maximum wave heights up to 4.6m, created in the flume, are shown. (Wenneker et al., 2016)

With a length of 300 m, a width of 5 m and a depth of 9.5 m the Delta flume can do storm wave simulations on a 1:1 scale experiment setup. Doing large scale test can save a lot of money, for example with regards to investments in flood protection. However, doing one test requires quite a big expense. The cost of electricity to fill the tank with 9 million litres of water and the generation of 4.6 m high waves is high (Morelle, 2015) , (Wenneker et al., 2016).

Waves that are created by wave generators in flumes are becoming more and more realistic. However, the representation of nature will never be perfect. And what if the experiments done in flumes are no longer representative? Research by van Gent (2008) and van Thiel de Vries et al. (2008b) are done, because they found out that the wave period T of waves in storms is bigger than the period used by Vellinga (1982), resulting in experiments that had to be redone, costing a lot of money.

Experiments conducted in the Delta flume led to dune erosion prediction methods that were discussed in chapter 1.1.4. The Delta flume is very successful for experiments where an object needs to be exposed to storm waves, to test the limits of the structure. However, multiple experiments are necessary when doing research on different parameters in the dune erosion process. These parameters can be different grain sizes, different dune face slopes, different dune heights, etc. These researches need multiple experiments, making it an expensive investigation.

Dune testing in the field is a good alternative, but it has some flaws too. In the field, it is difficult to separate specific parameters from each other. It is not possible to exclude the longshore sediment transport when you want to look at cross-shore sediment transport; longshore processes will have a major influence on the balance between eroded and deposited material within a cross-shore transect (van Bemmelen, 2018). Also, it is more difficult to do measurements. There is no specifically designed workplace nearby, as is the case for flume research. Moreover, during the experiments, you are dependent on the conditions at that time.

1.2. Problem definition

As 70% of the Gross National Product in the Netherlands is earned in floodable areas, the safety of the protective structures and nature is important. To test the strength of dunes along the Dutch coastline, wave flume tests are done to come up with prediction models, which have mapped dune erosion processes extensively. These lab experiments were conducted to investigate the safety of dunes under specific boundary conditions, such as long storm waves of a certain height.

To avoid scale problems, dune erosion tests are conducted in large flumes such as the Delta Flume. In these flumes, the wave climate can get close to natural conditions, but will never be fully the same. On the other hand, when conducting dune erosion test on natural beaches, it is difficult to focus on one specific process, because it is hard to exclude parameters such as longshore sediment transport. Therefore, a contained setup on the beach could be a solution. This might prevent the influence of longshore sediment transport, but reduces the cost significantly when comparing this new research method to the Delta Flume.

1.3. Research questions

A new research method is proposed. In this method, dune erosion processes can be investigated on a beach with a real wave climate, while longshore transport might be excluded. The new method consists of a 40 ft shipping container with open doors on the seaside. In this container research on dunes could be carried out. To investigate the effectiveness of the new research method, a research question was posed:

How can a contained erosion setup in the field be used to measure a realistic dune erosion process?

To answer the main research question several sub-questions are posed:

1. **How does the contained erosion setup influence the measurements?**
   With this question, influences caused by the container on the measurements are reviewed by looking at general observations. This includes container movement, the reflection of waves from the walls, the breaking of waves due to the entrance of the container and incident wave angles of wave rays travelling in the container.

2. **What is the difference in wave behaviour when comparing waves in and outside the container?**
   To answer this question, the wave behaviour inside and outside the container should be investigated by doing a wave-by-wave analysis. This includes the investigation of the wave height reduction and the propagation of the waves in and outside the container.

3. **How does the erosion process inside the container behave?**
   If the erosion process inside the container works according to the theory, the process is working the same inside as outside of the container. The following research hypotheses, that are mentioned in section 1.1, are tested:

   (a) Avalanching process is present.
   (Bosboom et al., 2015)

   (b) Higher dunes have a larger eroded volume under the same wave forcing.
   (Thiel de Vries et al., 2011),(de Winter et al., 2015)

   (c) The dune toe follows the rising water level
   (Bonte and Levoy, 2015),(Splinter et al., 2018)

   (d) The wet slope of the foredune stays at an equal steepness while the dry dune face slope increases in steepness due to scarp formation.
   (Larson et al., 2004)

   (e) The total amount of eroded volume inside the container can be predicted with existing models.
   (Vellinga, 1982),(van Gent et al., 2007)

1.4. Thesis outline

In order to answer the research questions presented above, this thesis is divided into six chapters. The configuration of these chapters is shown in figure 1.7.

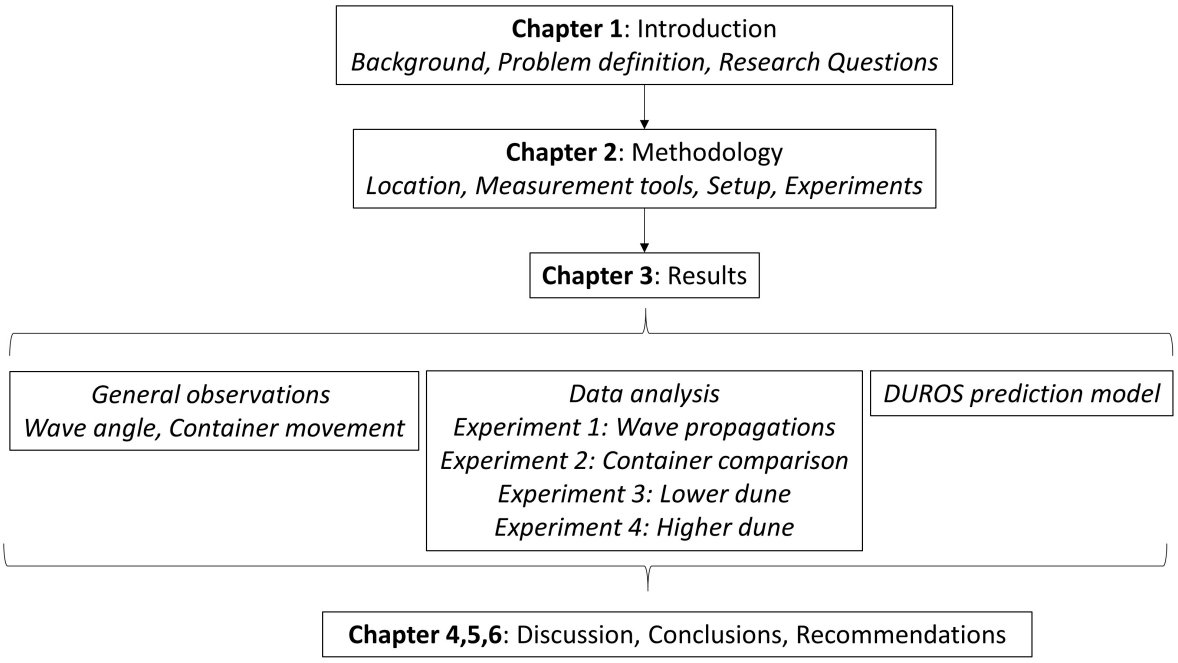

Figure 1.7: An overview of the general thesis outline

Chapter 1, the introduction, contains essential background information that leads to the problem this thesis addresses. Then several research questions have been posed. Chapter 2, the Methodology, evaluates the fieldwork. Its location, tools and experiments are extensively explained. The results are presented in chapter 3. This chapter is divided into three parts. The first part discusses general observations made during the fieldwork. The second part discusses data analysis per experiment and the final section discusses the implementation of two prediction models. Finally, chapter 4, 5 and 6 represent the discussion, conclusion and recommendations from this thesis.

In the Appendix, several subjects are explained in more detail. Appendix A discusses further background info. Appendix B gives some more info of the modelling of the Dutch coastline, focused on the process-based model, XBeach. Appendix C shows a data overview of the raw outputs of the measurements devices. Appendix D focuses on the processing of the raw data. Appendix E show visual dune crest observations. Finally, in appendix F the errors of the GPS and the lateral deviation of the GPS setup during the experiments is shown.

2

Methodology

Field experiments with a newly developed, contained erosion setup have been conducted at the Sand Engine. In this chapter the methodology of the experiments, the setup, the measurement tools and the local conditions will be discussed in further detail.

The Sand Engine is a 'mega nourishment' at the Dutch coastline where experiments are often conducted. As this location is naturally eroding, the nourishment provides a perfect setting for field experiments, where dune erosion processes are investigated. This will be further explained in section 2.2. To fill the knowledge gap between lab and field experiments a contained field experiment was executed. Two 40 ft sea containers were put close to the high water line, to function as a contained area where different dune erosion experiments can be executed. These containers were placed on the beach for one week from Friday 18-09-2020 until Friday 25-09-2020. In the first weekend, the measurement devices and the container setup was tested. After that, 4 days of experiments were conducted.

2.1. Contained erosion setup

Two 40 foot open top shipping containers were used as a movable lab where dune erosion experiments were carried out. The container is open on one short side and on the top, as shown in figure **??**. On the inside, experiments can be executed. In this case, an artificial dune is built. The container is placed at the high water line in such a way, that at low tide no water is entering the container, making it the perfect time to construct the tested dune.

Figure 2.1: 3D overview of an open-top shipping container with a yellow sail on top. This container is used as a contained dune erosion environment.

The walls of the containers are made of corrugated steel which improves the strength (Anish, 2019). For this experiment reinforced open-top containers are used. These containers were previously closed

40-ft containers. First, the top has been removed, then steel reinforcements containing a squared steel frame and a dozen steel crossbars are welded in the top. The front of the container has two steel, winched doors that can be opened. The dimensions of the container are shown in table 2.1.

Table 2.1: Container dimensions of a 40 ft open-top container, from the inside and outside. Results are obtained by measurements and sources (Lepage (2020),Hapag-Lloyd (2020)). [1]unclear due to steel reinforcements on the container.

Container dimensions	**Inside**	**Outside**
Length [mm]	12030	12190
Width [mm]	2350	2438
Height [mm]	2380	2590
Capacity [m^3]	67	-
Weight [kg]	-	3850-4050[1]

At high water, the waves are in the collision regime at the dune face, causing erosion of the dune inside the container. In figure 2.2a a container is shown during high tide and in figure 2.2b the dune construction inside the container is shown during low tide. The exact dimensions and specifications will be discussed in section 2.5, but first, the location of the fieldwork is explained.

(a) Overview an experiment conducted inside a container during high tide. The container functions as a contained erosion setup where wind and longshore currents should have no influence.

(b) Picture taken at low tide during dune construction. A dune of 1 m height is constructed and measurement tools are placed in, around and on top of the container.

Figure 2.2: Contained erosion measurement setup

2.2. Fieldwork location

At the Dutch coast, to the South of The Hague, a sandy 'mega nourishment' is built on which this research has taken place. This nourishment is called; the Sand Engine and is shown at the right top of figure 2.3.

The Sand Engine is a project that was created in 2011 between Monster and Kijkduin to provide sand to the beach of South Holland over the next 20 years by natural processes (Stive et al., 2013). Since then, the Sand Engine became an attraction not only for recreational activities and natural species but also for researchers and their experiments. This is one of those experiments. The exact location of this fieldwork will be at the tip of the sand engine at $52°03'21.9"$N and $4°11'17.6"$E, as shown in figure 2.3.

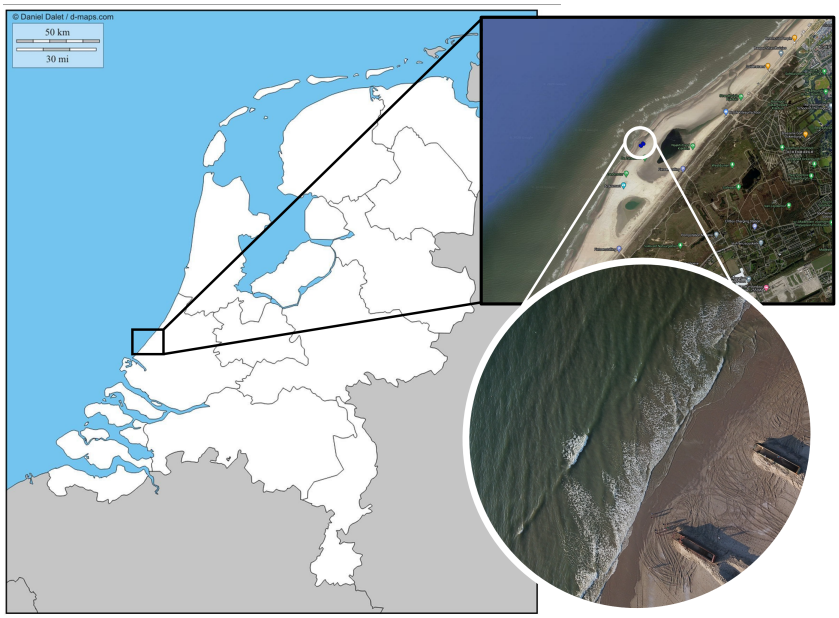

Figure 2.3: Location overview of the fieldwork experiment, I. Located at the tip of the Sand Engine between Monster and Kijkduin in the Netherlands.

The location of the containers on the sand engine has been determined based on several points:

- Hydraulic conditions: At the Sand Engine several tests have already been performed, therefore historic data of the hydraulic conditions was available. Furthermore, the tip of the sand engine has (when looking at yearly averages) NE waves arriving directly parallel to the shoreline. This meant that waves are moving straight in the container.
- Uncrowded beach: The tip of the sand engine is a 15 min walk from to closest beach entrance and a 20 min walk from the main beach entrance. Therefore this location is not visited by many people. As the two containers are not in a confined area, trespassers could disturb the measurements. Therefore, an uncrowded beach is preferred.
- Logistics: A beach close to the city of Rotterdam was preferred as the containers were transported from the port of Rotterdam.

2.3. Measurement tools

For this fieldwork different devices are used to measure various parameters.

2.3.1. Global Positioning System

The height of the dune profile was measured with a real-time kinematic global positioning system (RTK-GPS). The RTK-GPS automatically logs data from a stationary station nearby with known location and elevation to improve the data from the rover GPS. With the data of the reference base stations, positional corrections can be made, reducing errors. This results in an accuracy in the order of centimetres. The most nearby base station was the station at Hoek van Holland, which is approximately 9-10 km away from the Sand-Engine. The differential corrections work best if the distance from the rover to the base station is small, such that the atmospheric conditions could be assumed similar at both locations. The error of these GPS devices is tested and is in the order of 1.4-3.8 cm, as shown in Appendix F.

A GPS uses a satellite connection to function. Inside the container, the connection of the GPS with the satellites and the antennas of the GPS devices was fairly limited. The signal was disturbed by the walls of the containers. This meant that the antenna needed to be above the containers while measuring in the container. As the container is 2.59 m high (see table 2.1), an extension pole had to be used to higher the antenna. To reduce lateral movements of the GPS receiver a guidance system was

created for both containers. The guidance systems made it possible to conduct a survey on a straight line. Unfortunately, due to limited resources and logistical difficulties, two different systems were used, one for each container.

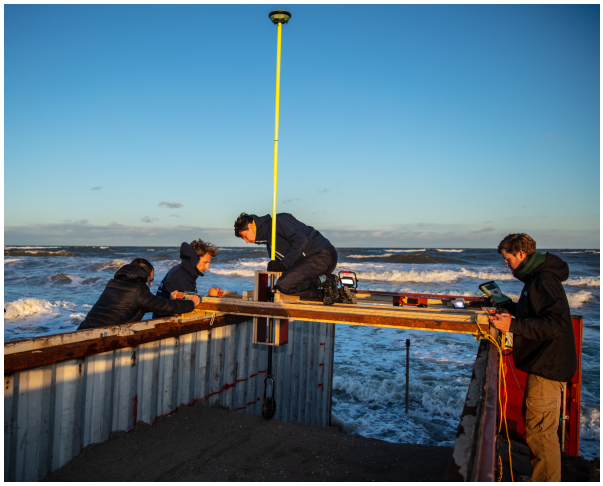

(a) GPS setup container 1. A cart on top of the container with a frame attached to it can guide a GPS pole through the container. This way transects of the dune face are taken.

(b) GPS setup of container 2. A wooden plank functions as a stabilizer for GPS pole. This way the point measurements of the dune face are stable.

Figure 2.4: Comparison of the two measurement systems.

System 1
This guidance system is only used in container 1. As the dune height varies in this container the system needed to be the most advanced system as high precision is required. This system consists of a cart with wheels underneath it, that can be rolled over the open-top container. On the cart, a wooden frame for the GPS pole was constructed. This wooden frame could be tilted and shifted in such a way that the pole could remain in a straight position at all times, as can be seen in figure 2.4a. In lateral direction, the frame was set to 59 cm from the southern side of the container. For the setup at container 1 an extension pole with an attached wheel was used (1.32 m) together with 2 extra regular extension poles (1.00 m each). The total length of the poles was therefore 3.32 m. When the cart with the GPS pole inside, was pushed from the back of the container to the front, a transect was made. After that, the cart was pulled back and the process was repeated until the measurement was finished. 80-120 transects were made per experiment with this system.

System 2
Due to some logistical and time management difficulties, there was no second cart built for container 2. This was not a problem as the second container only contained a reference dune during all of the dune experiments. Therefore a small wooden frame was build that was placed on the side of container 2, as can be seen in figure 2.4b. This frame made it possible to do point measurements at an equal distance from the side of the container and resulted in a straight measurement transect. The table was built to measure a transect at 59 cm from the southern side of container 2. As was the case with system 1. This was done to strive for equal measurement conditions in both containers. For container 2, one extension pole with a foot (1.80 m) and one regular extension pole (1.00 m) were used. The total length was therefore 2.80 m as is presented in table 2.2. A spirit level was attached to one of the poles to manually place the GPS receiver plumb over the foot. With these point measurements, 30-70 transects were made per measurement with this system.

2.3.2. RBR solo pressure sensor
To measure the wave heights and the water level, four pressure sensors of the type RBR Solo 8Hz were used, see figure 2.5a. To identify the sensors during and after the measurements, the sensors are numbered RBR1, RBR2, RBR3 and RBR4 and will be referred to as such from now on for clarity. Each sensor has a sensing element, which reacts to pressure changes and creates an output signal

Table 2.2: Summary of the GPS setups of both containers.

Parameter	System 1	System 2
Location	Container 1	Container 2
Extension poles	Two regular poles	One regular pole
Guidance system	Cart and stabilisation frame	Small wooden frame
Measurement technique	Continuous measurement	Point measurement
Total height receiver	3.32 m	2.80 m

that can be retrieved by connecting the pressure sensor to a laptop. The pressure sensors are able to measure a frequency of 8 Hz.

When a pressure sensor is installed outside the container, the sensor is attached to a metal frame by screws and a clamp. This metal frame is then pulled over a metal jet pole, which is jetted into the sand, and fixed in a way that the sensing element is 15 cm above the ground (before the experiment starts) to reduce sand intrusion in the pressure sensor. This distance varies during the different experiments due to bed erosion, as shown in figure 2.5c. When a sensor is installed inside the container, the sensor is attached to a short wooden pole, which is connected to the container floor by L-shaped metal plates and screws. The sensing elements are all 7 cm above the container floor. This height is assumed to be sufficient for the sensors to not get buried by possible accretion inside the container during high tide, but also to be fully submerged underwater long enough to record a proper wave signal during high tide, as shown in figure 2.5b.

(a) Pressure sensor RBR Solo 8 Hz with indication of the sensing element inside the sensor

(b) RBR horizontal mounting inside the container

(c) RBR vertical mounting in front of the container on a jet pole

Figure 2.5: RBR pressure sensor and mounting overview.

The pressure sensors are placed in three different setups, discussed in section 2.5, and are mounted to a pole with a clamp. This pole could be located inside the container, bolted to the floor (see figure 2.5b), or in front of the container, jetted in the ground. See figure 2.5c

When the pressure sensor is not submerged underwater, it measures the surrounding atmospheric pressure p_{atm}. When it is submerged in still water, the measured pressure is the absolute pressure which consists of the atmospheric pressure p_{atm} and the hydrostatic pressure $p_{hyd} = -\rho g z_p$, where z_p is the height of the sensor under the still water line. At z=0, ρ is the density of the water and g is the gravitational acceleration, which is taken to be 9.81 m/s^2. When waves are present, the recorded pressure sensor records (additionally to p_{atm} and p_{hyd}) the dynamic wave pressure p_{dyn}, which is further explained in Appendix D.1.

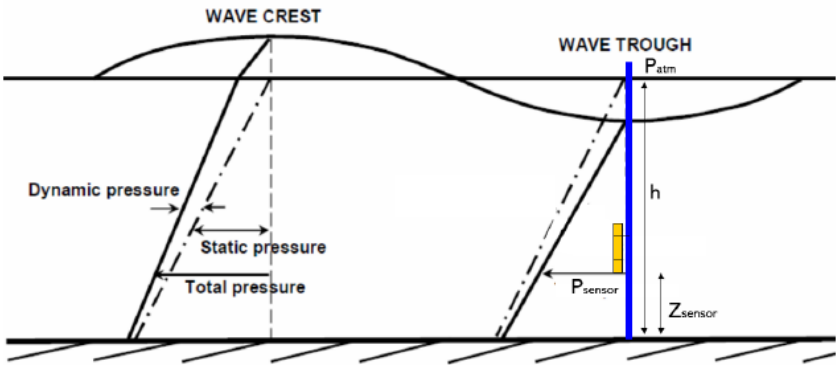

Figure 2.6: Wave-induced pressure superimposed on the hydrostatic pressure along the vertical, beneath a wave crest and a wave trough (amplitude exaggerated for illustrative purposes) with a crude approximation above the still-water line REF (Ocean wave lecture slides, 2019, adapted)

The four RBR's were placed in three different setups depending on the experiment that was carried out.

2.4. Experiments

During the fieldwork, four different experiments were conducted inside the containers. These experiments were carried out during a fieldwork week from the 18th until the 24th of September 2020. An overview of the experiments is given in table 2.3. All experiments were executed during high tide conditions, beginning approximately 1-2 hours before high tide and ending around 1 hour after high tide. This way the biggest wave action is present at the dune face during the measurement.

Table 2.3: Fieldwork experiments overview in September 2020.

Number	Description	Date	Time	Short explanation
Exp 1.1	Wave straightening	21-09	17:50-20:00	Test with two empty containers to investigate wave straightening
Exp 1.2	Wave propagation	22-09	06:00-09:10	Test with two empty containers to investigate wave propagation
Exp 2	Two reference dunes	22-09	18:09-20:06	Two similar reference dunes with a height of 1.3 m to check similarity
Exp 3	Low dune	23-09	18:30-20:13	One container with a ref dune of 1.3 m and one container with a low dune of 1.0m to check erosion speed differences
Exp 4	High dune	24-09	06:59-09:19	One container with a ref dune of 1.3 m and one container with a high dune of 1.6m to check erosion speed differences

2.4.1. Experiment 1

The first experiment is done to investigate the wave straightening and the wave propagation of the waves travelling inside both containers without any sand (or dunes). To investigate this, this experiment consists of two sub-experiments with different setups. The pressure sensors are the most important measurement devices in this sub-experiment. Experiment 1.1 is carried out on Monday evening during high tide between 17:50 and 20:00 and experiment 1.2 is carried out on Tuesday morning during high tide between 6:00 and 9:10. The GPS devices will not take measurements during these sub-experiments because there is no dune constructed in the containers. To have a visual of the waves in the experiment, the Go Pros will be on video mode. The pressure sensors are put in two different setups.

Experiment 1 setup 1: Wave straightening

The first setup of experiment 1, shown in figure 2.7, is used to estimate the straightening of the waves when travelling inside the container. For this, RBR2, RBR3 and RBR4 are placed in one line parallel to the water line about 2 m inside the container and RBR1 is placed 1 m in front of and in the middle of the container, as shown in figure 2.13a and will be discussed into more detail in section 2.5. If the RBR's register the incoming wave at the same time, the wave is considered straight.

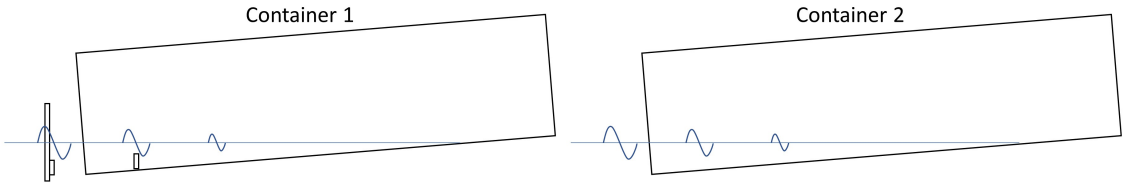

Figure 2.7: During experiment 1.1. Four pressure sensors are placed in and around container 1 to measure the wave straightening. Container 2 is empty.

Experiment 1 setup 2: Wave propagation

The second setup of experiment 1, as shown in figure 2.8, is used to register the wave propagation over the container entrance, which is 15 cm high. All four sensors are placed in one line perpendicular

to the waterline, where RBR 1 is 1m outside the container and the other three pressure sensors are inside the container, as shown in figure 2.13b and will also be discussed in more detail in section 2.5.

The sensors are installed in the same way as in setup 1. The sensing elements of RBR2 to RBR4 are 7 cm above the container floor, while the height of RBR1 decreased to 11.5 cm above the sea bed due to sedimentation in front of the container during the high tide of setup 1.

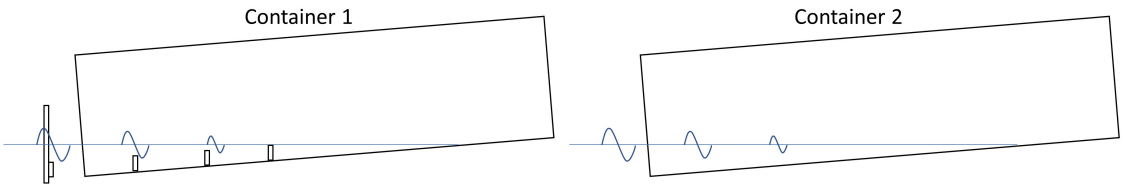

Figure 2.8: During experiment 1.2. Four pressure sensors are placed in and around container 1 to measure the wave propagation. Container 2 is empty.

2.4.2. Experiment 2: Two reference dunes

The second experiment takes place during high water on Tuesday evening between 18:09 and 20:06. At the previous low tide, a dune of 1.3 m in height, 2.35 m in width (=container width), a crest length of approximately 4-6 m and a slope of 1:1 starting 1 m from the entrance of the container, is constructed in each of the containers. This is shown in figure 2.9. A dune with this form is referred to as a reference dune, from now on. This is done to investigate the difference in erosion speed between the two containers, to see if the result of both containers can be compared.

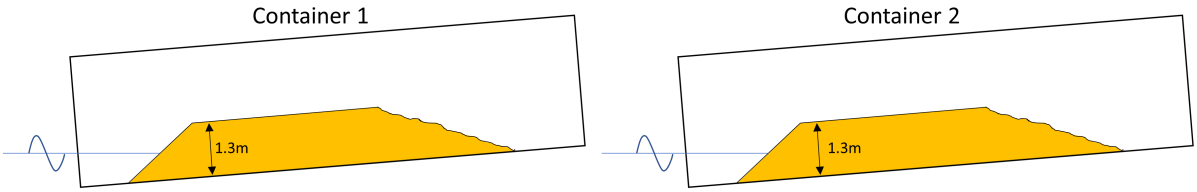

Figure 2.9: During experiment 2, container 1 contains a dune of 1.3 m (ref dune) and container 2 contains a dune of 1.3m (reference dune).

1.5 hours before high tide, the measurements of the GPS, Go Pro's and the RBR's start, at the same time. That means that at container 1 the cart with the GPS pole starts taking transects of the dune while waves erode the dune. In container 2, the GPS starts taking point measurements of the other reference dune. Go Pro 1 and Go Pro 2, located in the first container, simultaneously take two pictures per second. In the second container, the Go Pro Fusion is taking a video. All the RBR's are taken out of the container and put into the setup explained in figure 2.12. They will stay in this setup for the remainder of the fieldwork.

2.4.3. Experiment 3: Low dune

The third experiment represents a field test where 2 dunes with different heights are investigated and takes place Wednesday 23-09 between 18:30-20:13. During low tide on Wednesday, two dunes were constructed. In container 1 a low dune with a height of 1.0 m is constructed. In container 2 the reference dune with a height of 1.3 m is made, as shown in figure 2.10. The width (2.35m), crest length (4-6m), slope (1:1) and starting point (1m from entrance) are similar for all the constructed dunes in all experiments and will therefore not be mentioned again. This way the difference between the erosion speed of the two dunes solely based on height difference can be investigated as they start eroding at the same time. The third experiment takes place during high water on Wednesday evening between 18:30 and 20:13. The height of the low dune (1 m) is chosen in such a way that under normal wind conditions in September (approx 5m/s) at the Sand Engine, the collision regime is still valid.

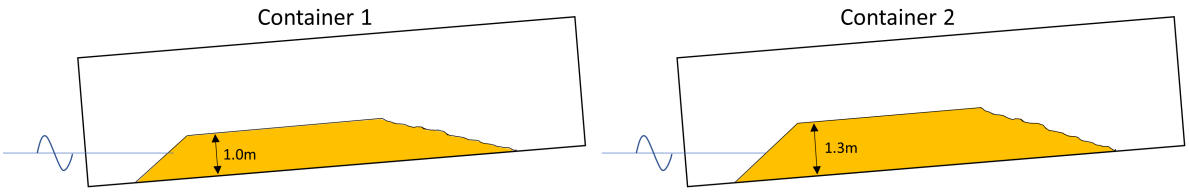

Figure 2.10: During experiment 3, container 1 contains a dune of 1.0 m and container 2 contains a dune of 1.3m (reference dune).

The GPS devices, Go Pro's and RBR's are all measuring from the start of this experiment. The GPS devices are taking transects of the dune front. The Go Pro's are taking a time-lapse with a frame rate of two pictures per second. And the RBR's are taking pressure measurements at an 8 HZ frequency.

2.4.4. Experiment 4: High dune

The fourth experiment also focuses on erosion speeds of dunes with different height. The difference is, that experiment 4 looks at the difference between a high dune and a reference dune instead of a low dune and a reference dune. This experiment takes place at high tide on Thursday morning between 6:59 and 9:19. In container 1 a high dune with a height of 1.6 m is built. In container 2 a reference dune is built with a height of 1.3 m, as shown in figure 2.11. The measurement devices function the same as in experiment 3.

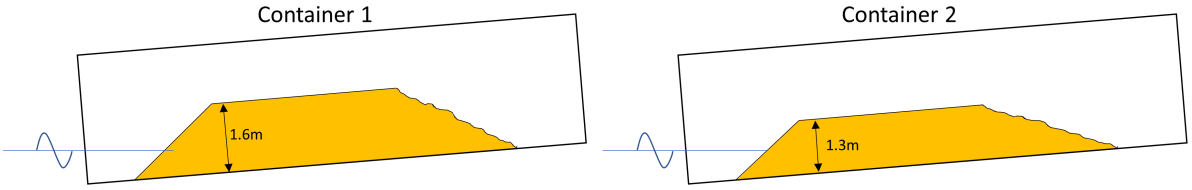

Figure 2.11: During experiment 4, container 1 contains a dune of 1.6 m and container 2 contains a dune of 1.3m (reference dune).

2.5. Fieldwork setup

The containers are placed between the low and high water line on the beach. The slope of the beach between the high water line and the low water line, is around 1:25, meaning that the distance between these two tidal marks is approximately 50 m. The containers were placed on the beach such that the opening is directed parallel to the incoming waves. This proved to be difficult. The containers were placed as far from the low waterline as possible, around 10-20 m from the high water line depending on the day. This will result in high wave action in the front of the container during high tide. During low tide, the containers are dry, which gives an ideal window to setup the next experiment. The containers will be secured with a steel chain and a concrete block and were kept at the same location during all experiments. The measurement devices in and around the container will, however, be moved in between experiments in 3 different setups.

Around the containers, a 2 m high dune was constructed, as is shown in the fieldwork setup plan in figure 2.12. This has multiple purposes. The friction between the sides of the container and the dune prevented the container from moving. The v-shaped dunes, placed from the container to the high water line, are also functioning as a precaution. Without these dunes, water could move freely around the container, causing big scour holes and therefore settlement or movement of the containers. As the return current is much more likely to cause this potentially dangerous scour, the v-shaped dunes were built up to and over the high water line to prevent this from happening. This is shown in figure 2.12.

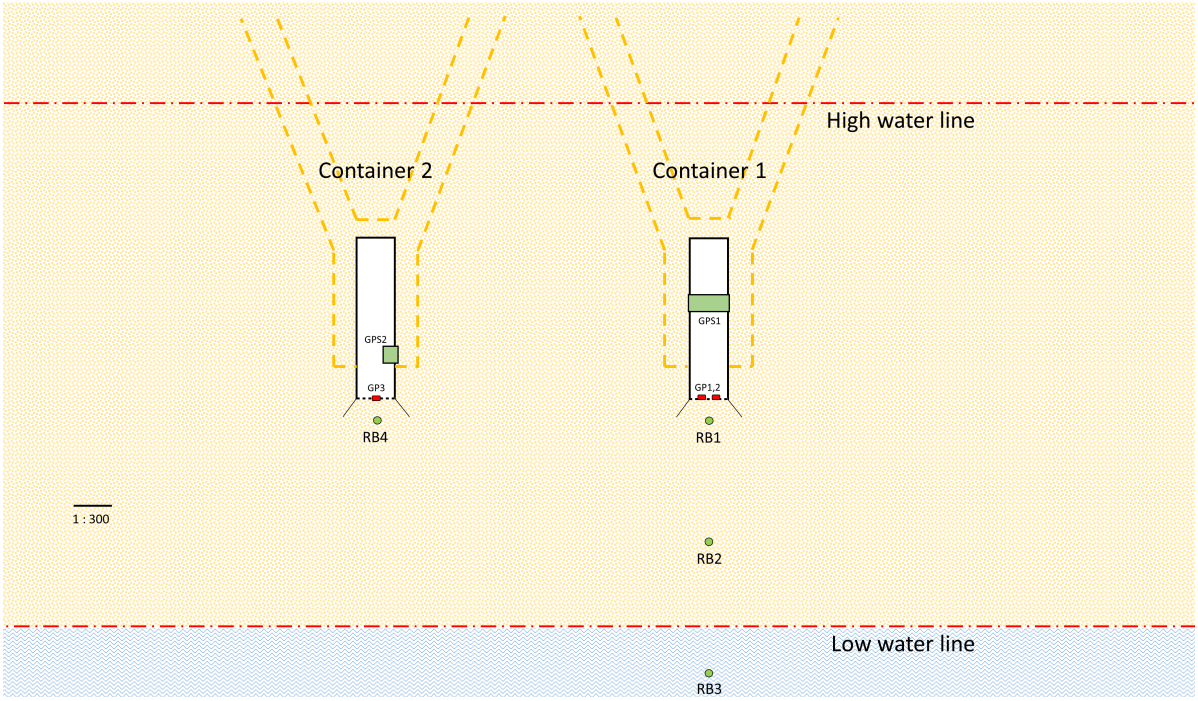

Figure 2.12: Overview of container placement during the fieldwork week. Two containers placed on the beach close to the high water line, containing 3 Go Pro's, and a GPS setup in each container. Furthermore, 4 RBR solo pressure sensors are placed in front of both containers. Around the containers, dunes are constructed to prevent movement of the containers and for experiment accessibility during measurements at high water. The location of the measurement devices varies during different experiments. Scale is 1:300.

The measurement tools are installed in and around the container, as explained in section 2.3. Next to the pressure sensors and the GPS systems, two Go Pro's Hero 7 are installed at the entrance of the two containers. These will not have a big function in this thesis, but they are used to make movies and photos of the experiments. The Go Pro's faced the inside of the container and will remain in the same position during all experiments.

The pressure sensors are placed in 3 different setups. Setup 1 and 2 are used in the first experiment, each half a day (1 high tide) and setup 3 is used for experiment 2,3 and 4, for 3 days (6 high tides).

2.5.1. RBR setup 1

RBR setup 1 is shown in figure 2.13a, and shows a positioning of the RBR's in experiment 1.1 on Monday evening. RBR 1 is placed 1.03 m in front of the container. RBR 2, 3 and 4 are place parallel to the shore inside the container, 3m from RBR 1. RBR 2 and 4 are mounted close to the container walls, but with enough space between the wall and the sensor to exclude the noise of turbulence that is generated by the irregular container walls. This setup is used to measure if waves travel straight inside the container. No dune is built while RBR's are placed inside the container.

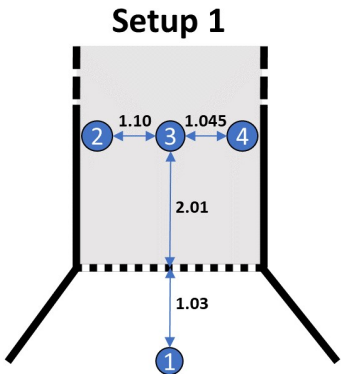

(a) RBR setup 1, situated in container 1 on Monday evening. 3 RBR's are placed inside the container and 1 RBR is placed in front.

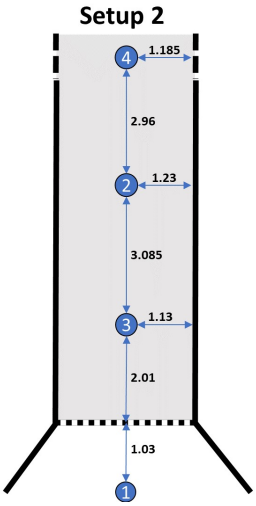

(b) RBR setup 2, situated in container 1 on Tuesday morning. All sensors are placed in a straight line perpendicular to the shoreline.

Figure 2.13: RBR setup 1 and setup 2

2.5.2. RBR setup 2

RBR setup 2 is shown in figure 2.13a, and shows a positioning of the RBR's in experiment 1.2 on Tuesday morning. All the RBR's are in a straight line perpendicular to the shoreline. 3 sensors are placed inside the container and 1 sensor is placed 1.03m in front of the container. The distance between the sensors is based on the average wavelength of waves that travel inside the container. This setup is used to test the progression of the wave inside the container.

2.5.3. RBR setup 3

RBR setup 3 is used for most experiments, experiment 2, 3 and 4. In front of container 1, 3 RBR pressure sensors are installed. RBR 1 and 4 are installed on a pole approximately 1 m in front of the containers. RBR 2 and 3 are installed on a jet pole, parallel with RBR1, with approximately 40 m between the poles. RBR3 is installed as far offshore as was logistically possible. This setup is called setup 3 and is shown in figure 2.14. The first two setups of the RBR's (on Monday) are only used for half a day each. Setup 3 is used for 3 days for all dune erosion experiments.

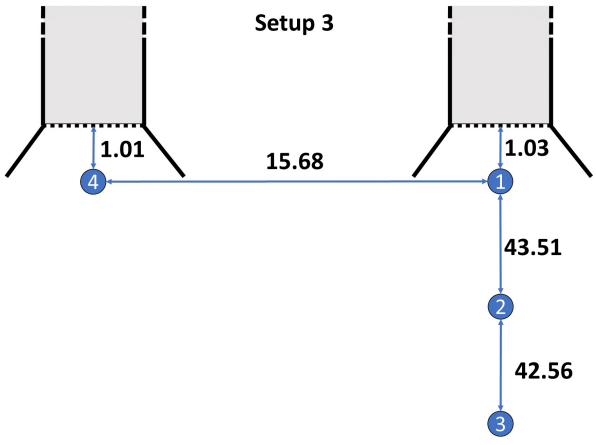

Figure 2.14: RBR setup 3, situated in front of container 1 and 2 from Tuesday evening until Thursday. In this setup all sensors are placed in front of the container, similar to figure 2.12.

2.6. Local conditions

The local conditions include the water level, the spectral wave height, the wind speed and the wind direction. These are determined based on offshore buoy data from Rijkswaterstaat. The Water level,

wind speed and wind direction are from the same buoy at Hoek van Holland. Just 10 km SE from the Sand Engine. This means that, for example, the water level peaks arrive approximately 13 minutes later than predicted at the fieldwork location. The wave data (second graph) is from a buoy in the Maasgeul Maasvlakte Noord in front of the port of Rotterdam.

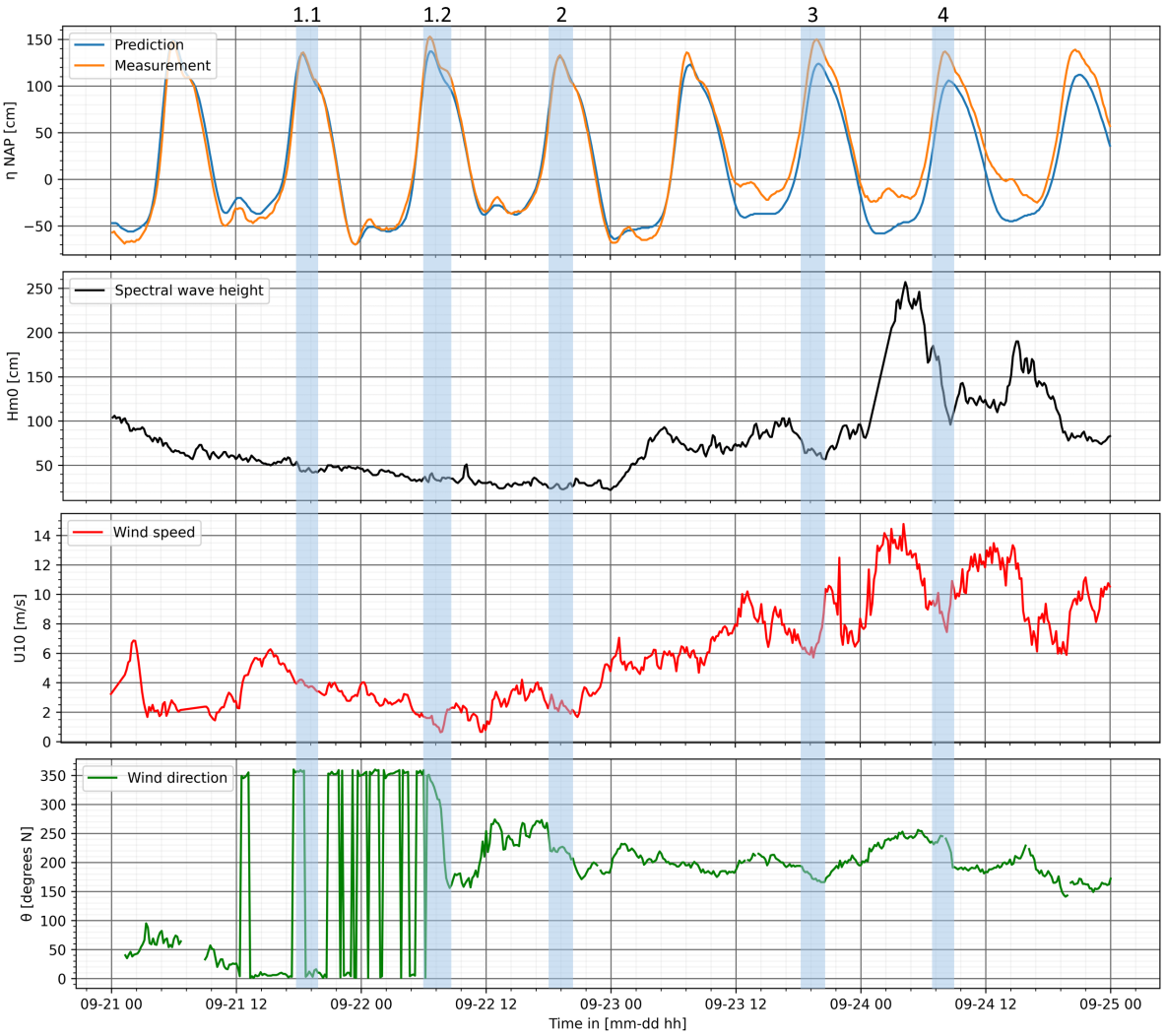

Figure 2.15: Overview of the hydraulic conditions from Monday 21 September 2012 to Friday 25 September 2021 at Hoek van Holland. From top to bottom: Water level, Spectral wave height, Wind speed, wind direction. In light blue the different experiments, which will be introduced in section 2.4

In figure 2.15, four graphs are shown. these graphs have different data on the y-axis but they have a similar x-axis. On the x-axis, the time during the four experiments is shown in [mm-dd hh]. Measurement points are averaged per 10 minutes. From the second and third graph, representing the wave height and the wind speed, an increasing trend towards Thursday the 24^{th} is visible. This trend shows an increase in wind speed, an increase in wave height. Also, a change in wind direction from East to North is visible in the last graph. This shows that a small storm was hitting the Dutch coast on Thursday during the fieldwork.

2.6.1. Wind angles

In table 2.4 an overview of the wind directions is given. These are used for the evaluation of the straightening of the waves in section 3.1.1.

Table 2.4: Overview of the wind directions during the four experiments. Wind directions are based on KNMI data, as shown in figure 2.15.

Experiment	Date	Time	Average wind direction	Average wind speed	Wave height Maasgeul
Exp 1 setup 1	21-09	17:50-20:00	4.1 °	3.77 [m/s]	44.79 [cm]
Exp 1 setup 2	22-09	06:00-09:10	260.5 °	1.62 [m/s]	34.85 [cm]
Exp 2	22-09	18:09-20:06	211.3 °	2.41 [m/s]	25.73 [cm]
Exp 3	23-09	18:30-20:13	175.3 °	6.46 [m/s]	65.17 [cm]
Exp 4	24-09	06:59-09:19	222.9 °	9.30 [m/s]	138.06 [cm]

In table 2.4, an increase in wind speed is visible. Also, the direction of the wind changed a lot during the different experiments. This means that also the wave angle changes during the experiments and that therefore the wave did not arrive at a straight angle at the entrance of the container. In figure 2.16, the different wind angles per experiment are visualized.

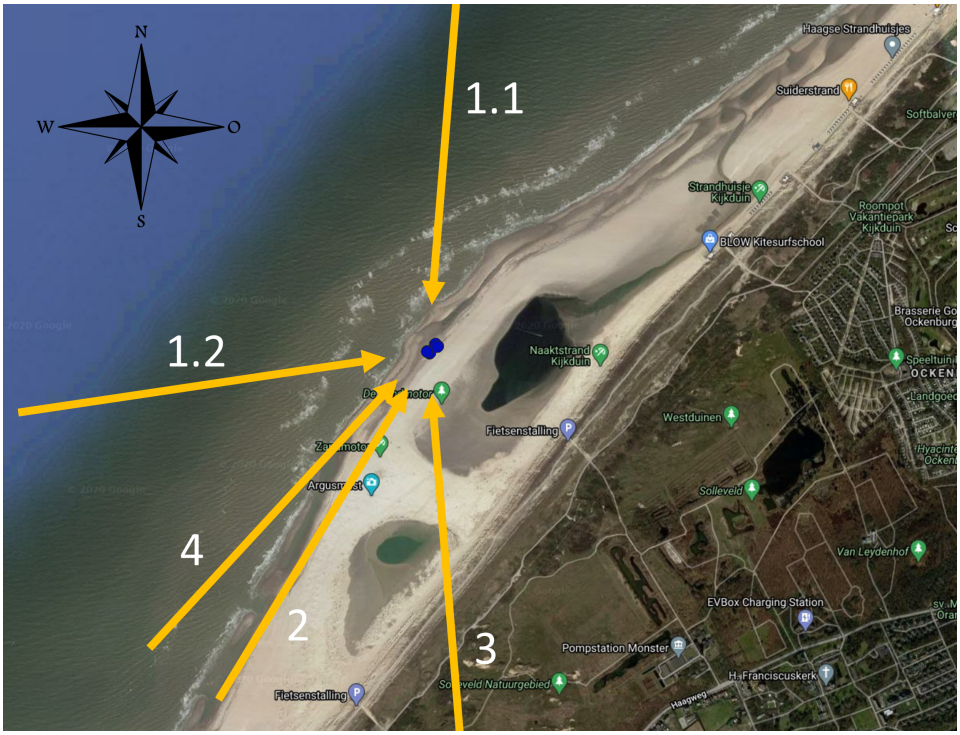

Figure 2.16: Wind direction per experiment. The two blue dots represent the containers. The yellow arrow with 1.1 is the wind direction during experiment 1 setup 1, 1.2 is during experiment 1 setup 2, etc.

3

Results

In this chapter, the results of the experiments are evaluated in three sections: General Observations, Data analysis and DUROS prediction model. First, the 'General observations' section includes an evaluation of the wave angle inside the container and a description of the movement of the two containers during the experiments. These observations are both visible and measured observations.

Secondly, the 'Data analysis' section contains an evaluation of the wave characteristics, the eroded volumes, the dune toe evolution and the wet/dry slope is shown. This is done per experiment. This evaluation is done based on the measured data by the two GPS systems and the RBR's.

Finally, the third section contains a prediction of the amount of dune erosion of experiment 4 and the post-storm dune profile in container 1 is made. This is done by using the DUROS and DUROS+ model. These two models are explained in 1.1.4. If the dune erosion inside the containers can be predicted by these models, the effectiveness of this new research method can be evaluated.

Before the experiments can be evaluated the raw pressure data, that has been measured by the RBR's, is transformed to surface elevation taking the dynamic wave pressure into account. An overview of the raw data output of the RBR's and the GPS devices is given in Appendix D.1.

3.1. General observations

In this section, some general observations are discussed. The visual observations of the wave angle change are evaluated. Also, as the containers were in big wave action during the experiments, the location, and especially the movement of the containers is discussed.

3.1.1. Wave angle inside the container

The first observation that is made is the changing wave angle of incoming waves. When conducting the experiments, both the wind direction and the wave direction changed over time. In table 2.4 a brief overview of the wind directions during the experiments is presented. Due to these changes in wind direction, oblique incident waves arrive at different angles during different experiments, as can be seen in figure 3.1.

When obliquely incident waves arrive at the shoreline the wave rays refract towards the coastline. This is a natural phenomenon that is due to depth changes in the bathymetry. When waves arrive at shallow water, the wave speed decreases, giving an oblique wave time to catch up before arriving at the shallower bathymetry itself. Hence the turning of the wave. However, when waves arrive at the container, they are not entirely straight yet. The angle of the wave rays arriving at the container and propagating inside the container can be observed from drone images.

(a) An oblige wave of approx. 5°N (red line) on Monday.

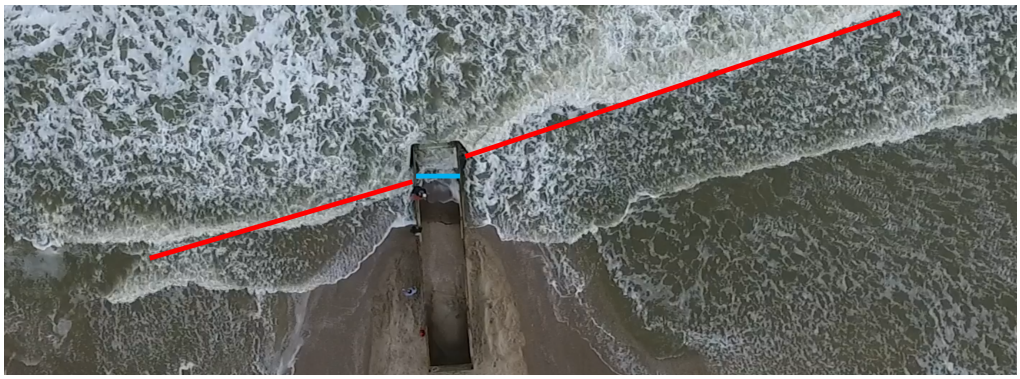

(b) An oblige wave of approx. 245°N (red line) on Thursday.

Figure 3.1: Overview of two extreme oblige waves (red lines) that turn straight (blue lines) inside the container because of refraction due to a change in bathymetry and diffraction around the container corner.

In figure 3.1 two drone images from Monday and Thursday are shown. It is clear that the waves arrive from an opposite angle at the container. From these drone images, it has been concluded that the incoming waves straighten out inside the container. Therefore, the effect of the waves coming from different directions has been concluded to be negligible. In addition, the waves cause an erosion pattern that is perpendicular to the shoreline. This observation is made by visual inspection.

The cause of the straightening of the waves inside the container is somewhat unclear. A shoaling wave still arrives under an angle at the container, but inside the container, the wave almost immediately straightens out. A combination of refraction due to a changed bathymetry around the container and diffraction around the container corners is most probable.

Figure 3.1 shows just a momentary shot of the incoming waves. In order to understand if the straightening of the waves inside the container is repeatable, the dune crest is also investigated over time. A comparison is made between a picture at the beginning of a dune experiment and at the end of a dune experiment. These two pictures are then superimposed over each other. An example of the dune crest comparison of Tuesday is shown in figure E.1.

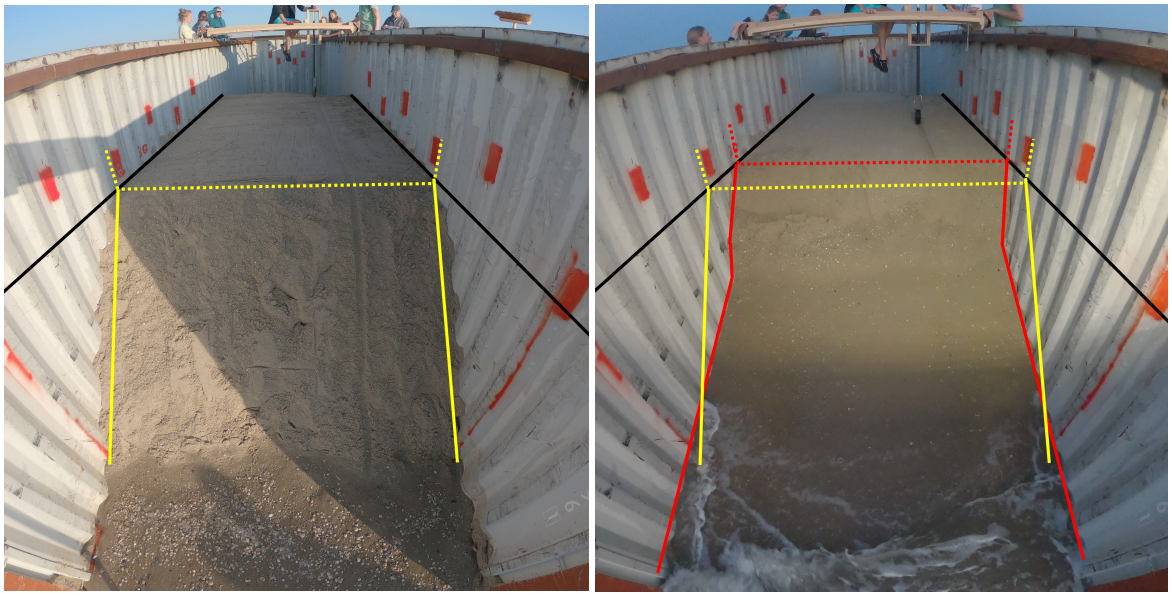

(a) Starting position of the dune face 22-09-2020 18:24.

(b) Ending position of the dune face 22-09-2020 19:54.

Figure 3.2: Two go pro pictures of the dune face of experiment 2 compared to each other. In black the sides of the dune. In yellow the start position of the dune. In red the end position after +-1.5 hours.

Based on red squares that have been painted on the container walls, an estimation of the straightness of the dune phase is determined. The error of this investigation is approximately 5 to 10 cm. The results are shown in table 3.1 and the pictures of all comparisons, taken by a GoPro Hero 7 are shown in Appendix E

Table 3.1: Visual check if the dune crest is straight before and after the experiments. The point where the dune crest touches the container wall on the right side of the picture is considered the base point. Offsets are the difference in cross-shore direction from the base point. The bigger the difference in offset the more oblique the dune crest. Pictures are shown in Appendix E.

Name	Date	Time	Left offset	Right offset
Exp 2 start	22-09	18:24	0 cm	0 cm
Exp 2 end	22-09	19:54	5 cm	0 cm
Exp 3 start	23-09	18:43	-5 cm	0 cm
Exp 3 end	23-09	19:27	35 cm	0 cm
Exp 4 start	24-09	07:05	0 cm	0 cm
Exp 4 end	24-09	08:39	15 cm	0 cm

3.1.2. Container movement

The second observation that has been made is the movement of the container. The stability of the container is important for reliable measurements. If the containers move during an experiment, the measurement inside the container could be influenced. Horizontal movement could be caused by heavy wave impact, and vertical movement could be caused by soil settlement due to liquefaction of the soil. Therefore the stability of the container is measured during the fieldwork week. Horizontal and vertical movement is checked by measuring the corners of container 1 in between the experiments. The container corners are numbered in order to list the movement of each corner. This is shown in figure 3.3

Figure 3.3: The corners of the container are numbered in order to list the movement per corner. The results of the movement are shown in table 3.2 and 3.3. Corner 1 is the Northern corner, 2 is West, 3 is East and 4 is South.

The results of the movement of container 1 are shown in table 3.2, and the movement of the corners of container 2 is shown in 3.3. The GPS device that measured the x,y and z-position has an error of 1-3 cm. If a value of movement of a corner is within these margins, it is assumed that this corner did not move. When the x,y offsets of the corners are compared to the original measurement on Tuesday 11:41, it is notable that most offsets remain within the error margin of the GPS-device. Four exceptions are highlighted in red.

Table 3.2: Measurements of the corner movement of container 1 during the experiments. Numbers are in m and are relative to a corner measurement on Tuesday at 11:41. 1 is the Northern corner, 2 is West, 3 is East and 4 is South. Highlighted in red are movements of a corner that are larger than the error of measurement device (GPS)

	Wed 11:46			Thu 11:00		
Container 1	x	y	z	x	y	z
1	-0.051	0.015	0.007	0.007	-0.047	0.072
2	0.000	0.000	0.008	0.012	-0.040	0.032
3	0.008	-0.014	-0.003	-0.002	-0.014	-0.004
4	0.009	0.008	-0.008	-0.001	-0.018	-0.012

Table 3.3: Measurements of the corner movement of container 2 during the experiments. Numbers are in m and are relative to a corner measurement on Tuesday at 11:41. 1 is the Northern corner, 2 is West, 3 is East and 4 is South. No movements were larger than the error of the measurement device (GPS)

	Wed 11:46			Thu 11:00		
Container 2	x	y	z	x	y	z
1	-0.027	-0.005	0.012	0.030	0.013	-0.016
2	0.012	0.022	0.008	0.013	-0.005	-0.025
3	0.021	-0.012	0.008	-0.004	0.020	0.005
4	0.002	0.013	-0.006	-0.006	-0.013	-0.015

The four corner measurements that have a bigger offset than the error of the GPS-device are highlighted in red in table 3.2. These vary from 4-7 cm and will therefore be explained. 2 offsets were in x-direction, 1 in y-direction and 1 in z-direction. First, the bigger x-offset is discussed. The x-offset on Wednesday moved significantly. But, the x-offset on Thursday only moved 7mm compared to the measurement of Tuesday. This could mean that the container has moved back and forward by 5 cm. Looking at the movement of other corners, it is more likely that this particular x-offset is caused by a slightly bigger error of the GPS device.

Secondly, both the y-coordinates of corner 1 and 2 of container 1 on Thursday have moved 4-4.7 cm. It can be assumed that the front of container 1 has moved 4-4.7cm in y-direction during experiment 3. This is probably caused by heavy wave impact during experiment 3.

Finally, the z-coordinate of corner 1 of container 1 has sunken 7 cm. This was also visible in pictures taken from the front of the container. Looking at the z-offset of corner 1 and 2 on Thursday, it is notable that both corners moved downward 3-7 cm, causing a slope of the front of the container of 1:61. This slope is assumed to have no effect on the measurements inside the container. As this has no effect on the measurements, it is therefore assumed that the container did not move during the experiments.

3.2. Data analysis

In this section an evaluation of the results per experiment is discussed. Experiment 1 is about reviewing the wave propagation and the straightening of the waves inside the containers. This is evaluated in two different setups: experiment 1 setup 1 and experiment 1 setup 2. In experiment 2, 3 and 4, dunes are built inside the containers. Depending on the experiment, the height of the dunes will differ, as explained in section 2.4. These three experiments will be evaluated based on the wave characteristics, the eroded volume of the dunes, the dune toe evolution and the wet/dry slope change.

3.2.1. Experiment 1: setup 1

The first experiment on Monday is done to investigate if the straightness of the waves that are propagating inside the container. As explained in section 2.4, the first setup of the first experiment is a setup of 3 pressure sensors horizontally (longshore) aligned in the container. This is done to check if the incoming wave field is alongshore uniform and straight. If waves are not straight or alongshore uniform inside the container, the erosion processes could be influenced by an irregular wave pattern or by reflection of the walls. The reflection of the walls is discussed in chapter 4. No dunes are built in the containers yet.

To prove the quality of the visual analysis done in section 3.1.1, a wave by wave analysis is done, using a zero-down crossing method is performed. First, the raw pressure is converted to surface elevation taking also the dynamic wave pressure into account. This is done by taking the pressure time series of approximately 2.5 hours and dividing it into 5 blocks of 30 min. Then a fast Fourier transformation is done per block to get the Energy (E(p)) per wave frequency. The wavenumber (k) per frequency is determined just as a dynamic wave factor T. Finally the data is changed to surface elevation by using an inverted fast Fourier transformation. From this surface elevation data set, a spectral analysis is done to get the different wave heights shown in 3.4.

Table 3.4: Experiment 1 setup 1, wave characteristics in m for RBR1, 2, 3 and 4 during an interval of 30 min during high tide on Monday 21/9, 18:45:50-19:15:50.

Wave characteristic	RBR1	RBR2	RBR3	RBR4
H_m	0.24	0.15	0.14	0.19
H_{rms}	0.29	0.17	0.17	0.23
$H_{1/3}$	0.43	0.25	0.24	0.34

From table 3.4 it can be seen that the average wave height H_m decreases from outside of the container (RBR1) towards the inside (RBR2, RBR3, RBR4). This is concluded from the visual observation as well. Over a travelling distance of 3.04 m, the waves decrease about 0.1m in height. Similar results can be obtained by comparing the value of H_{rms}s of RBR1 to the values of RBR2, RBR3 and RBR4, which indicates that energy is dissipated while waves travel inside the container. Comparing the wave heights inside the container to each other, RBR4 shows much higher wave heights than RBR2 and RBR3. Especially the value of $H_{1/3}$ is remarkable since it is about 0.1 m higher at location 4 than at location 2 and 3. This means, that the high waves at location 4 must have been significantly higher compared to location 2 and 3 during the high water on Monday evening. Reflection of the sidewalls of the container is not noticeable with this setup, although some bouncing was visible during the experiments.

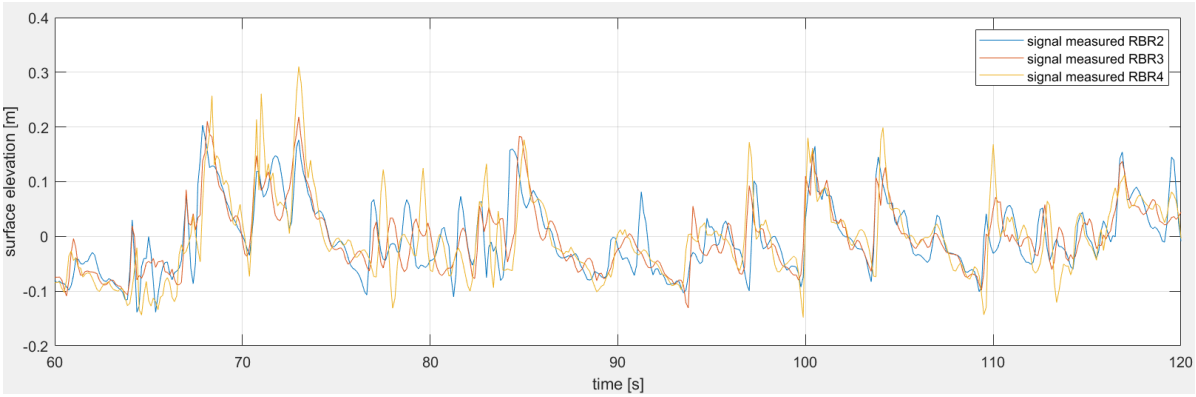

Figure 3.4: Sea surface elevation for RBR2, RBR3 and RBR4 for setup 1 during 60 seconds of high tide on Monday evening. The wave shape is similar at all three sensors.

When comparing the surface elevation of RBR2, 3 and 4, which are placed inside the container, the wave propagation is visible. This is shown in figure 3.4. When looking at the high wave at 73 seconds it can be seen that there is almost no difference in the time lag between the pressure sensor signals. This indicates that, with a correct calibration of the sensors, the waves are propagating in the main direction of the container, as they hit the sensors almost at the same time. This straightness of the waves is consistent with the analysis of your drone images.

3.2.2. Experiment 1: setup 2

In setup 2 an analysis of the propagation of the waves from outside to the inside of the container is done. This is important as the container entrance could have an influence on the waves. Disturbed waves could consequentially influence the erosion process inside the container. This setup has a different placement of the pressure sensors to make this evaluation. This setup is shown in figure 2.13b. The raw pressure time series is again transformed to surface elevation, taking the dynamic wave pressures into account. Then a wave-by-wave analysis is done to get the wave heights and the wave period shown in table 3.5.

Table 3.5: Experiment 1 setup 2, wave characteristics for RBR1, 2, 3 and 4 during an interval of 30 min during high tide on Tuesday 22/09, 06:58:20-07:28:30.

Wave characteristic	RBR1	RBR3	RBR2	RBR4
H_m	0.22	0.21	0.17	0.14
H_{rms}	0.27	0.27	0.20	0.17
$H_{1/3}$	0.40	0.39	0.29	0.24
T_m	3.26	2.93	2.74	2.58
N	275	306	328	347

The mean wave height decreases as the waves progress from further onshore from RBR1 to RBR3 to RBR2 to RBR4, as shown in table 3.5. The number of waves N observed with a zero-down crossing is smallest outside the container at RBR1 and then increases continuously further inside the container (N is largest at RBR4). This results in a highest mean period Tm outside the container and a smallest mean period T_m furthest inside the container. As the wave height does not decrease heavily when the waves progress over the edge of the container, the influence of the edge of the container on the decrease of the waves is neglected.

To get a better impression of a single wave progression inside the container, a randomly picked 60 sec out of the 305 min interval is taken and evaluated, as shown figure 3.5. It can be seen that waves become steeper at the front and flatter and longer in the through when they are travelling inside the container. The incoming wave crests can be followed clearly when travelling from one sensor to another. This is made visible with coloured dots in figure 3.5.

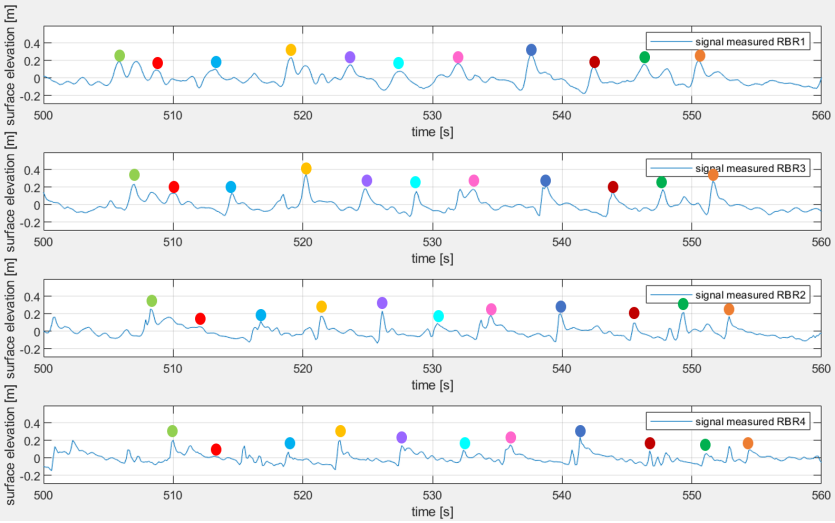

Figure 3.5: Sea surface elevation for RBR1, RBR2, RBR3 and RBR4 for setup 2 during 60 seconds of high tide on Tuesday 22/09, 07:06:40-07:07:40. The points in different colours follow the wave crest travelling past RBR1, RBR3, RBR3 and RBR4 (one colour per wave crest).

3.2.3. Experiment 2

Experiments 2, 3 and 4 contain the dune erosion tests and are evaluated based on the difference in waves characteristics, erosion volume, dune toe evolution and wet/dry slope development in both containers. At the end of the explanation of each experiment and its result, an overview table is given to summarize the results per experiment, see table 3.7. Experiment 2 contains two of the same reference dunes (1.3m in height) in both containers, as explained in section 2.4. This experiment is done to see if the two containers function the same.

Wave characteristics

The second experiment is an evaluation of the differences in erosion between the two containers to test consistency. This experiment takes place from 18:08-20:06. The wave characteristics are determined and shown in table 3.6. The pressure sensors are placed in setup 3 as shown in figure 2.14. This means that all four sensors are placed outside the containers. RBR1, 2 and 3 are placed in front of container 1 and RBR4 is placed in front of container 2. Also, the offshore wave height in the Maasgeul Maasvlakte Noord, measured by a buoy of Rijkswaterstaat, is mentioned. This is the significant wave height in the spectral domain of the surface water wave frequency between 30 and 500 MHz. This should therefore be compared to the $H_{1/3}$ of the most offshore pressure sensor, RBR3. All wave heights are in meters.

Table 3.6: Experiment 2, wave characteristics in m for RBR1, 2, 3 and 4 for setup 3.

Wave characteristics	RBR1	RBR2	RBR3	RBR4
H_m	0.218	0.150	0.143	0.185
H_{rms}	0.257	0.173	0.164	0.216
$H_{1/3}$	0.372	0.245	0.231	0.313
$H_{maasgeul}$			0.260	

RBR1 and RBR4 are both placed 1 m from the entrance of the containers. Therefore they should have similar wave conditions values. From table 3.6 it can be seen that there is a difference of 0.03 m in H_m when comparing these two sensors. A cause of these could be changing beach bathymetry around the containers causing waves to reduce in height earlier around container 2 (RBR4).

Erosion volume

If the two dunes of 1.3 m height in experiment 2 erode equally, the erosion process is assumed to be the same for container 1 as for container 2. For the evaluation of the expected eroded volumes of the dunes, the raw GPS data is processed. The raw data of the GPS, as shown in figure C.3 in Appendix C, contains (x,y,z) coordinates in the form of transects. One movement of the GPS pole from the back of the dune to the front of the dune where the GPS measures a coordinate every second is being referred to as a transect. The amount of transects per experiment depends on the GPS system that is used and the length of the experiment. This can vary from 20 to 120 transects. In figure 3.6 all transects made during experiment 2 in container 1 and container 2 are combined in order to see the dune evolution over time.

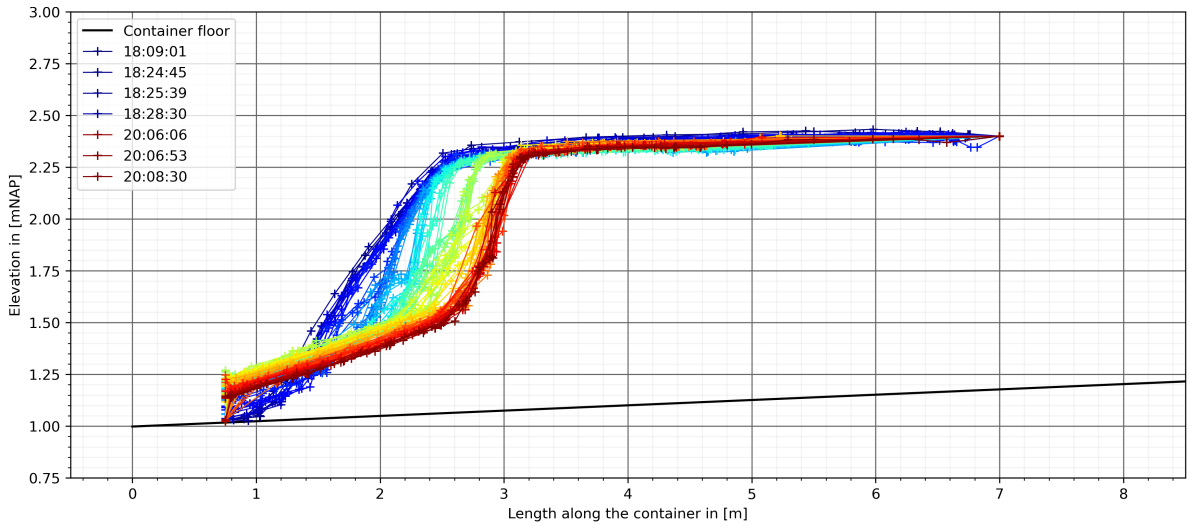

(a) Overview of the transects taken by GPS system 1 in container 1, during experiment 2 on Tuesday

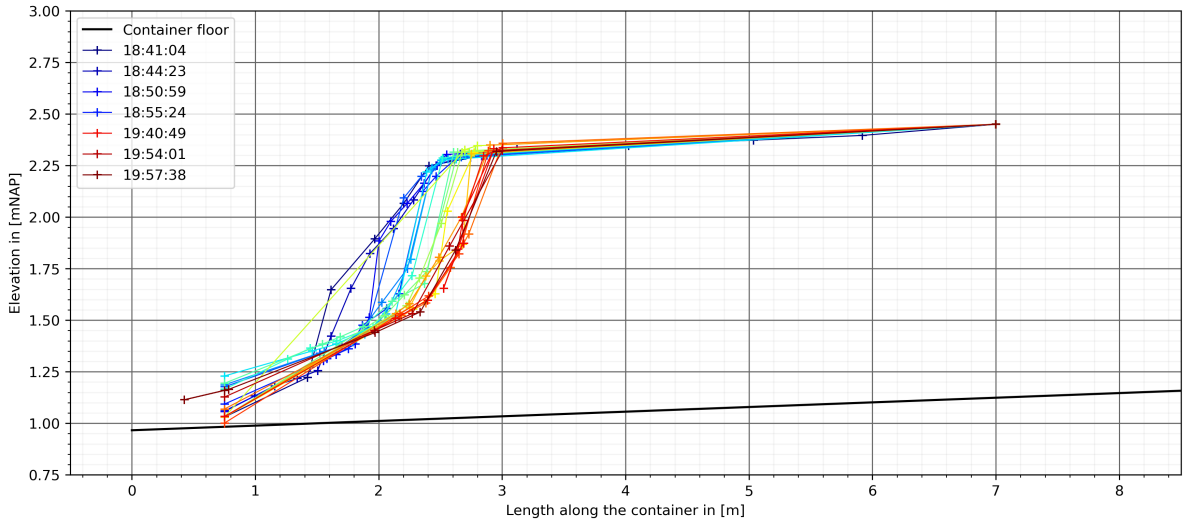

(b) Overview of the transects taken by GPS system 2 in container 2, during experiment 2 on Tuesday

Figure 3.6: Overview of the extended transects per experiment per container. Container 1 (with cart) on the left and container 2 (without cart) on the right. In every figure the transects, taken with the GPS pole, are shown in colour. The colour varies from blue at the start of the measurement to red at the end of the measurement. The container floor is shown in black.

For the comparison of the expected erosion volume and the expected erosion speed, all transect must have the same length to investigate the amount of erosion per transect. During the experiment, it was not possible to measure every transect from the same starting point to the same endpoint. Therefore, transects that do not reach the starting and endpoint are extended to those points, using linear extrapolation. These transect boundaries vary per experiment and per container. An overview of the boundaries can be found in table D.1 in appendix D.

Figure 3.6a shows the transects measured in container 1 during experiment 2 and figure 3.6b shows the transects of experiment 2 in container 2. In these figures every transect is shown in a different colour varying from dark blue to red. Transects with blue colour are taken at the start of the experiment. The red colour represents the end of the experiment. In container 1, 95 transects were taken with the GPS cart (system 1, as discussed in section 2.3.1). All of these 95 transects had to be extended to the toe of the dune and towards the end of the dune, at 7 meters. This is done because the transects did not have the same length and could therefore not subtracted to calculate the volume. In container 2 only 21 were taken and all of them had to be extended to the toe and to the end of the dune, at 7 meters. The transect boundaries can be found in table D.1.

When comparing these two graphs it has to be taken into account that there are significantly fewer transects taken in container 2 due to the use of a different GPS system. In figure 3.7 it can be seen that chunks of sand have fallen from the crest of the dune from one transect measurement to the other. This indicates that the avalanching process is happening inside the container.

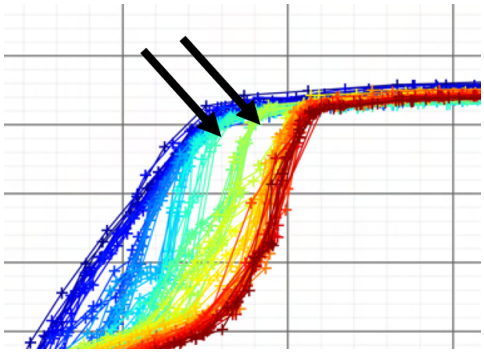

Figure 3.7: Zoom of the transects of experiment 2 container 1. The black arrows indicate where the avalanching process is visible.

Based on the amount of eroded volume, an indication of the similarity between the containers can be made. The cumulative eroded volume is calculated in the following way:

$$C(i) = -(V(i) - V(0)) \tag{3.1}$$

where:

- C(i) = the cumulative eroded volume at transect i
- V(i) = The volume of transect i, which is calculated by taking the trapezoidal rule of a transect i from end to start.
- V(0) = The volume of the first transect

The cumulative eroded volume is calculated per transect and figure 3.8a shows an overview of the cumulative eroded volume over time. The black crosses indicate the $C(i)$ per transect of container 1. The inside width of the container, and therefore the width of the dune is 2.35 m. This width is excluded from figure 3.8a. The actual amount of erosion of container 1 is therefore $2.35[m] * 1.034[m^2] = 2.43[m^3]$. The amount of erosion in container 2 is $2.35[m] * 0.475[m^2] = 1.12[m^3]$, which is a little more than half of the eroded volume from container 1. It has to be taken into account that the measurements in container 2 were started 32 minutes later due to some technical problems. Also, the measurement was stopped 11 minutes earlier, making the experiment in total 43 minutes shorter. This was also the first time that the GPS systems were put in use. Therefore a better indication of the similarity of the two measurements is the erosion speed.

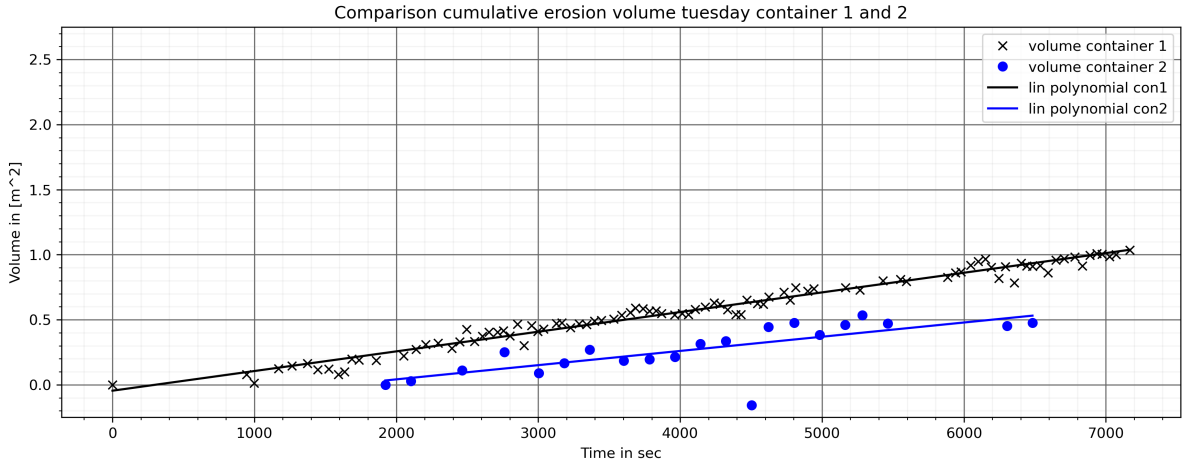

(a) Cumulative erosion $C(i)$ in $[\frac{m^3}{ms}]$. In black the $C(i)$ in container 1 and in blue the $C(i)$ in container 2.

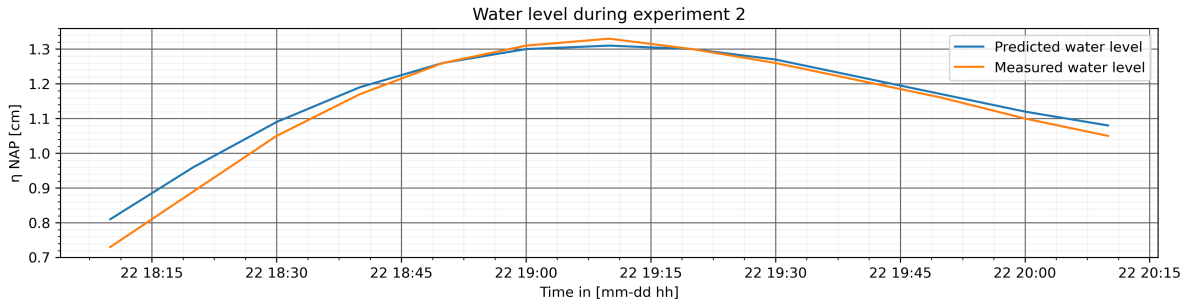

(b) Water level in Hoek van Holland (13min phase difference compared to the Sand Engine) during experiment 2.

Figure 3.8: Overview of cumulative eroded volume increase $C(i)$ for experiment 2 per container.

When looking at the speed of erosion, the slope of the black and blue (best) linear fits from figure 3.8a are determined. The formula of the polynomial of container 1 determines the slope of the line and therefore the speed of erosion of container 1 is $1.511 \cdot 10^{-4}[\frac{m^3}{ms}]$. The slope and therefore the speed of erosion of container 2 is $1.096 \cdot 10^{-4}[\frac{m^3}{ms}]$.

In figure 3.8b the predicted and measured water level at Hoek van Holland is shown. This graph is shown to see if the changing water level has an influence on the erosion volume change. The time on the x-axis of this graph corresponds to the timestamps of figure 3.8a. It is worth noting that the erosion speed does not change when the tide is falling. This could be due to the fact that the water level change is smaller and therefore insignificant compared to the wave impact, causing erosion.

Dune toe evolution

According to Larson et al. (2004, 2016), the dune toe is expected to follow the mean water level. As the mean water level varies during the experiment due to the moving tide, the toe should move up with the upcoming tide and then stay at the same height when the tide is falling. This should therefore be visible during the experiment. As the dune toe movement is independent of the height of the dune, the theory that the dune toe should follow the mean water level should be valid for all experiments.

The dune toe and crest are calculated by taking the minimum and maximum value of the second derivative of the transects. This is done for every transect per container and gives the x and y-values of two inflexion points. These inflexion points represent the dune toe and the dune crest. Therefore, a plot per experiment per container is made where the toe of the extended transects is plotted in figure 3.9.

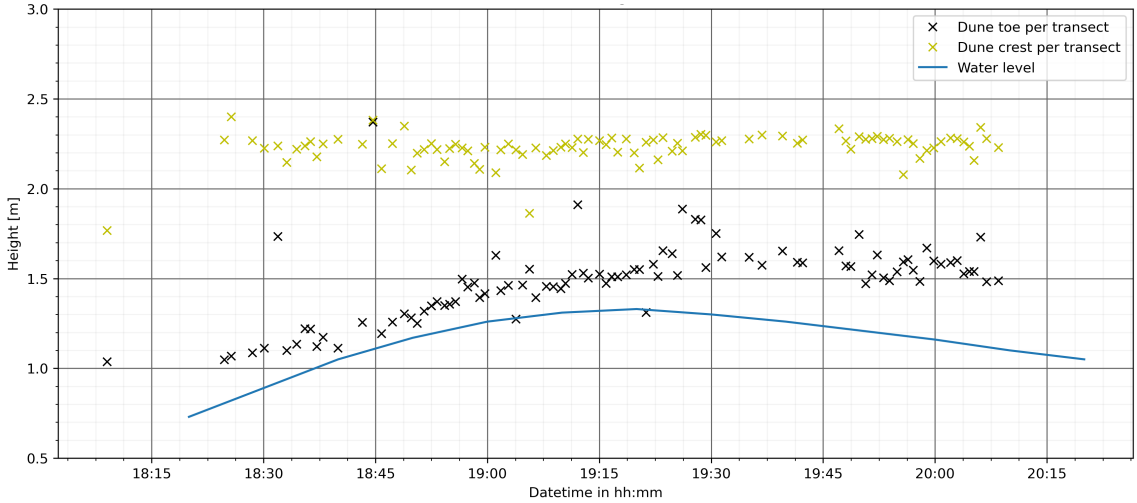

(a) Dune crest and dune toe height evolution Tuesday with cart in Container 1 during experiment 2.

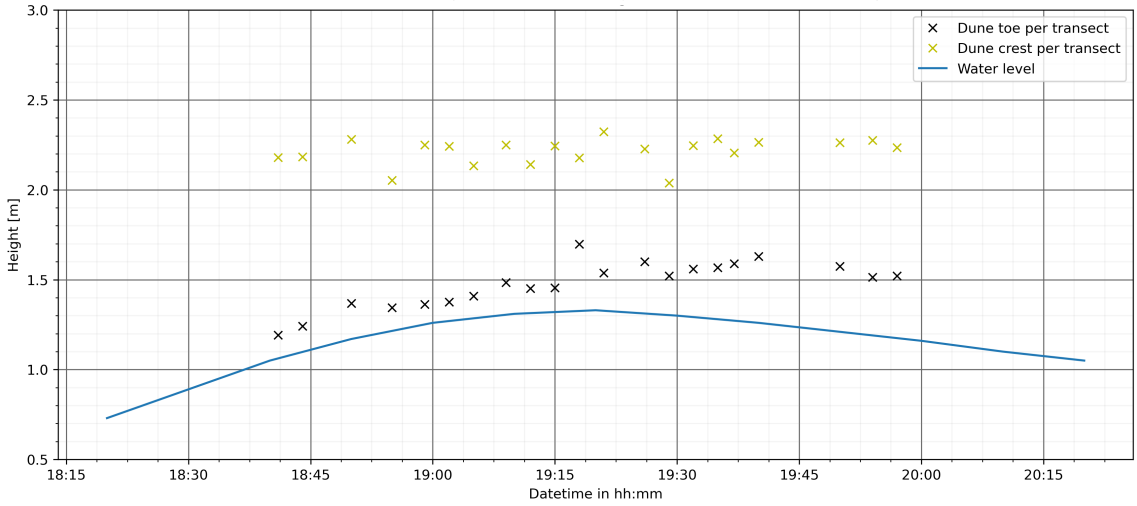

(b) Dune crest and dune toe height evolution Tuesday no cart in Container 1 during experiment 2.

Figure 3.9: Overview of vertical dune toe movement over time, per experiment per container.

In figure 3.9, the black crosses represent the dune toe elevation per transect in time. The yellow crosses represent the dune crest evolution per transect in time. In blue the measured water level in Hoek van Holland is shown. A 10 min phase difference is applied to make the water level of Hoek van Holland representable for the Sand Engine.

In container 1, the dune crest stays relatively the same at 2.3 m during the whole experiment. The dune toe, on the other hand, increases while the water level rises as well. The dune toe stays at this height when the water level falls again. The values of the rise of the toe and the rise of the water level are shown in 3.7 and are taken at the start of the dune toe rise at 18:24 and at the water level maximum, to understand the difference in height during the rising period. The total increase of height of the dune toe is 0.55 and the total increase of the water level is 0.52. The difference between these numbers is 0.03, meaning that the dune toe had almost the same rise in height as the water level and therefore follows the water level, which is what is expected according to the theory.

In container 2, the dune crest also stays relatively the same at 2.3 m. Starting at 18:41, the dune toe rises with the rise of the water level. When the tide falls the dune toe stays at the same level. This means that the total increase of height of the dune toe is 0.35 and the total increase of the water level is 0.28. The difference between these numbers is 0.07 meaning that just as in container 1 the dune toe had almost the same rise in height as the water level and therefore follows the water level, which

is what is expected according to the theory.

Wet and dry slope evolution

The dunes in the container consist of three types of 'slopes'. The first 'slope' is the foredune (beach) which is a wet slope and start in front of the container and ends at the dune toe. From the dune toe to the dune crest, the semi-dry dune face is present. This is considered to be the second 'slope'. The third one is the slope of the dune crest, which starts at the crest and goes to the end of the dune. The slopes that are considered in this section are shown in figure 3.10.

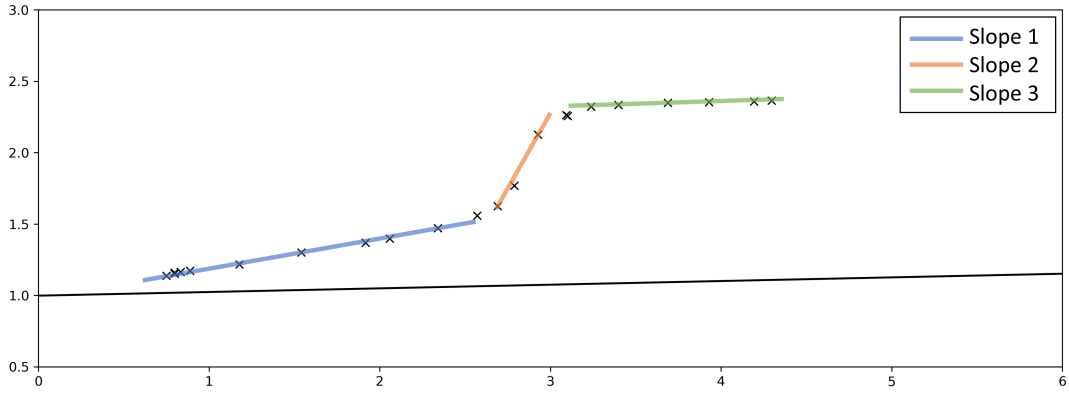

Figure 3.10: 1 transect with an indication of the three defined slopes. The blue slope of the foredune is slope 1, the slope of the dune face is slope 2 and the slope of the dune crest is slope 3.

During the experiment, the avalanching process causes volumes of sand to be replaced from the dune face to the foreshore. This causes the dune face to steepen and the foreshore to increase in length. One might think that the foreshore would also increase in steepness but due to the return current, sand gets diverted away from the foredune into the sea. As the water level is changing in this experiment the dune toe is rising with the water level, however, the angle of the wet slope should stay the same. This is evaluated in figure 3.11.

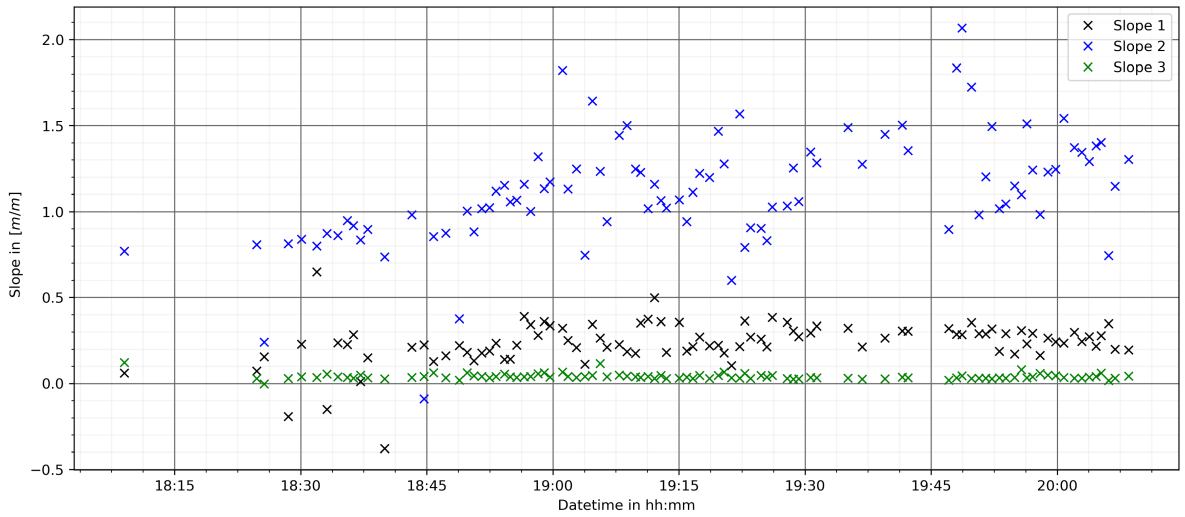

(a) Dune slope evolution of container 1 experiment 2 on Tuesday.

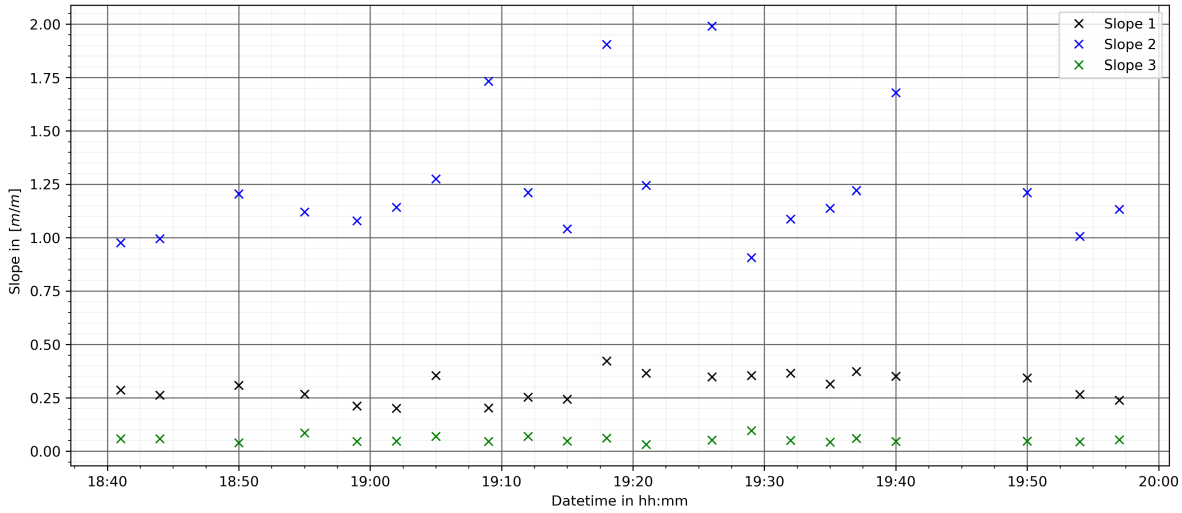

(b) Dune slope evolution of container 2 experiment 2 on Tuesday.

Figure 3.11: Slope evolution in time of all transect during experiment 2. Slope 1 is the wet foreshore, slope 2 is the semi-dry dune face and slope 3 is the dry dune crest. Slope 1 and 3 (respectively the foreshore and the crest) remain very stable throughout the experiment. The dune face is increasing in steepness due to scarp formation.

In figure 3.11a the slopes of experiment 2 in container 1 are shown. There is a similarity between the dune face slopes in the two containers. The foredunes and the dune crests stay relatively the same, while the dune face increases slightly due to crest forming.

In container 1, the foredune (slope 1) remains around 0.237, which is 1:4.22. The dune face (slope 2) increases slightly from 0.8 to 1.35 indicating a steepening slope from 1:1.25 to 1:0.74. The dune crest (slope 3) remains the same around 0.040 which is 1:25. In container 2, the foredune (slope 1) remains around 0.30, which is 1:3.32. The dune face (slope 2) increases slightly from 1 to 1.25 indicating a steepening slope from 1:1 to 1:0.8. This is however hard to determine with the limited amount of data available. Arguably it could be said as well that the slope stays roughly the same with a mean of 1.25 which is a steepness of 1:0.8. The dune crest (slope 3) remains the same around 0.054 which is 1:18.

A small summary of the results of experiment 2 is shown in table 3.7. Here the results per parameter for each container are shown. In the third column, the difference in percentage between the two containers is shown, with container 1 as a reference. In the last column, an indication of similarity is done.

Table 3.7: Experiment 2: Comparison of the results of container 1 and container 2.

Parameter	Container 1	Container 2	Difference Con 1 vs Con 2	Conclusion
H_m, rbr1, 4 in [m]	0.218	0.185	-15.2%	Similar
$H_{maasgeul}$ in [m]	0.257	0.257		
Wind direction in °	211.3	211.3		
Wind speed in $[\frac{m}{s}]$	2.41	2.41		
Erosion volume in $[\frac{m^3}{m}]$	1.034	0.475	-54.1 %	Different
Erosion speed in $[\frac{m^3}{ms}]$	$1.5 \cdot 10^{-4}$	$1.1 \cdot 10^{-}4$	-26.7 %	Similar
Rise dune toe [m]	0.55	0.35		
Rise water level [m]	0.52	0.28		
Difference rise water level and rise of the dune toe in [m]	0.03	0.07		Similar
Foredune slope	1:4.22	1:3.32		
Dune face slope	1:1.25 to 1:0.74	1:1 to 1:0.8		

3.2.4. Experiment 3

Experiment 3 is a dune erosion test where container 1 contained a low dune of 1 m in height and container 2 contained a reference dune of 1.3 m. This experiment is done to see the difference in erosion speed between these two dunes. As the wave climate is the same for the two containers, this experiment could represent an example of the kind of experiments that can be done inside the containers. It has to be noted that during the experiment in container 1 the cart had some technical malfunctioning. The GPS pole broke due to enthusiastic pulling of the cart. This resulted in a halt in the measurements around 4000 sec after the start of the measurement as is visible in figure 3.13a. After the incident the cart could not be repaired so measurements were carried out by foot, resulting in larger measurement errors.

Wave characteristics

The wave characteristics for experiment 3 are shown in table 3.8. These numbers are obtained by the measurements of the RBR's in setup 3. This setup was the same in experiment 2. The wave conditions are higher in this experiment compared to the previous experiment.

Table 3.8: Experiment 3, wave characteristics in m for RBR1, 2, 3 and 4 for setup 3.

Wave characteristics	RBR1	RBR2	RBR3	RBR4
H_m	0.2306	0.3998	0.4123	0.2571
H_{rms}	0.2787	0.4392	0.4533	0.3015
$H_{1/3}$	0.4144	0.6019	0.6221	0.4287
$H_{maasgeul}$			0.625	

Erosion Volume

The transects that were made inside the containers with the two systems are shown in figure 3.12. In these figures it is visible that in container 1 (figure 3.12a) the dune was 1 m in height and in container 2 (figure 3.12b) the dune was 1.3 m in height. Again system 2 with the pole performed much fewer transects than system 1 with the car, respectively 44 transects taken in container 2 compared to 82 transects in container 1. 82 of the 82 transects of container 1 were extended to the toe. And 59 of 82 transects were extended to value= 7. In container 2, all transect were extended to the toe and all transects were extended to value= 7.

In container 1 the dune is eroded much further than in container 2. It even reached a new collision phase, overwash. This had to do with the increased wave height (due to increased wind speeds compared to experiment 2) and also with the low dune height. In container 2 this overwash regime was not reached, mainly due to the fact that the dune was 0.3 m higher. As this thesis is about the comparison of dune erosion in the collision regime the eroded volume is calculated by taking the area under the transects up until 7m, not taking the overwash into account.

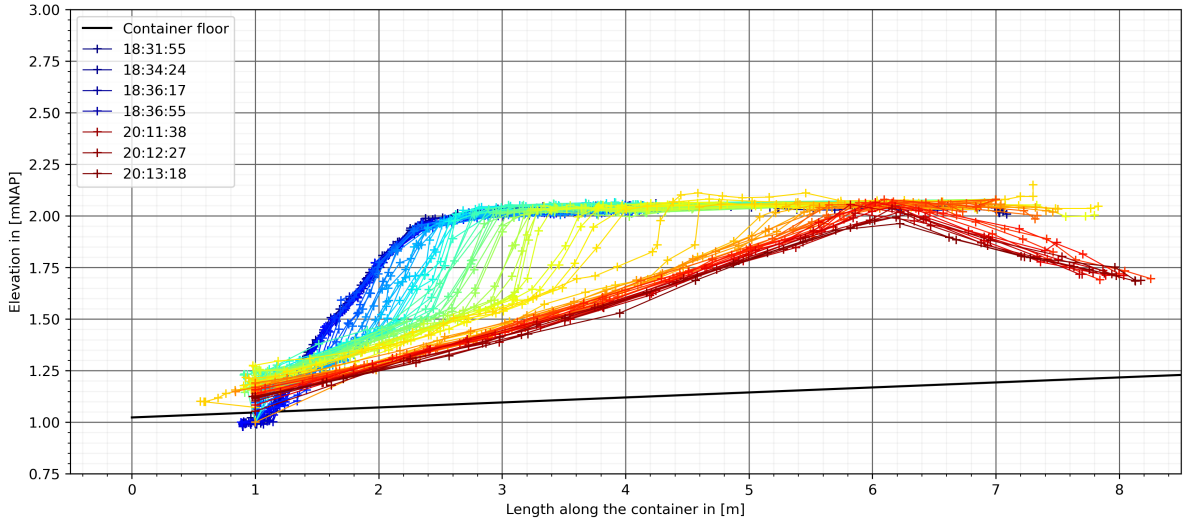

(a) Overview of the transects taken by GPS system 1 in container 1, during experiment 3 on Wednesday

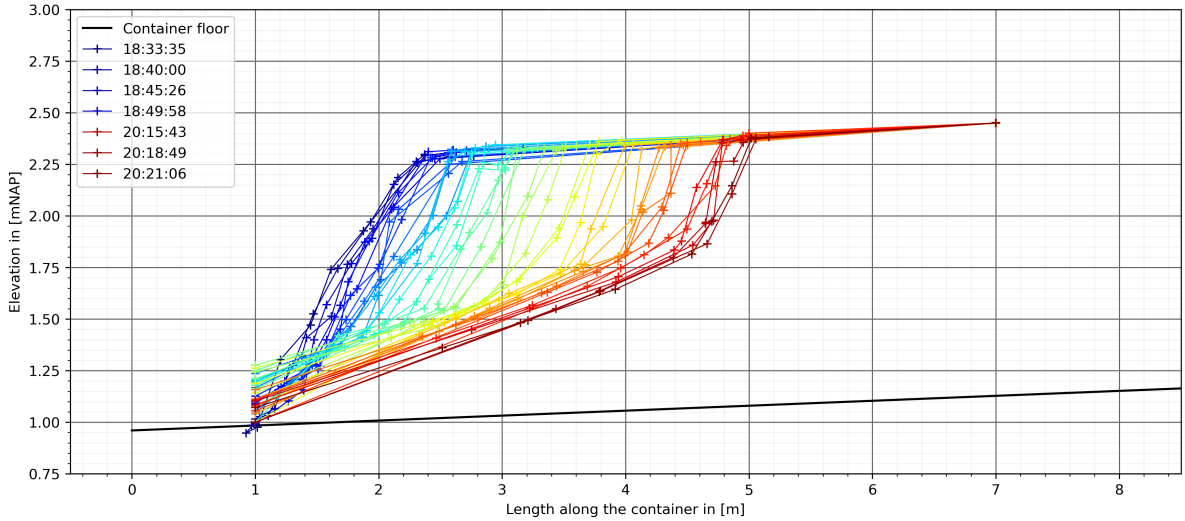

(b) Overview of the transects taken by GPS system 2 in container 2, during experiment 3 on Wednesday

Figure 3.12: Overview of the extended transects per experiment per container. Container 1 (with cart) on the left and container 2 (without cart) on the right. In every figure the transects, taken with the GPS pole, are shown in colour. The colour varies from blue at the start of the measurement to red at the end of the measurement. The container floor is shown in black.

Again, there are significantly fewer transects taken in container 2 due to the two different GPS systems that were used. However based on the retreat of the dune front, thus the amount of eroded volume, an indication of the difference between the containers can be made. In figure 3.13 an overview of the cumulative eroded volume over time is shown. The inside width of the container, and therefore the width of the dune is 2.35 m. This width is excluded from figure 3.13. The actual amount of erosion of container 1 is therefore $2.35[m] * 1.60[m^2] = 3.77[m^3]$. The amount of erosion in container 2 is $2.35[m] * 2.53[m^2] = 5.94[m^3]$, which is significantly less than the eroded volume in container 1. The measurements in container 2 were started 2 minutes later and stopped 8 minutes later, making the experiment in total 10 minutes longer, this is visible from the legend of figure 3.12.

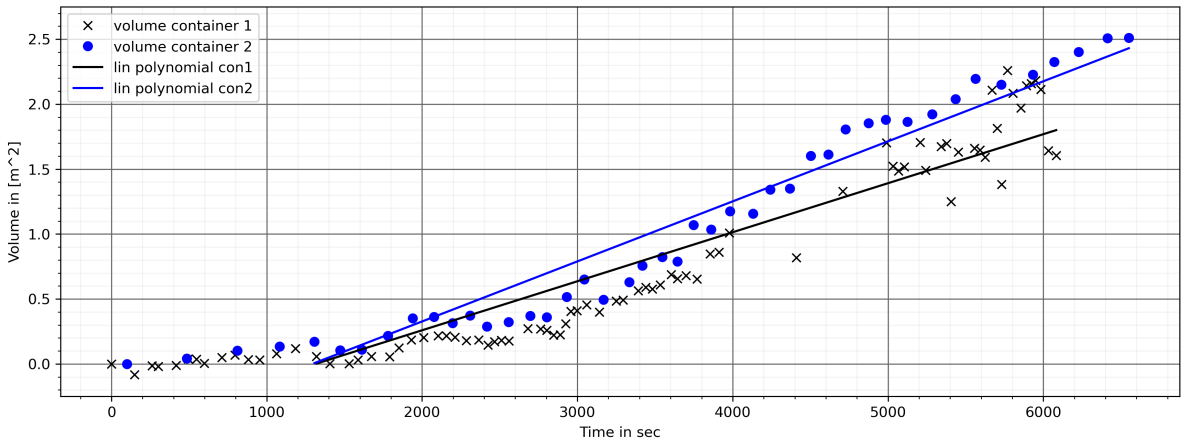

(a) Cumulative erosion volume of experiment 3 in $[\frac{m^3}{ms}]$. In black the eroded volume in container 1 and in blue the eroded volume in container 2. The pole of system 1 in container 1 broke around 4000 sec.

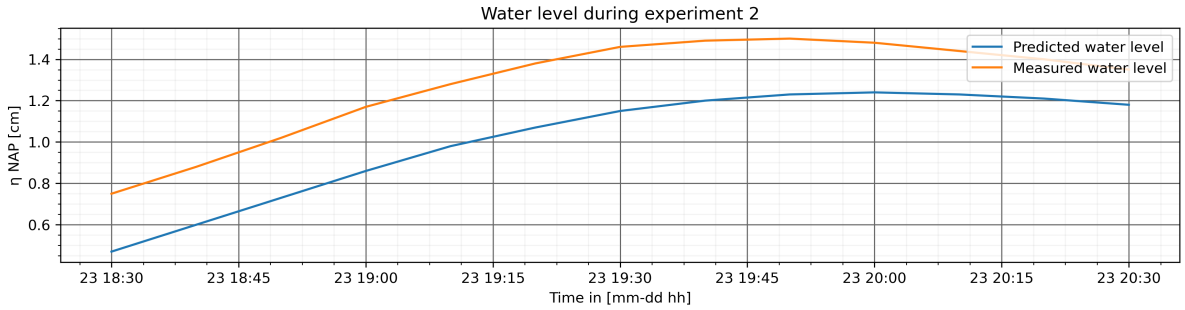

(b) Water level in Hoek van Holland (13min phase difference compared to the Sand Engine) during experiment 3.

Figure 3.13: During the first 4000 sec of experiment 3 the eroded volume increased exponentially due to a rising water level. When the water level is lowering the eroded volume increased linearly.

When looking at the speed of erosion, the slope of the blue linear fit from figure 3.13a is determined. The slope of the fit and therefore the speed of erosion of container 1 is $3.774 \cdot 10^{-4}[\frac{m^3}{ms}]$. The slope and therefore the speed of erosion of container 2 is $4.675 \cdot 10^{-4}[\frac{m^3}{ms}]$.

In figure 3.13a it is visible that in container 1, between 4000 and 5000 seconds there was no transect taken due to technical issues. Between 5000 and 6000 seconds, the measurements have an increased variability (bigger error). This is due to the fact that the measurements could not be resumed with the more precise cart of GPS system 1 but had to be resumed by foot.

Although a linear fit is plotted through the cumulative erosion plot, the data looks not linear. From 2000 sec the erosion is increasing more rapidly per transect. The tide is increasing, reaching a maximum and then decreasing again. During the time that the tide is max, the water level is at its highest point, causing more collision impact of waves at the dune face. This increases the amount of erosion. The maximum tidal elevation is reached at 19:40 at Hoek van Holland according to measurements of RWS. Assuming that the maximum tide reaches the Sand Engine 13 minutes later the high tide at the sand engine was at 19:53 (timestamp = +/-5040 sec) and was 1.5 m.

Dune toe evolution

Figure 3.14 shows the dune toe and dune crest evolution in both containers, to see if the dune toe follows the rising water level. The black crosses represent the dune toe elevation per transect in time. The yellow crosses represent the dune crest evolution per transect in time. In blue, the measured water level in Hoek van Holland is shown. A 10 min phase differences is applied to make the water level of Hoek van Holland representable for the Sand Engine.

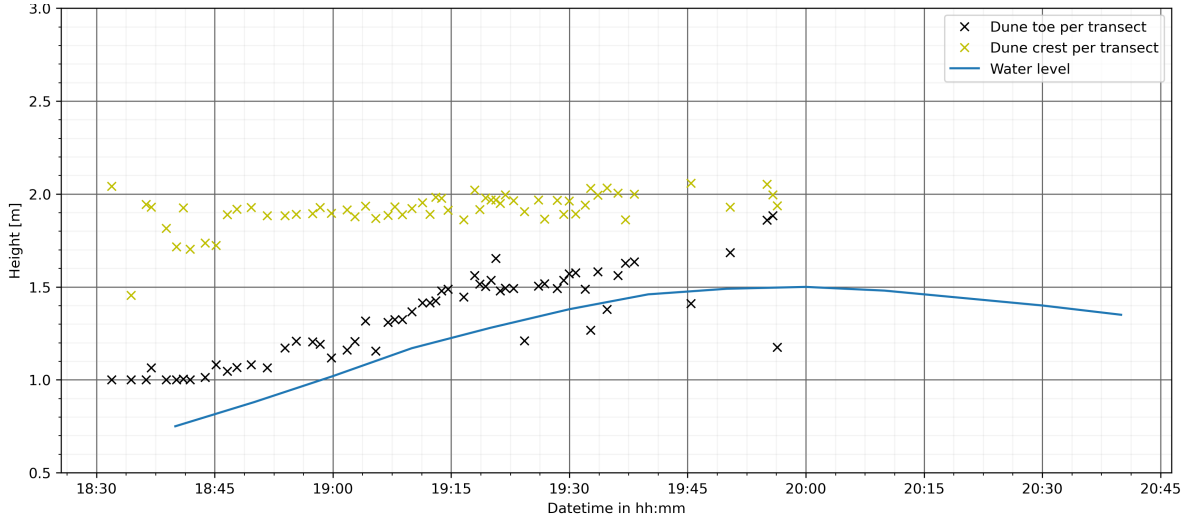

(a) Dune crest and dune toe height evolution Wednesday with cart in container 1 during experiment 3.

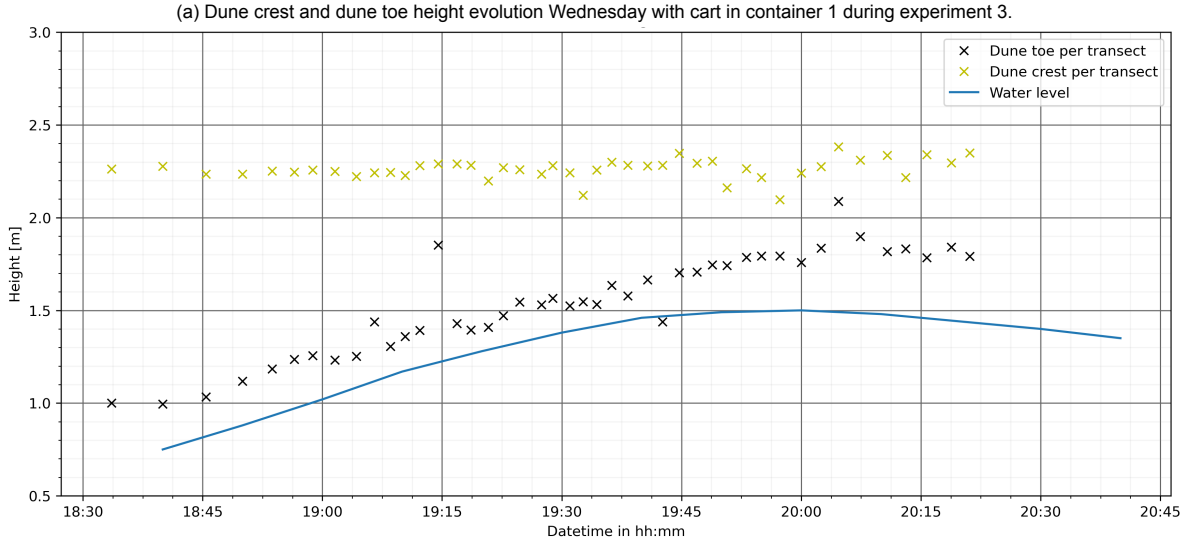

(b) Dune crest and dune toe height evolution Wednesday no cart in container 2 during experiment 3.

Figure 3.14: Vertical dune toe movement over time, for experiment 3 per container. In yellow the dune crest movement per transect, in black the dune toe per transect.

The dune toe and crest are calculated in the same way as was discussed in experiment 2. In container 1, the dune crest stays relatively the same at 1.95 m during the whole experiment. The dune toe on the other hand increases from 1.0 to approximately 1.9 m while the water level rises from 0.75 to 1.5 m, and it stays at this height when the water level falls again. These values are taken at the start of the dune toe rise at 18:40 and at the water level maximum, to understand the difference in height during the rising period. The total increase of height of the dune toe is 0.9 and the total increase of the water level is 0.75. The difference between these numbers is 0.15, which is slightly higher than previously measured differences but still the assumption that the dune toe follows the water level is valid. This difference might be due to a difference in runup due to rougher wave conditions. It has to be noted that the pole broke just as the overwash regime is reached. The comparison of the dune toe with the water level is only valid for the collision phase as there is no dune toe anymore in the overwash phase. Therefore the timeline in container 1 is stopped when the overwash phase is reached and the dune toe becomes the same height as the crest around 19:55. This is only the case in container 1.

In container 2, the dune crest also stays relatively the same at 2.3 m. Starting at 18:45, the dune toe rises from 1.05 m to 1.8 m, while the water level increased from 0.815 m to 1.5 m. These values are taken at the start of the dune toe rising and at the water level maximum, to only understand the

difference in height during the rising period. When the tide falls the dune toe stays at the same level. This means that the total increase of height of the dune toe is 0.75 and the total increase of the water level is 0.685. The difference between these numbers is 0.065 and that means that just as in container 1 the dune toe had almost the same rise in height as the water level and therefore follows the water level.

Wet and dry slope evolution

The wet and dry slope evolution of the dunes of experiment 3 are shown in figure 3.15 and represent the 'wet' foredune (slope 1), the 'dry' dune face (slope 2) and the slope of the dune crest (slope 3), as shown in figure 3.10.

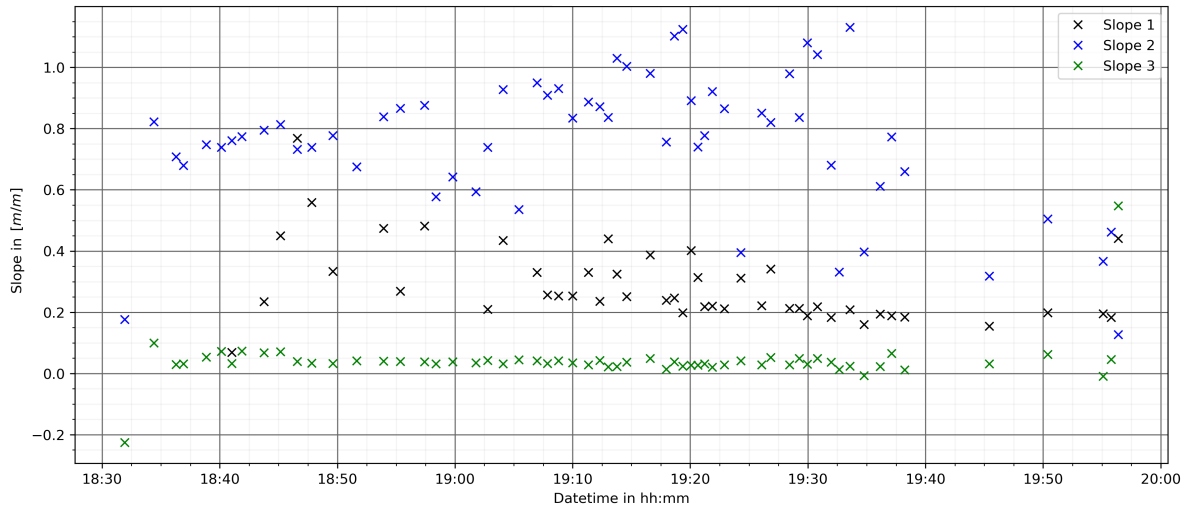

(a) Dune slope evolution of container 1 experiment 3 on Tuesday.

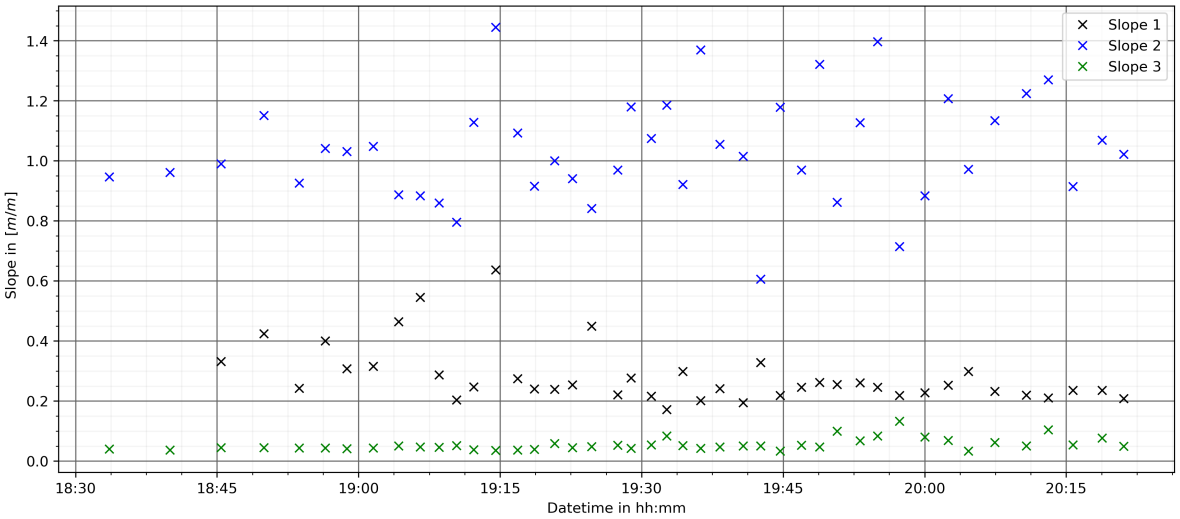

(b) Dune slope evolution of container 2 experiment 3 on Tuesday.

Figure 3.15: Slope evolution in time of all transect during experiment 3. Slope 1 is the wet foreshore, slope 2 is the dry dune face and slope 3 is the dry dune crest. Slope 1 and 3 (respectively the foreshore and the crest) remain very stable throughout the experiment. The dune face is increasing in steepness due to scarp formation.

As the pole of system 1 broke around 19:40 the slopes in figure 3.15a are difficult to define and there not very accurate. In container 1 the black crosses represent slope 1, which is the foredune. This slope decreases a little bit but stays roughly the same at around 0.285 which is 1:3.51. The blue crosses, which represent the dune face are slightly increasing from 0.8 to 1 during the collision phase indicating a steepening slope from 1:1.25 to 1:1. During the overwash phase, this sharply reduces. The slope of the dune crest stays the same during the whole experiment, until the overwash regime, at 0.041, which

is 1:24, which the roughly the same as the slope of the beach and the slope of the container.

In container 2 the slopes behave similar to container 1. Slope 1, the foredune decreases slightly but stays roughly the same at 0.25 which is 1:4. Slope 2, the dune face is slightly increasing from 0.95 to 1.2 indicating a steepening slope from 1:1.05 to 1:0.83, which indicates the forming of a scarp. Slope 3, the crest stays the same at 0.035, which is the same as the angle of the container, and the slope of the beach.

The results of experiment 3 are shown in table 3.9. Here the difference between the two containers, and therefore between the 1 m high dune of container 1 and the 1.3 m high dune of container 2 is shown. In the third column, the difference in percentage between the two containers is shown, with container 1 as a reference. In the last column, an indication of similarity is done.

Table 3.9: Experiment 3: Comparison of the results of container 1 and container 2.

Parameter	Container 1	Container 2	Difference Con 1 vs Con 2	Conclusion
H_m, rbr1, 4 in [m]	0.231	0.257	+11.5%	Similar
$H_{maasgeul}$ in [m]	0.652	0.652		
Wind direction in °	175.3	175.3		
Wind speed in [m/s]	6.46	6.46		
Erosion volume in [$\frac{m^3}{m}$]	5.94	3.77	-57.6 %	Different
Erosion speed in [$\frac{m^3}{ms}$]	$3.77 \cdot 10^{-4}$	$4.68 \cdot 10^{-4}$	+19.4 %	Similar
Rise dune toe in [m]	0.9	0.75		
Rise water level in [m]	0.75	0.685		
Difference rise water level and rise dune toe in [m]	0.15	0.06		Similar
Foredune slope in [m/m]	1:3.51	1:4.00		
Dune face slope in [m/m]	1:1.25 to 1:1	1:1.05 to 1:0.83		

3.2.5. Experiment 4

The fourth experiment is done to review the difference between the erosion speeds of a higher dune of 1.6m. This experiment is carried out the same way as experiment 2 and 3. But during the experiment, the wind was at 6 BF causing very big waves. The difference between the two containers, and therefore the two dunes is evaluated by looking at the difference in erosion volume, erosion speed and dune toe evolution.

Wave characteristics

The wave characteristics are shown in table 3.10. The pressure sensors were still in setup 3, where RBR3 is the most offshore sensor and RBR1 and RBR4 are placed 1 m in front of the container. Looking at the most offshore sensor, RBR3, it can be seen that waves were much higher offshore than in previous experiments due to high wind speeds. However, wave therefore break earlier and reach the container with relative low wave energy as can be seen from RBR1 and RBR4. Interesting RBR 1 and 4 register similar wave heights to experiment 2 and 3.

Table 3.10: Experiment 4: Wave characteristics in [m] for RBR1, 2, 3 and 4 for setup 3.

Wave characteristics	RBR1	RBR2	RBR3	RBR4
H_m	0.1959	0.484	0.8273	0.1987
H_{rms}	0.2325	0.571	0.9316	0.2413
$H_{1/3}$	0.3439	0.8198	1.3067	0.3581
$H_{maasgeul}$			1.38	

Erosion volume

The results of the transects taking by the two GPS systems in the containers are shown in figure 3.16. From these figures the difference in dune height is clearly visible. 1.6 m in container 1, figure 3.16a, and 1.3 m in container 2, figure 3.16b. System 2 performed fewer transects than system 1, but the amount due to increased experience of the students who helped out with taking the measurements, the measurements could be taken faster and therefore more transect were taken during experiment 4. In total 118 transects were taken in container 1 and all of them were extended to the toe. Also, almost all of them were extended to 7 m. In container 2 more than 70 transects were taken but only 42 could be used for evaluation. All transect were extended at the bottom to the toe and they were extended at the top to 7m.

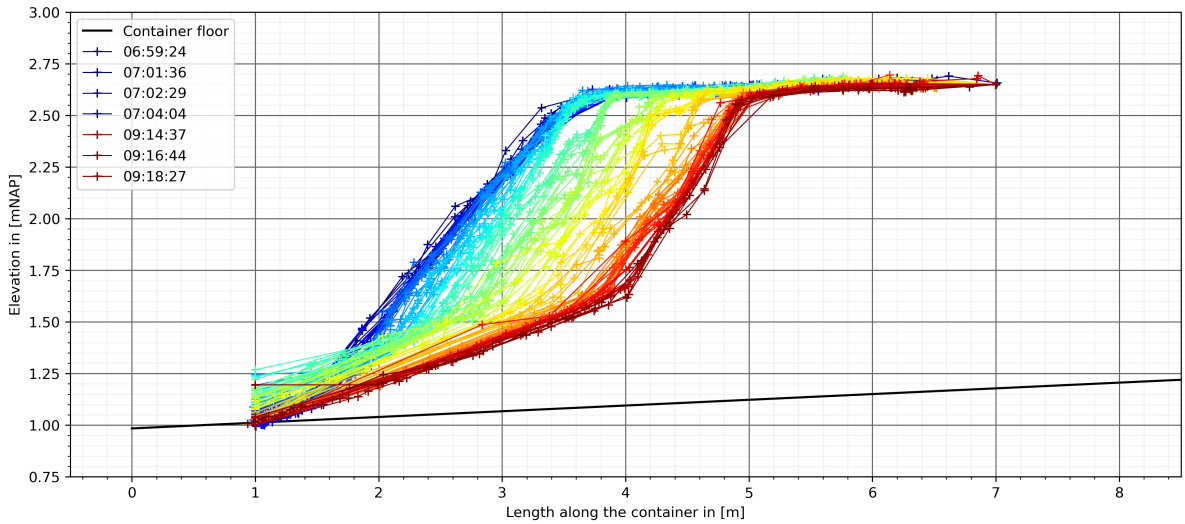

(a) Overview of the transects taken by GPS system 1 in container 1, during experiment 4 on Thursday

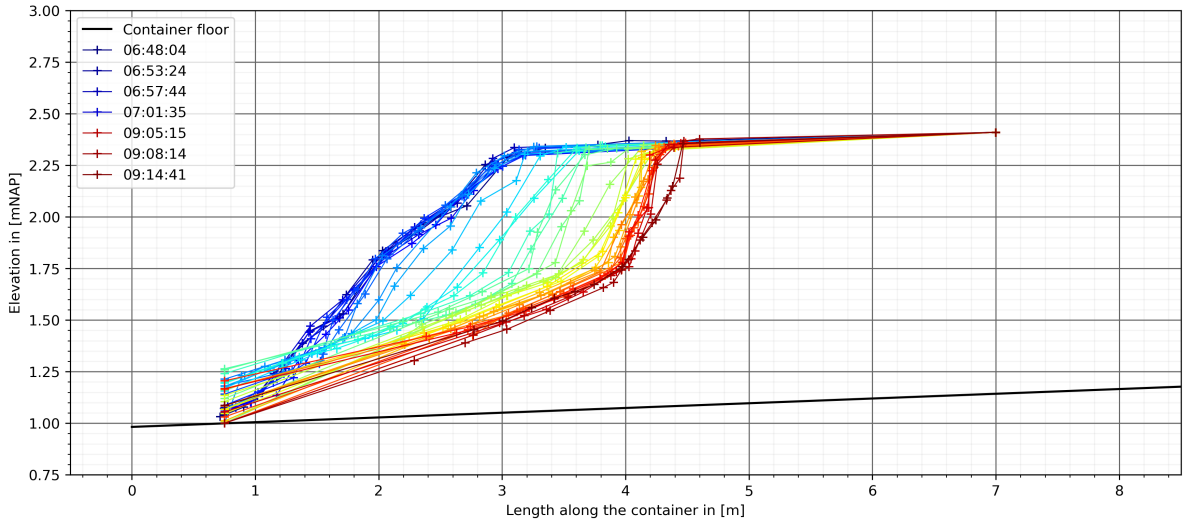

(b) Overview of the transects taken by GPS system 2 in container 2, during experiment 4 on Thursday

Figure 3.16: Overview of the extended transects per experiment per container. Container 1 (with cart) on the left and container 2 (without cart) on the right. In every figure the transects, taken with the GPS pole, are shown in colour. The colour varies from blue at the start of the measurement to red at the end of the measurement. The container floor is shown in black.

In figure 3.16a, the avalanching process is visible when looking at the time evolution of the dune crest. T3.16bhis is harder to see because the measurements were taken at a slower pace. The measurements in container 1 started at 6:59 but in container 2 the measurement started 11 min earlier and stopped 4 min earlier. This makes the measurement 7 min shorter in container 2 than in container 1. As the width of the dune (2.35m) is not taken into account in figure 3.16, the total amount of erosion is different than presented in the graph. A quick calculation show that the total amount of erosion of container 1 is $2.35[m] * 2.33[m^2] = 5.48[m^3]$. The amount of erosion in container 2 is $2.35[m] * 1.72[m^2] = 4.04[m^3]$, which is significantly less than the eroded volume in container 1.

The use of the measurement systems improves from experiment 2 to 4. This is visible in the more neat transects in figure **??** compared to figure 3.6. Working with the cart went smoother and faster in experiment 4, thus the time between two transects in container 1 reduced. This was also the case for system 2 in container 2. On Tuesday the amount of transects taken by system 2 was 21 but on Thursday already 42 transects were taken.

For the evaluation of the total erosion volume, the speed of the erosion process figure 3.17 is

investigated. In this figure the increase in cumulative eroded volume per transect is shown for container 1 (black crosses) and container 2 (blue crosses). The slope of the polynomials is determined to find the erosion speed in $[\frac{m^3}{ms}]$. The speed of erosion of container 1 is 3.20 $\cdot 10^{-4}$ $[\frac{m^3}{ms}]$ and in container 2 the speed of erosion is 2.56 $\cdot 10^{-4}$ $[\frac{m^3}{ms}]$. These speeds will be compared to experiment 2 and 3 in chapter 4.

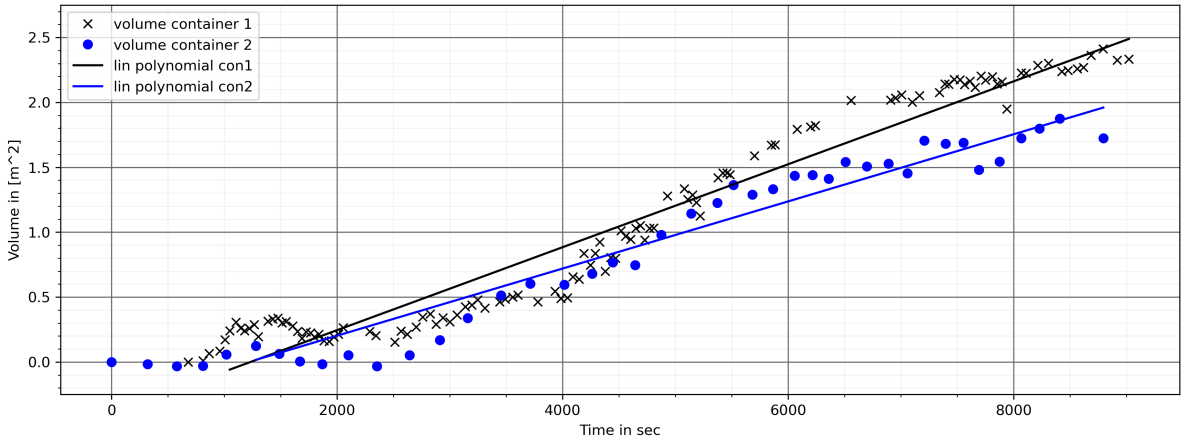

(a) Cumulative erosion volume of experiment 4 in $[\frac{m^3}{ms}]$. In black the eroded volume in container 1 and in blue the eroded volume in container 2. The pole of system 1 in container 1 broke around 4000 sec.

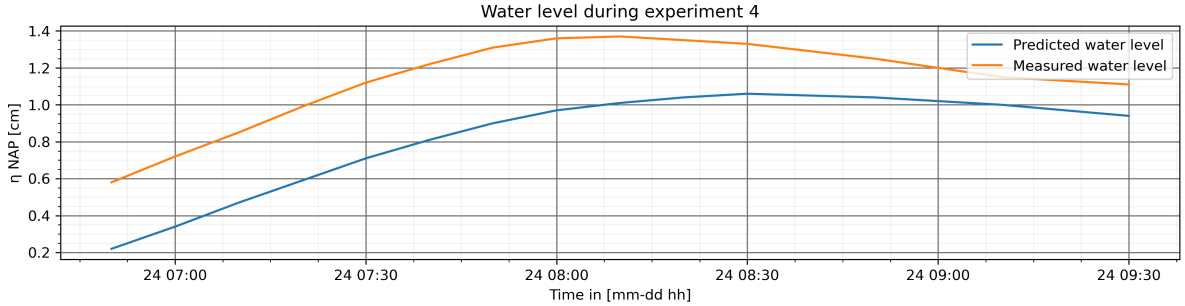

(b) Water level, orange is the measured water level and blue is the predicted water level.

Figure 3.17: Overview of cumulative erosion volume increase of experiment 4 per container.

The tidal water surface elevation measured in Hoek van Holland by RWS resulted in a maximum mean water level of 1.37 m at 8:10 (timestamp = +/- 4260 sec) at the Sand Engine. This includes the 10 min phase shift of the tidal motion when comparing the Sand Engine and Hoek van Holland.

Also, the erosion pattern looks, just as in experiment 3, not linear. From 2000 sec an increase in slop is visible. In contrast to experiment 3, also a decrease in slope is visible from 6000 sec. This increase and decrease have to do with the fact that the mean water level at the dune face is changing due to the tide. This causes an increase in wave action, and therefore erosion when the tide is high (rising) and a decrease in wave action, and therefore erosion, when the tide is lower (falling).

Dune toe evolution

When looking at the dune toe evolution, a difference is visible between container 1 and container 2, because the toe of both dunes do follow the water level, however, the toe of the high dune in container 2 does not rise at the same pace as the rise of the water level. This is visible in figure 3.18a. In this figure the black crosses show the location of the dune toe per transect and the yellow crosses show the location of the dune crest per transect. The blue line shows the water level. Both containers show a rise of the dune toe during the rise of the water level. Also, they both show a steady dune crest during the whole experiment. The increase of the dune toes in both containers stop when the water level reaches its maximum of 1.37 m.

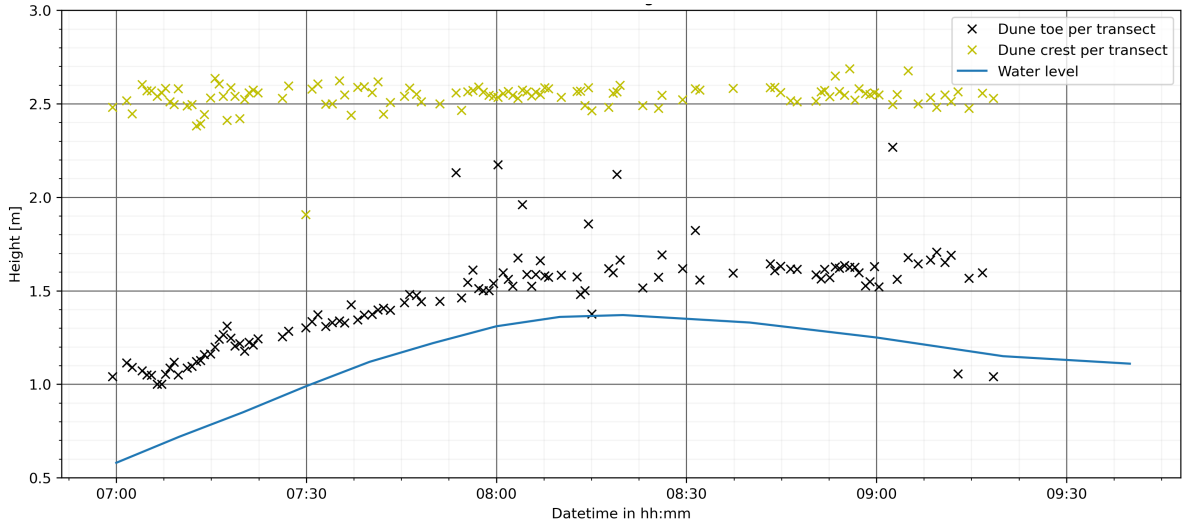

(a) Dune crest and dune toe height evolution Wednesday no cart in container 1 during experiment 4.

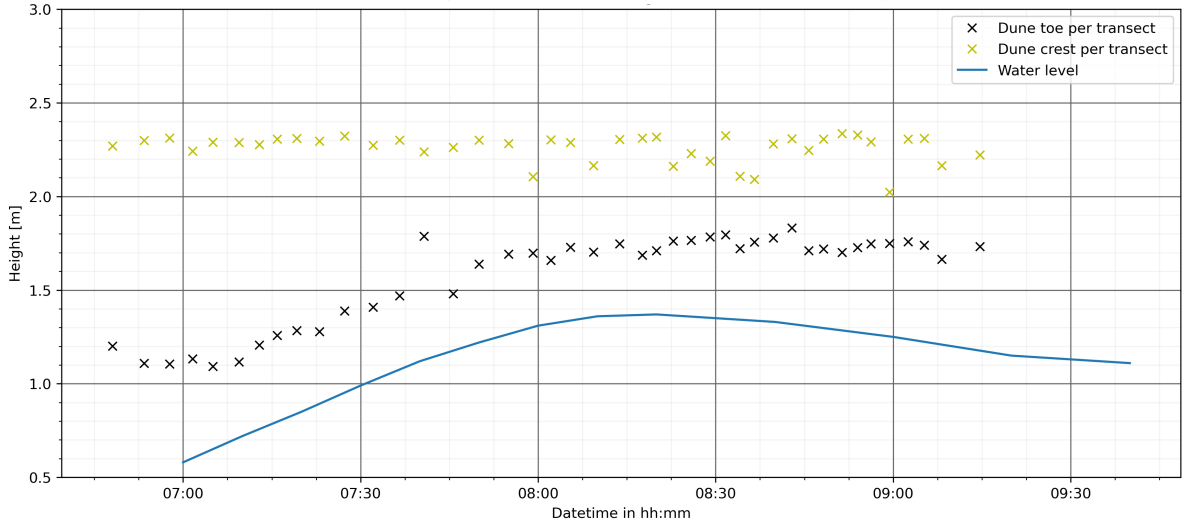

(b) Dune crest and dune toe height evolution Wednesday no cart in container 2 during experiment 4.

Figure 3.18: Vertical dune toe movement over time, for experiment 4 per container. In yellow the dune crest movement per transect, in black the dune toe per transect.

The dune toe and crest are calculated in the same way as was discussed in experiment 2 and 3. In container 1, the dune crest stays relatively the same at 2.55 m during the whole experiment. Starting at 7:10, the dune toe on the other hand increases from 1.05 m to 1.6 m while the water level rises from 0.72 m to 1.37 m. The toe stays at this height when the water level falls again, which means that the total height increase toe is 0.55 and the total increase of the water level is 0.65. The difference in rise is 0.10 m, which could be caused by the difference in dune height. As this is value is very low, the theory that the dune toe follows the water level is valid.

In container 2, the dune crest also stays relatively the same at 2.3 m. The dune toe rises from 1.1 m to 1.75 m, while the water level increased from 0.72 m to 1.37 m. These values are taken at the start of the dune toe rise at 7:10 and at the water level maximum. This is done to understand the difference in height during the rising period. When the tide falls the dune toe stays at the same level. The total increase of height of the dune toe is 0.65 m and the total increase of the water level is also 0.65 m. The difference between these heights is 0.0 m, which means that just as in container 1 the dune toe had almost the same rise in height as the water level and therefore follows the water level.

Wet and dry slope evolution

As explained in experiment 2 and 3 the dunes consist of three slopes: the wet foredune, the dry dune face and the crest slope. As the water level is changing in this experiment the dune toe is rising with the water level, however, the angle of the wet slope should stay the same due to a distribution of the eroded volume along the foredune. This is evaluated in figure 3.11.

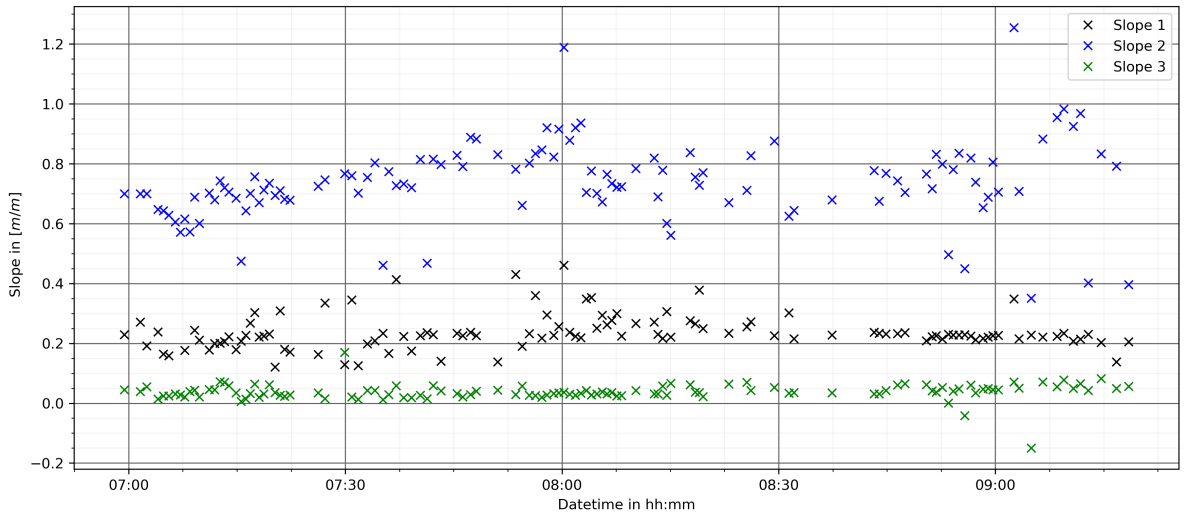

(a) Dune slope evolution of container 1 experiment 4 on Thursday.

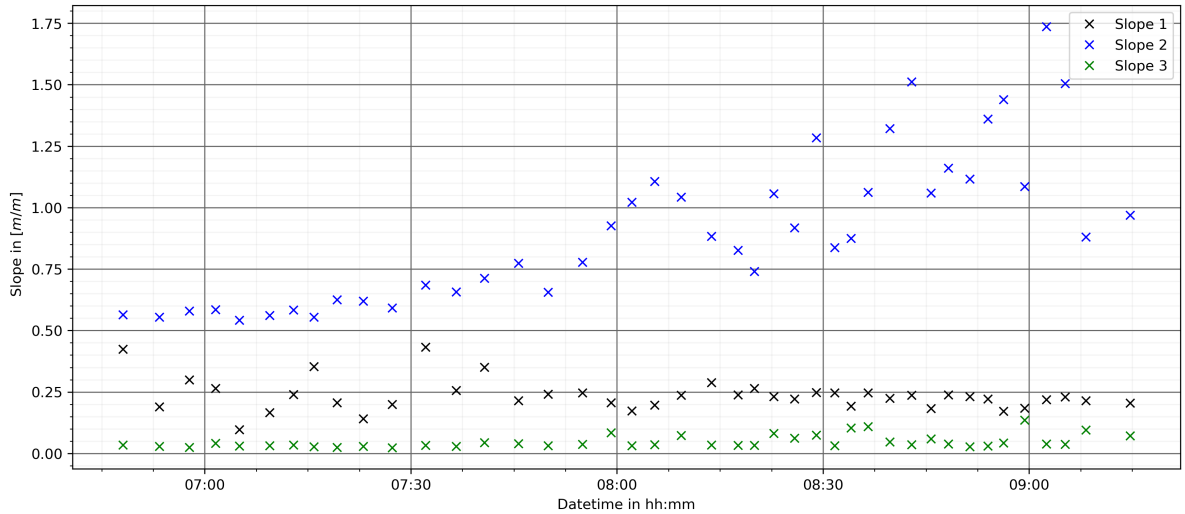

(b) Dune slope evolution of container 2 experiment 4 on Thursday.

Figure 3.19: Slope evolution in time of all transect during experiment 4. Slope 1 is the wet foreshore, slope 2 is the semi-dry dune face and slope 3 is the dry dune crest. Slope 1 and 3 (respectively the foreshore and the crest) remain very stable throughout the experiment. The dune face is increasing in steepness due to scarp formation.

A clear difference between the dune face slopes in the two containers is visible, while the foredunes and the dune crests stay relatively the same. In container 1, the foredune (slope 1) remains around 0.236, which is 1:4.23. The dune face (slope 2) increases slightly from 0.65 to 0.85 respectively 1:1.54 to 1:1.18 with a mean of 0.74 which is 1:1.36. The dune crest (slope 3) remains the same around 0.038 which is 1:26. In container 2, the foredune (slope 1) remains around 0.235, which is 1:4.25. The dune face (slope 2) increases strongly from 0.6 to 1.25 which is an increase in steepness from 1:1.67 to 1:0.8. This is due to scarp formation. The dune crest (slope 3) remains the same around 0.047 which is 1:21.

The results of experiment 4 are shown in table 3.11. Here the difference between the two containers, and therefore between the 1.6 m high dune of container 1 and the 1.3 m high dune of container 2 is

shown. In the third column, the difference in percentage between the two containers is shown, with container 1 as reference. In the last column, an indication of similarity is done.

Table 3.11: Experiment 4: Comparison of the results of container 1 and container 2.

Parameter	Container 1	Container 2	Difference Con 1 vs Con 2	Conclusion
H_m, rbr1, 4 in [m]	0.196	0.199	+1.4%	Similar
$H_{maasgeul}$ in [m]	1.38	1.38		
Wind direction in °	222.9	222.9		
Wind speed in [m/s]	9.30	9.30		
Erosion volume in [$\frac{m^3}{m}$]	5.48	4.04	-35.6 %	Different
Erosion speed in [$\frac{m^3}{ms}$]	$3.20 \cdot 10^{-4}$	$2.56 \cdot 10^{-4}$	-25 %	Similar
Rise dune toe in [m]	0.55	0.65		
Rise water level in [m]	0.65	0.65		
Difference rise water level and rise dune toe in [m]	-0.10	0.0		Similar
Foredune slope in [m/m]	1:4.23	1:4.25		
Dune face slope in [m/m]	1:1.54 to 1:1.18	1:1.67 to 1:0.8		

3.3. DUROS prediction model

Previous research on dune erosion has led to prediction models for the amount of erosion during a storm, which can be used to evaluate the dune erosion results inside the container. This thesis focuses on two models, DUROS and DUROS+. As explained in section1.1.4 the DUROS model was made by Vellinga in 1986. This model shifts the dune face land inwards until the eroded volume is equal to the accreted volume on the foreshore. The parameters are the wave height, the fall velocity, which is based on the grain size of the sand, and the storm surge level. The DUROS+ model made by van Gent in 2008 also uses the peak wave period in the model as long waves cause more erosion than short waves.

The dune of experiment 4 of container 1 on Thursday is taken for comparison with the dune erosion models. In figure 3.20 the results of the models, compared to the measured profiles are shown. The bathymetry that has been used as input is based on three components to get a full transect of the beach. A Jarkus cross-section of the Sand Engine of 2020 is used as a base profile from -12 to -0.8 m height. Then a bathymetry-transect taken during the fieldwork in September 2020 is added from -0.8 to +0.8 to get an accurate beach profile. The third component is the dune transect measured by system 1 in container 1 at the start of the experiment. These three profiles together form the base bathymetry that is used as input for the prediction models.

Input parameters DUROS and DUROS+:

- H_s = 0.827 m, which is the H_m of RBR3 during experiment 4 on Thursday.
- ssl = 1.5 m, the input parameter for the storm surge level is the maximum tide of experiment 4.
- d = 350 μm, for the sieve size, the measured D_{50} is taken
- Tm = 12 sec, the peak wave period, only used by DUROS+ is also measured by RBR3. 12sec is the minimum value that is used in DUROS+

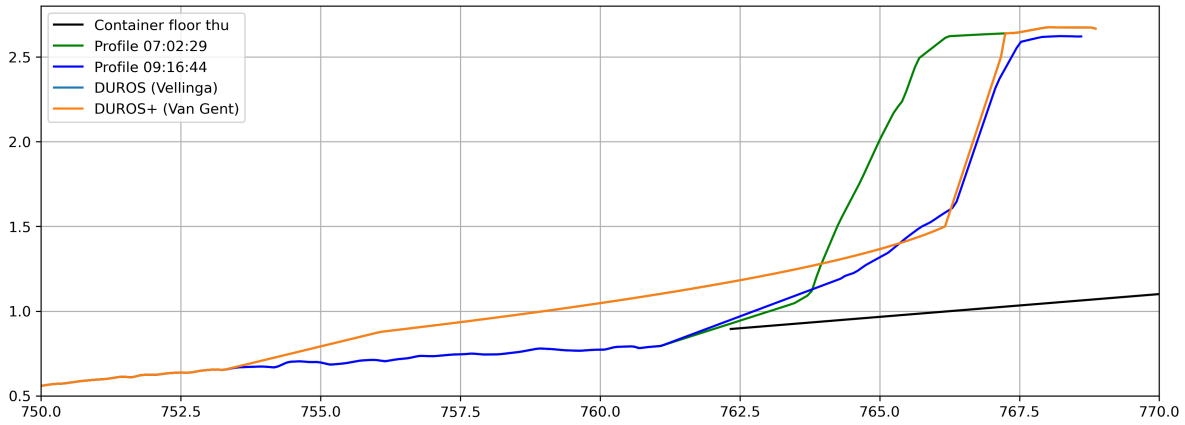

Figure 3.20: A comparison of DUROS and DUROS+ to the measured transects of the dune of experiment 4 container 1. In black the floor of the container, in green and blue the measured transects at the beginning and at the end of experiment 4. In orange and light blue the calculated DUROS and DUROS+ profiles. The light blue line is exactly the same as the orange line, as the wave period is the standard period used by DUROS.

In figure 3.20 a comparison between the DUROS, DUROS+ and the transects in the container are given. In orange, a transect at 7:02 at the beginning of the experiment is shown. The blue line represents a transect at 9:16 at the end of the experiment. The black line is the container floor and the red line is the outcome of the DUROS model. The DUROS+ line is not shown as it is exactly the same as the DUROS line due to the fact that the Tp is a standard value.

The measured transect at the end of the experiment (blue line) and the DUROS model (red line) are compared. The DUROS model seems to resemble the actual dune erosion of the container quite well.

The crests of both the model and the measurement have an almost similar starting point. Also, the dune toe height begins at approximately the same height. In DUROS this height is determined by the input parameter of the storm surge. For this input, the maximum tidal elevation is taken which works well. The difference between the models is visible in the bottom part of the profile. As the DUROS model works on the basis of a volume balance, the eroded volume of the dune is placed directly on the foreshore by the model. This is not happening in the measured profile. It has to be said that the measurements of the dune only go to 1 m inside the container and that the measurement of the foredune is only measured from 1 m outside of the container. The bathymetry of the blue and the orange line is therefore not entirely accurate from 1 m inside the container to 1 m outside of the container (x-direction). Also, the measurement of the foredune is only done before the experiment. Therefore the actual change in height of the foredune is not registered. This partly explains the difference in height of the foredune between the model and the measurement. It also has to be said that the return current out of the container was strong. This was observed in visual observations. This means that the eroded volume can be distributed quickly out of the container and across the beach, resulting in a 3D spread of the eroded volume on the beach. Therefore the height of the foredune will not be as high as the 2D model predicts.

It is important to realize that: according to Deltares (Vellinga, 1982) the DUROS method is only valid for situations in which:

1. the maximum storm surge level minus $1\ \mathrm{m}$ is exceeded for 5 to 6 hours
2. the grain size diameter is $150\mu\mathrm{m} < D_{50} < 400\mu\mathrm{m}$
3. the wave steepness is larger than $H_{0s}/L_0 = 0.02$

It is also noted that a post-storm beach profile as measured shortly after the storm will be a little lower than the predicted profile, because of a redistribution of sand after the peak of the storm. Furthermore, these two models are made for storm erosion, therefore they do not take changing water levels such as the tidal influence into account.

The first situation of Deltares where the maximum storm surge minus 1 m needs to be exceeded for 5-6 hours is of course not true for this measurement. The measurement time is 2.5 hours and the surge (=tide) varies between 0.75 to 1.37 and back to 1.15 as is visible in figure 3.17b. This reduces the accuracy of the DUROS comparison.

The second requirement is being acknowledged because de grain size of the tip of the Sand Engine is between 250 and 350 μm.

The third requirement, stating that the wave steepness must larger than 0.02 is true for this case. With a H_s of 1.3 m and an average wavelength of 6 m, the steepness is around 0.21.

Finally, Deltares (Vellinga, 1982) says that the post-storm profile will lower than the predicted profile, because of the redistribution of the sand. This is not accurately measured but as explained before the measured profile is almost certainly lower than the predicted profile. On pictures an increase of 5-15 cm of the beach profile height around the container was visible. So it can be concluded that the DUROS and DUROS+ profile make an accurate comparison with the actual measurements, but based on the literature behind the models, these models are not designed for this particular comparison, mainly because there is no storm, the water level was moving and the measuring time was too short.

4

Discussion

In this thesis, a new method to measure dune erosion on a large scale has been tested. Dune erosion tests are normally done in the field or in a flume in a lab. The new method is a contained environment that can be placed on a flat beach of choice. It uses the natural wind-generated waves and tidal motion but it limits boundary conditions such as longshore currents and aeolian transport. The contained environment consists of a 40-foot open-top sea container where dune transects can be taken by using a GPS device. Multiple containers can be placed next to each other to increase the amount of research that can be done.

To obtain knowledge on the workability of the new method, two containers were put on the Sand Engine near Kijkduin. Four experiments were conducted inside these containers. In these experiments, measurements were done using RBR pressure sensors and GPS measuring devices. The first experiment included two setups of the pressure sensors, cross-shore and long-shore, and was done to indicate wave movement inside the container. In the second experiment, two dunes of 1.3 m high were built in both containers to see if both containers have the same dune erosion process. The third experiment contained a lower dune of 1 m height and a dune of 1.3 m high, to see if the erosion process differs. Finally, the fourth experiment contained a higher dune of 1.6 m and a dune of 1.3 m. This was also done to see what the difference in the erosion process is and if it works according to the theory.

In general, it was found that the contained erosion setup works according to theory. Depending on the tidal motion and the wave conditions the erosion process can be well measured using a GPS device. The measurement system turned out to be quite critical as the GPS cart in system 1 performed significantly better than the GPS pole of system 2. In this chapter, the general findings of this master thesis are discussed. It will start with a discussion and reflection of all aspects of the methodology applied. Experimental shortcomings made assumptions, and discrepancies in results will be clarified and evaluated.

This discussion covers the following aspects:

1. Methodology:
    - Scalability
    - Container location
    - Fieldwork shortcomings
    - GPS system 1 versus GPS system 2
    - Precision of the measurement devices
    - Workability
2. General observations:
    - Turning of incident waves

- Container movement

3. Data anlysis:
    - Wave reflection
    - Wave propagation
    - Erosion speed
    - Dune toe evolution
    - Slope evolution
    - Duros predictions models

4.1. Methodology

Scalability

During this thesis, two containers are used simultaneously. This way two measurements can be done at the same time. A benefit of the container is that is easily scalable. As long as the distance between the containers is sufficient, the number of containers could be scaled up. This would be preferable when research on the dependency of erosion processes on grain sizes of dunes is done. If 5 types of grain sizes need to be tested, 5 containers could be used at the same time. It has to be noted that research in multiple containers has to be done at the same time to have the same hydraulic conditions.

Container Location

During this research, the containers were placed on the Sand Engine. As this is a flat beach, there were no deformations in the beach profile that could cause disturbance in the hydraulic conditions. A straight beach without big rocks or other objects is preferred. These could cause a change in the hydraulic conditions. Furthermore, the location in cross-shore direction is also important. The back of the containers was placed 10 cm below the average high water during the fieldwork week. This turned out to be a good approach, as there was enough time to make dunes during low water, but there was also enough wave action on the dune face during high water.

Fieldwork shortcomings

The fieldwork week took place in September 2020. During the fieldwork week, there were several aspects that could be improved as this was the first time that this method was tested.

GPS system 1 versus GPS system 2

The GPS systems proved to be a successful method to measure dune erosion in 2D. Due to time and logistical reasons, two different systems were used inside the containers. In container 1 a cart with a GPS pole was used. In container 2 a stability plank with a GPS pole was used. System 1 with the cart proved to be a much faster and more accurate method than system 2. With system 2, several different point measurements were taken. With every measurement, the pole needed to be straightened according to a spirit level to reduce errors. Then the device did 5 point measurement and took the average of those points to come up with one point measurement. This was done for every measurement in the transect and it took 2-4 times as long as system 1. This time improved during the fieldwork week due to experience, but as the time between two point reduced, the error of the measurements increased. An example of this is the measurement of experiment 4 on Thursday where almost 75 transects were measured by system 2, but 35 had to be removed because of accuracy.

System 1 had its own flaws. The handling of the car was sometimes more difficult than expected and required good teamwork. The GPS pole in the cart automatically took 1 measurement per second therefore the focus of the people handling the cart could be on a smooth consistent movement of the cart from the back to the front of the container. However, when a transect is measured, the car needs

to be pulled, back up the dune, to the back of the container to start a new transect. In this process, the pole needs to be pulled up by someone sitting on the cart. When the car is pulled back earlier than the pole is pulled back up, the pole gets stuck and breaks. This has happened in experiment 3 on Wednesday and is also visible in the figure 3.12a and figure 3.13a.

Precision of the GPS measurement devices

The validity of the experiments depends on the precision of the measurement devices and the precision of the data analysis. The precision of the GPS devices is determined in Appendix **??**. An example of the GPS, that is used in container 1, is shown in figure 4.1. This is a stationary test to see the error of the device when measuring around 1000 points in the same location. The error of this device is 0.0375 m and the error of the GPS, used in container 2, is 0.0140 m. This is only the error of the device itself.

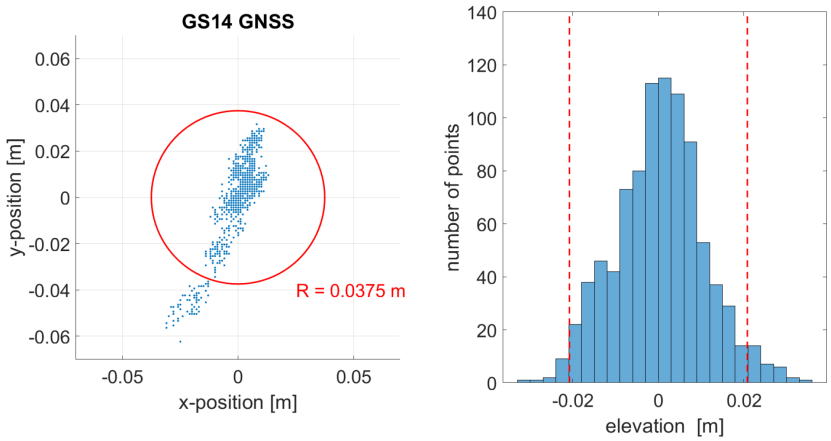

Figure 4.1: Results of the stationary test for the GS14 GPS. This GPS device is used in container 1 and has a remote controller. On the left is the distribution of the horizontal position coordinates depicted. The blue dots represent the measurements and the red circle is the 95% confidence interval based on these results. The right figure shows the distribution of the measured elevation. Here the 95% interval is highlighted y the red dashed lines.

Factors that contribute to errors in the measurement are: the moving car, the long wobbly pole, the wheel sinking in the sand, lateral deviation of the transects. The car was not mounted on rails, but on the top beam of the container. This could cause some sliding in longshore direction. As the GPS pole in container 1 had to be high enough to receive satellite connection, the movement of this pole due to wind gusts, and car movement could cause small errors in x, y-direction. The weight of this pole caused the wheel to sink in the wet sand for a couple of cms, causing small errors in the z-direction. And when looking from the top to the GPS transects, a lateral deviation in the order of cm is visible. This is shown in Appendix F as well. All these small imperfections are important to register but do not have a major effect on the final dune results.

Workability

To use these containers as a new method was challenging. Especially the logistics around the containers such as getting them into place, removing them, etc. Also, the beach is not entirely straight. Therefore it was chosen to put one container under a slight angle. It was difficult to manage this angle during installation. This can be seen from the drone shot in figure 4.2. Luckily this had no effect on the measurements as the waves straighten out inside the container.

Figure 4.2: Drone shot from the container setup. There is a slight angle between the two containers.

Doing the measurements itself was fun and not that hard under normal conditions. Pushing a cart with a GPS device on top across a container, with wind power of 6 Bft and high waves hitting the container makes it a little more challenging though. The installation of the dunes inside the container took time. The length of installation depended solely on the number of shovel buckets that were shovelled inside the container. One bucket could contain 4 m^3 of sand. If this bucket was accidentally put into the container, due to poor vision. It could result in an extra hour of preparing the dune inside the container and removing the excessive amount of sand.

4.2. General observations

Turning of incident waves

As shown in section 3.1.1, incident waves that are arriving at the entrance of the container straighten out inside the container. This straightening was a visual observation and was not measured. Also, waves do not always arrive entirely straight at the dune face. An explanation for the straightening could be the change in bathymetry around the container. An equilibrium profile around the container is formed during the experiments. This profile showed a small accumulation of sand around the container, causing waves to shoal towards the container. The sudden change in bathymetry when the wave enters the container causes a bend in the wave rays. The change in angle of the waves due to the change of the bathymetry when entering the container is an interesting phenomenon that works in favour of the method validation.

Container movement

In section 3.1.2, the movement of the container is discussed. As this was the first time that this method was tested, it was not certain that the containers would stay stable during the whole experiment. The

only measurable movement was on Thursday when heavy wind and high wave impact hit the container. This caused settlement of the front of the container with 4-7 cm. It has to be pointed out that this settlement was based on GPS data. However, the bathymetry around the container changed to an equilibrium in such a way that the front of the container was not 4-7 cm lower than the surrounding beach. Therefore it is assumed that the incoming waves were not affected by this small settlement.

4.3. Data analysis

Wave reflection

Experiment 1 measured the wave propagation inside the container. However, with the cross-shore and longshore setups (setup 1 and setup 2), the reflection of the waves from the side walls could not be measured accurately. As there was a visible reflection of certain waves coming in the container, it is not possible to exclude this. In setup 2 the container entrance was evaluated. The average wave height reduced by only 1 cm between RBR1, which located 1 m in front of the container, and RBR3, which was 2 m inside the container. Therefore, it is assumed that the entrance of the container does not have an influence on wave propagation. Interestingly the amount of wave registered by the pressure sensors increases when going more inside the container, as is shown in table 3.5. This could be due to the reflection of waves from the sides. RBR4, which is most far inside the container, registered a 26% increase in the amount of waves. This could be due to waves reflecting from the back of the container wall.

Wave propagation

During the experiments, the offshore wave height changed due to weather changes. However, the difference in wave height in front of the containers was not big. In table 4.1, it is shown that the offshore wave height ranged from 0.349 m to 1.38 m, and the wave height of 1 m in front of the container only ranged from 0.185 m to 0.257 m. One could argue, that while the weather conditions changed significantly, the conditions, with respect to wave height, inside the container were relatively stable, as all waves did already break before arriving at the pressure sensor.

Table 4.1: Comparison of the wave heights inside the containers during different experiments. The offshore wave height in the Maasgeul $H_{maasgeul}$ is shown. Also, the measured wave height H_m, registered by RBR1 and RBR4, which were placed 1 m in front of both containers, is shown.

Experiment	Parameter in [m]	Container 1	Container 2
Experiment 1 setup 1	H_m RBR1, 3	0.240	-
	$H_{maasgeul}$	0.448	0.448
Experiment 1 setup 2	H_m RBR1, 3	0.220	-
	$H_{maasgeul}$	0.349	0.349
Experiment 2	H_m RBR1, 4	0.218	0.185
	$H_{maasgeul}$	0.257	0.257
Experiment 3	H_m RBR1, 4	0.231	0.257
	$H_{maasgeul}$	0.652	0.652
Experiment 4	H_m RBR1, 4	0.196	0.199
	$H_{maasgeul}$	1.38	1.38

Erosion speed

Evaluation of the erosion speed can only be done per experiment, as the hydraulic conditions, and therefore the wave energy differs per experiment. Three points are worth noting.

Firstly, the erosion speed is determined by looking at a linear fit through a plot that shows the volume per transect. It has to be pointed out that this was not always a linear fit. Looking at experiment 4, container 1, the dune eroded faster when the water level reached the dune foot at η=1.20 m. Then dune also eroded slower when the water level decreased, 90 minutes later, to 1.20 m. This is visible in figure 3.2.5.

Secondly, there is a significant difference between the erosion speed of the two containers in experiment 2, where the dunes were the same height. While the dune height and the wave conditions were similar, the erosion speed was 1.5 $\cdot 10^{-4}$ [$\frac{m^3}{ms}$] in container 1 and 1.1 $\cdot 10^{-4}$ [$\frac{m^3}{ms}$] in container 2. In section 3.2.3, figure 3.2.3 it is visible that in container 2 there were significantly fewer transects measured by system 2, than by system 1 in container 1. This was a result of doing a new test for the first time. As there were only 20 points available for evaluation of the erosion speed, the accuracy was not high. Therefore this test does not represent a good comparison between the two containers.

Finally, during the fieldwork week experience in using the measurement systems resulted in more accurate transect measurements. Therefore a comparison of the erosion speed and the dune heights can be done for experiment 3 and 4. As is explained in section 3.3, Van Thiel de Vries et. all (2011) found in XBeach runs that the higher the dune, the more the eroded volume. The total eroded volume is in this thesis hard to compare, as the measurements in the containers were of different lengths. Therefore, the average erosion speed is compared, which is the total volume per total measurement time. In experiment 3, container 1 contained a 1 m high dune and container 2 contained a 1.3 m high dune. Here the erosion speed was significantly lower in container 1 than in container 2, 3.77 $\cdot 10^{-4}$ [$\frac{m^3}{ms}$] compared to 4.68 $\cdot 10^{-4}$ [$\frac{m^3}{ms}$]. This is shown in table 4.2 and is in agreement with van Thiel de Vries et al. (2011). In experiment 4, container 1 contained a 1.6 m high dune and container 2 contained a 1.3 m high dune. Here the erosion speed was significantly lower in container 2, which now has the lower dune. The speed was 3.20 $\cdot 10^{-4}$ [$\frac{m^3}{ms}$] compared to 2.56 $\cdot 10^{-4}$ [$\frac{m^3}{ms}$]. So both experiment 3 and experiment 4 confirm the theory of Thiel de Vries et al. (2011) that the higher the dune, the more volume erodes.

Table 4.2: Comparison of the erosion speed of experiment 2, 3 and 4. The erosion speed calculated in chapter 3 is shown. Also, the measured wave height H_m, registered by RBR1 and RBR4, which were placed 1 m in front of both containers, is shown.

Experiment	Parameter	Container 1	Container 2
Experiment 2	Erosion speed in [$\frac{m^3}{ms}$]	1.5 $\cdot 10^{-4}$	1.1 $\cdot 10^{-4}$
	Dune height in [m]	1.3	1.3
	Wave height in [m]	0.218	0.185
Experiment 3	Erosion speed in [$\frac{m^3}{ms}$]	3.77 $\cdot 10^{-4}$	4.68 $\cdot 10^{-4}$
	Dune height in [m]	1.0	1.3
	Wave height in [m]	0.231	0.257
Experiment 4	Erosion speed in [$\frac{m^3}{ms}$]	3.20 $\cdot 10^{-4}$	2.56 $\cdot 10^{-4}$
	Dune height in [m]	1.6	1.3
	Wave height in [m]	0.196	0.199

Dune toe evolution

In all 3 dune experiments, the dune toe rose in the vertical direction with approximately the same speed as the rising water level, which is in agreement with the findings of Bonte and Levoy (2015). The difference between the rise of the dune toe and the rise of the water level shows that the dune toe is following the water level. The values in table 4.3 are determined from the start of the increase to the end, which is at the maximum water level. This starting and endpoint is determined per experiment. The rise of the water level and the increase of the dune toe were comparable in every container. The difference varies between -0.10 m and 0.07 m. The conclusion of experiment 3, container 1 is not been taken into account as the overwash phase was reached in this experiment due to low dune height and high wave action. This caused the dune toe to rise to the top of the dune crest as overwash occurred and no clear dune toe could be identified anymore. This resulted in an incomparable conclusion of this particular experiment.

Table 4.3: Comparison of the dune toe increase and the water level rise of experiment 2, 3 and 4, which is determined in chapter 3. The increase of the dune foot and the water level is shown per container. The difference between these values shows that the dune toe is following the water level. The values are determined from the start of the increase to the end, which is at the maximum water level. This starting and endpoint are determined per experiment. [1]This comparison is not accurate as the overwash phase was reached in this experiment. Therefore the dune toe rose up to the top of the dune.

Experiment	Parameter	Container 1	Container 2
Experiment 2	Rise dune toe in [m]	0.55	0.35
	Rise water level in [m]	0.52	0.28
	Difference is rise in [m]	0.03	0.07
Experiment 3	Rise dune toe in [m]	0.90	0.75
	Rise water level in [m]	0.75	0.69
	Difference is rise in [m]	0.15[1]	0.06
Experiment 4	Rise dune toe in [m]	0.55	0.65
	Rise water level in [m]	0.65	0.65
	Difference is rise in [m]	-0.10	0.00

Slope evolution

Form the three slope compared in chapter 3, only two are of importance: the foredune slope, which should stay the same during the experiments, and the dune face slope which should steepen during the experiments due to scarp formation according to Larson et al. (2004). In table 4.4comparison of these two slopes, per container, per experiment is shown. Two observations are made.

Firstly, the foreda unes of all experiments stayed at the same slope during the experiments, as shown in chapter 3. The slope of the foredune during all dune experiments, ranged between 13.34 deg and 16.76 deg (1:4.25 to 1:3.32) and therefore remained more or less constant. This could be due to difference in hydraulic conditions, which means different return currents due to different wave speeds. But it could be argued that experiment 2 container 2 could be excluded, because of pore measurements and experiment 3 container 1 could be excluded, because of the overwash phase that was reached. This leaves four results in which the slopes of the foredunes are the same, deviating from 1:4.25 to 1:4.00, which is 13.34° to 14.04°. This result suggests that the foredune stays in a constant slope, regarding the wave conditions.

Secondly, the dune face slope increased in steepness in all experiments. In container 2 this was a constant increase from 1:1 to 1:0.8, which is an increase from 45.00° to 54.34°. But in container 1 this increase was different per experiment, but also different within an experiment comparing the two containers. As shown in figures 3.11, 3.15 and 3.19, the slopes of the dune faces do not have a consistent value or trend. Therefore the only conclusion that can be taken from this data is that scarp formation is present due to the steepening of the slopes of the dune faces.

Table 4.4: Comparison of the slopes of the dunes of experiment 2, 3 and 4. The erosion speed calculated in chapter 3 is shown. Also, the measured wave height H_m, registered by RBR1 and RBR4, which were placed 1 m in front of both containers, is shown.

Experiment	Parameter	Container 1	Container 2
Experiment 2	Foredune slope	1:4.22	1:3.32
	Dune face slope	1:1.25 to 1:0.74	1:1 to 1:0.8
Experiment 3	Foredune slope	1:3.51	1:4.00
	Dune face slope	1:1.25 to 1:1	1:1.05 to 1:0.83
Experiment 4	Foredune slope	1:4.23	1:4.25
	Dune face slope	1:1.54 to 1:1.18	1:1.67 to 1:0.8

DUROS erosion predictions models

In section 3.3, the DUROS prediction model has been applied to the specific case of experiment 4 in container 1. As input parameters the wave height, the storm surge level, the grain size and the wave period were necessary. From these parameters, the storm surge parameter was filled in with the maximum tide level. DUROS and DUROS+, are models that should be used for evaluating erosion after a storm of at least 5 hours. Although this was not the case in this thesis, the model results give

similar results as the measurements.

5

Conclusions

The main objective of this master thesis was to investigate the effectiveness of a new method to measure dune erosion processes in the field by using a contained environment in the form of a shipping container. Experiments have been conducted in this contained environment and it was found that on most occasions the measurements of dune erosion in the new method was similar to the expectations, therefore making the container a valid way for measuring dune erosion processes on specific occasions.

The main research question of this thesis is:

How can a contained erosion setup in the field be used to measure a realistic erosion process?

To answer this question, the 3 sub-questions are evaluated. The conclusion, with respect to each individual sub-question, is given per sub-question below:

1. *How does the contained erosion setup influence the measurements*
   The container does have some influences on the measurement. Section 3.1 analysed general observations of the container on the measurements. These observations can be divided into several categories:

   (a) Container movement:
   During experiment 2, 3 and 4, the movement of the containers was determined by measuring the corners of the two containers with a GPS system with an error of 1-3 cm. It can be concluded that during experiment 2 both containers did not move. During experiment 3, the front of container 1 moved around 4-5 cm in y-directions (East) and settled around 3-7 cm in the sand, due to heavy wave impact and the subsequent return currents. These small movements are considered as not enough movement to influence the measurements.

   (b) Bending of wave rays travelling in the container:
   Hydraulic conditions, such as incoming wave angles, cannot be controlled when doing experiments in the field. During experiment 1 and 4 on Monday and Thursday, the waves approached the container at different angles. The difference was around 40-45 degrees. This had a small effect on the angle of the dune crest compared to the incident wave angles. This effect was only small because waves tend to straighten out when travelling through the entrance of the container. This straightening of the wave rays when entering the containers was observed during all experiments.

2. *What is the difference in wave behaviour when comparing waves in and outside the container?*
   In chapter 3.2.1 and 3.2.2, a wave-by-wave analysis is performed to understand the wave behaviour of waves travelling inside the container. From experiment 1 setup 1, where 3 pressure sensors were put in longshore direction inside the container, it can be concluded that reflection of the sidewalls of the container was not noticeable with this setup. However, some wave reflection

was observed during the experiments.
From experiment 1 setup 2, where the pressure sensors were put in cross-shore direction inside the container, it is concluded that the influence of the entrance of the container can be neglected because there was no significant reduction in wave height measured when waves travel from the outside to the inside of the container.

3. *How does the erosion process inside the container behave?*
It is assumed, that if the erosion process inside the container works according to the theories explained in chapter 1, the erosion process is working the same inside as outside of the container, and therefore the container does not influence the processes. To see if this statement is valid, the following theories are tested:

   (a) Avalanching process is present:
   (Bosboom et al., 2015)
   During experiment 2, 3 and 4, dunes were made inside the container with varying heights. In container 2, avalanching could not be noticed due to the use of a different measurement system, where taking a transect took a longer time. This resulted in fewer transects during the whole experiment and therefore no measurable avalanching. However, visual observations confirm the avalanching process taking place in both containers. In section 3.2.3 and 3.2.5, it is concluded that avalanching was happening during experiment 2 and 4 in container 1. During experiment 3 the process could also not be measured in container 1, as a malfunctioning GPS pole reduced the number of transects, but the avalanching was also spotted visually in container 1 during all experiments. It can therefore be concluded that a normal avalanching process occurred during experiment 2,3 and 4 in both containers, but that is was not always visible in the time series of the transects.

   (b) Higher dunes have a larger eroded volume under the same wave forcing:
   (Thiel de Vries et al., 2011),(de Winter et al., 2015)
   During experiment 3 and 4 a variation in dune height between the two containers is tested. In chapter 3.2.4 and 3.2.5it is shown that during both experiments the higher dune eroded faster than the lower dune in terms of dune volume, confirming the theory of Van Thiel de Vries and De Winter, who noticed this from XBeach runs and flume experiments.

   (c) The dune toe follows the rising water level:
   (Bonte and Levoy, 2015),(Splinter et al., 2018) In chapter 3.2.3, 3.2.4 and 3.2.5, the evolution of the dune toe during the experiments is discussed. It is concluded from all three experiments that the dune toe rises with the water level until the water level is at its maximum. When the water level lowers again, the toe stays at a constant level.

   (d) The wet slope of the foredune remains constant, while the dry dune face slope increases in steepness due to scarp formation:
   (Larson et al., 2004)
   In chapter 3.2.3, 3.2.4 and 3.2.5, the stability of the wet and dry slopes of the dunes are discussed. In all three experiments, the 'wet' slope of the foredune stays around the same slope steepness. This steepness varies slightly per experiment from 1:3.32 to 1:4.25. It can also be concluded that the 'dry' slope of the dune face steepens in all experiments in both containers. The exact quantification of this steepness proved to be difficult with the applied method.

   (e) The total amount of eroded volume can be predicted by existing models:
   (Vellinga, 1982),(van Gent et al., 2007)
   Experiment 4 container 1 is taken as an example case for the comparison of the DUROS and DUROS+ models. It can be concluded that these models give a good indication of the actual erosion happening in the container, although these models were intended to be used for storm erosion events that last for 5 hours, where the water level is not varying. This is not the case in this thesis. The water level is varying due to tidal motion, the experiments have an average length of 2.5 hours and the waves are a combination of wind waves and swell, not storm waves.

6

Recommendations

Based on the findings in Chapter 3 and Chapter 4, recommendations for further research are made. These recommendations include suggestions of different methods that could have been used. Furthermore, this chapter contains a section that functions as a guideline for the use of this new method; the contained erosion setup.

6.1. Recommendations for further research with the new method

The contained erosion setup can be used for various new researches. in process-based dune erosion prediction models such as XBeach, the influence of grain size and wet/dry slopes is not yet been evaluated extensively. To improve this model, a new research of dune erosion with dune made of different grain size should be carried out. This method could be beneficial for those experiments. Different container with different dunes inside them could be evaluated at the same time to investigate the influence of the grain size.

Another interesting fact is that the container can be transported. This means that a container could be transported to the Stevin lab of the Faculty Civil Engineering. There a dune could be prepared inside the container and it could then be transported back to the beach. This has an advantage, namely that you could grow plants on dunes inside the container, as there is no time pressure. Marram grass or European beachgrass could grow on dunes inside the container. These dunes could then be tested with respect to safety when they are transported back to the beach. Another example could be the growth of a grass foreshore.

As said before, the containers could be used for the validation of XBeach, especially for the evaluation of dune erosion of different grain sizes. But XBeach could also be used for the validation of the containers themselves. Now the models DUROS and DUROS+ are used to see if the erosion inside the container is comparable. These methods are empirical and do not include varying water levels. These models are designed for storm conditions, which is not the case here. The use of a process-based model such as XBeach could provide a more accurate prediction of the erosion inside the container.

6.2. Recommendations for using the contained erosion setup

In the experiments, a comparison between the two containers is made. In experiment 2 two dunes of the same height were compared. It turned out that the results of these containers were not entirely similar. The cause of this was the use of different systems in both containers. It would be very interesting to compare two containers with the same dune height with the same measurement systems. It is advised to use system 1 in both containers as it was faster and more precise than system 2.

The measurement systems that were used for the GPS measurement of the dune shapes were only able to measure inside the container. A better way to do measurements is to use a laser on an extension rail. This rail of 10-15 m could be attached parallel to the top of the container, extending

from the top in seaward direction. On this rail, a down-facing laser could be attached. This laser could not only measure faster and more precise, but it could also measure the bathymetry changes of the foredune outside the container better.

During experiment 1 the influence of the walls of the containers on the erosion process is evaluated. This needs more extensive research. Different configurations of the incoming waves should be tested. Also, the walls of these particular containers have a sheet pile shape. This shape could cause more reflections and turbulence than straight walls.

Furthermore, it is advised that when another erosion experiment is carried out inside the container, the length of the taken transects is the same. This reduces the errors of the post-processing significantly. Especially the transect length at the bottom of the dune is important to measure accurately with the same length. The reason for this is the fact that the dune toe is moving with the rising water level. As can be seen in Figure C.3 in Appendix C the raw measurements of the transect were not taken to the same length. Therefore the extension of the transect was necessary. This can be avoided when measuring all transects with the same length.

When doing new experiments with these containers it is highly recommended to limit access to the containers. When the experiments for this thesis were carried out, the access was not limited and bypassers would take a look inside the container. Sometimes even when the experiments were carried out. The placement of information boards could reduce the curiosity of people on the beach.

A

Theoretical background

This appendix, provides more background information on dunes. These sections were part of a literature study of dunes and their erosion processes. It mainly focuses on its shape and formation.

A.1. Sand dunes formation

Sand dunes are found in three types of landscapes: sea coasts and lakeshores, river valleys and arid regions (Maun and Maun, 2009). Coastal dunes are formed along coasts in areas above the high watermark of sandy beaches. They occur all over the world from the northern Arctic to the equator to southern Antarctica. Coastal dunes tend to exist wherever barrier islands or wave-dominated depositional coastal landforms occur, see figure A.1.(Martínez and Psuty, 2004)

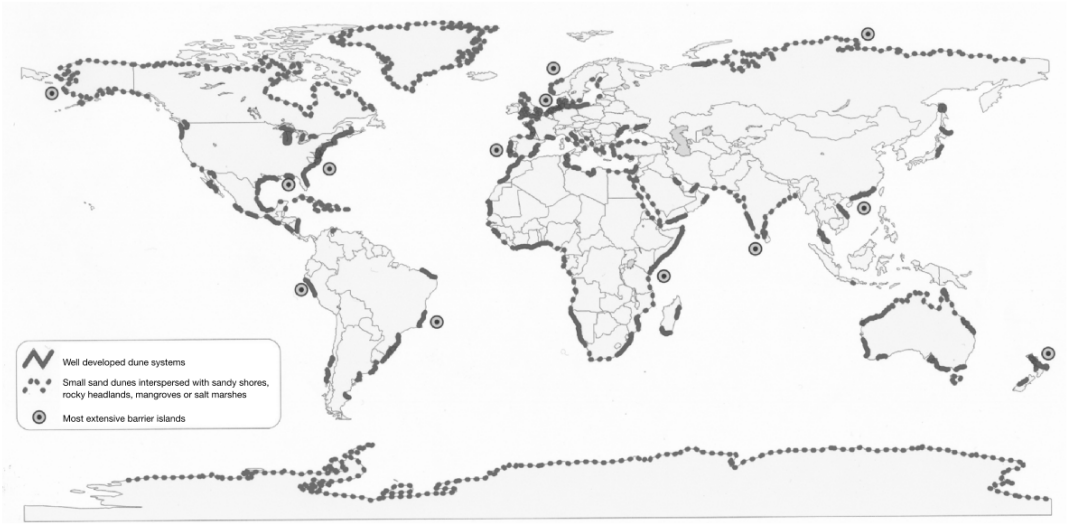

Figure A.1: Locations of coastal dunes around the world (Martínez and Psuty, 2004).

Coastal dunes are aeolian landforms that develop in coastal situations where an ample supply of loose, sand-sized sediment is available to be transported inland by ambient winds (Martínez and Psuty, 2004). These aeolian processes determine the shape of the landforms. Wind erosion tends to enforce the concentration of soil resources in islands of fertility (Okin and Gillette, 2001). It is thus important to understand the detailed mechanisms by which wind interacts with the land surface. Wind erosion mechanisms include deflation and abrasion. Deflation is the removal of loose, fine-grained particles due to the turbulent action of the wind. Abrasion is the wearing of the bedrock by grinding action of sand particles carried by the wind (Paris et al., 2019).

Before these two small scale erosion effects can take place, the wind has to transport the sediment.

Three principal mechanisms for the transport of sediment by wind are suspension, saltation and creep (Okin et al., 2006).

Where suspension occurs when very fine sand and dust particles (20-70 μm) are lifted in the wind through impact with other particles or by the wind itself. Once in the atmosphere, these particles can be carried very high and be transported over extremely long distances (Huang, 2020).

In saltation, fine soil particles (70-500 μm) are lifted into the air by the wind and drift horizontally across the surface increasing in velocity travelling up to four times longer in distance than in height. Soil particles moved in this process of saltation can cause severe damage to the soil surface and vegetation when they strike the surface again they either rebound back into the air or knock other particles into the air (Huang, 2020).

Creep refers to the movement of grains (>500 μm) by rolling over the surface (Schwartz, 2006). Figure A.2 shows these three processes.

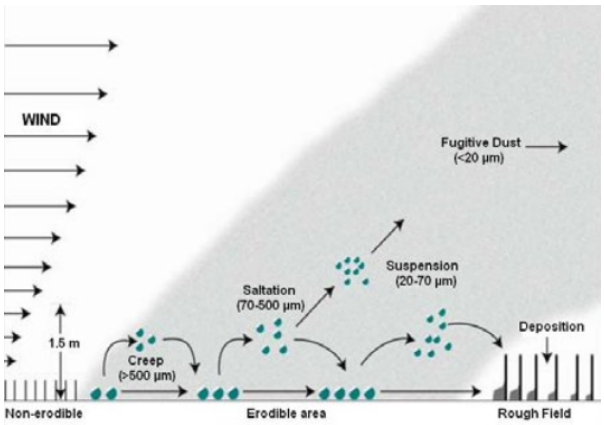

Figure A.2: Illustration of suspension, saltation and creep of soil particulates during an erosion event (Burger, 2010).

The smaller the sediment the more likely it is to be picked up by the wind. This means that the wind and the grain size of the soil have a big influence in determining the shape of a sand dune. (Burger, 2010)

A.2. Dune shape

Shapes of sand dunes are determined by wind speed, wind direction, grain size, possible vegetation, climate, etc. These factors have created numerous types of sand dunes such as: Reversing dunes, Nebkhas, Star dunes, Barchans, Transverse dunes, Longitudinal dunes, Barchanoid dunes, Dome dunes and Parabolic dunes. These are some examples of sand dunes and an illustration of the wide variety of sand dunes is shown in figure A.3.

Figure A.3: Illustration of nine different dune types. From left to right, top to bottom: Reversing dunes, Nebkhas, Star dunes, Barchans, Transverse dunes, Longitudinal dunes, Barchanoid dunes, Dome dunes and Parabolic dunes, shown in figure (Burger, 2010).

Along the dutch coastline, sand dunes contain vegetation. Salt-loving plants collect and hold sediment that was in transport due to the wind processes as discussed in section A.1. Due to these effects dunes grow in height and therefore also in length and width. The climate along the Dutch coastline is such that marrams will settle on top of the dunes after the growth. This type of vegetation holds the sand together and is resistant to dryness.

All small dunes eventually form a closed dune row. This dune row can develop into a sea strip: a solid seawall that is high enough to dam water during a storm flood. A sea strip can grow to more than 20 metres high and can either settle towards an existent sea strip.

B

Modelling of the Dutch coastline

This appendix focuses on the modelling of the Dutch coastline, with special attention to the use of the process-based model XBeach. This program is not used in this thesis but the use of it is highly recommended at the end of the thesis in chapter 6.

B.1. Evaluation of the Dutch coastline

The protection of the Dutch coastline is regulated in the law; the Dutch water act. This law states the flooding probability per dike segment. (van Haegen-Maas Geesteranus, 2016). To meet these regulations the Dutch coastline must be evaluated to understand the safety of the dikes. Presently, the safety assessment is based on the relatively simple cross-shore dune erosion model DUROS. The empirical DUROS-model is designed for alongshore uniform coastlines. Since the DUROS-model is not qualified to assess storm impact in complex cases, a more generic model that includes the long-shore dimension can be a helpful instrument. In this research the process based model XBeach (Roelvink et al., 2009) is used.

There are two kinds of programs that are used; behaviour-based models and process-based models. A behaviour model is a model where an equilibrium is forced such as Unibest-CL+ and Asmita. Process-based models are models where equilibrium follows from the balance of forces/transport contributions such as Delft3D and Xbeach. This results in smaller errors but longer computational times compared to the behaviour-based models.

For the modelling of extreme storms on a coastline, resulting in typical processes such as overwash, erosion and avalanching, the process-based model Xbeach is be used. Xbeach Roelvink et al. (2009) is an open-source numerical model which is originally developed to simulate hydrodynamic and morphodynamic processes and impacts on sandy coasts with a domain size of kilometres and on the time scale of storms. Since then, the model has been applied to other types of coasts and purposes (Roelvink et al., 2015).

B.2. Avalanching in Xbeach

To account for the slumping/avalanching of sandy material from the dune face to the foreshore during storm-induced dune erosion avalanching (Xbeach keyword: avalanching) is introduced to update the bed evolution. Avalanching is introduced via the use of a critical bed slope for both the dry and wet area (Xbeach keyword: wetslp and dryslp). It is considered that inundated areas are much more prone to slumping and therefore two separate critical slopes for dry and wet points are used. The default values are 1.0 and 0.3 respectively. When this critical slope is exceeded, the material is exchanged between the adjacent cells to the amount needed to bring the slope back to the critical slope (Roelvink et al., 2015).

$$\left|\frac{\partial z_b}{\partial x}\right| > m_{cr} \tag{B.1}$$

To prevent the generation of large shockwaves due to sudden changes of the bottom level, bottom updating due to avalanching has been limited to a maximum speed of vav,max (xbeach keyword: dzmax). Equation B.3 shows the resulting bed level change within one-time step (Roelvink et al., 2015).

$$\Delta z_b = \min\left(\left(\left|\frac{\partial z_b}{\partial x}\right| - m_{cr}\right)\Delta x, v_{av,\max}\Delta t\right), \frac{\partial z_b}{\partial x} > 0 \tag{B.2}$$

$$\Delta z_b = \max\left(-\left(\left|\frac{\partial z_b}{\partial x}\right| - m_{cr}\right)\Delta x, -v_{av,\max}\Delta t\right), \frac{\partial z_b}{\partial x} < 0 \tag{B.3}$$

B.3. XBeach base case

To test if this process-based model does register the difference between grain sizes a test model is made to evaluate this. A storm is simulated with a wave height of 2.5m and a peak period of 8.8 sec. The storm duration is 6 hours and the result is simulated in figure B.1. This is a momentary shot from t = 6000 sec. The red line is the water level (with waves), the black line is the original bathymetry at t =0, the green line is the eroding bed level with grain size = 0.2 mm and the blue line is the eroding bed level with grain size = 0.4 mm.

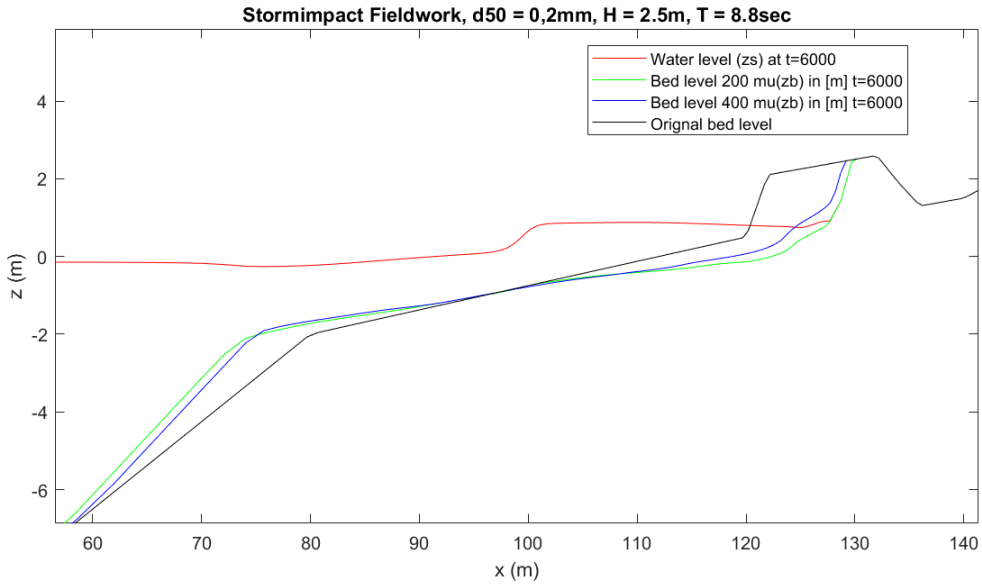

Figure B.1: Results of a test setup with H=2.5m, T_p= 8.8 sec. A storm of 6 hours is simulated and this figure is a momentary shot from t = 6000 sec. The red line is the water level (with waves), the black line is the original bathymetry at t =0, the green line is the eroding bed level with grain size = 0.2 mm and the blue line is the eroding bed level with grain size = 0.4 mm.

In this test, it can be concluded that the program does register the difference between 0.2 mm and 0.4 mm grain size. In the next couple of weeks, it is necessary to investigate how this process works exactly in the program. And if there is a big difference between using a storm or using the upcoming tide.

C

Data overview

In this appendix an overview of the raw data per instrument is given. Starting with the pressure sensors in different setups and ending with the raw GPS data without the extension of the transects.

C.1. RBR's

The RBR Solos pressure sensors give absolute pressure as raw output. Outside the water, this output is the atmospheric pressure, but when the device is put inside the water, this pressure relates to water pressure which can be converted to surface elevation. First the raw output of sensor RBR1, RBR2, RBR3, RBR4, on Monday setup 1 (left four pictures) and setup 2 (right four pictures) are shown in figure C.1.

Setup 1 and 2 are shown in figure 2.13a and figure 2.13b. In setup 1 on Monday afternoon the sensors are placed in a T-shape profile. Where RBR1 is placed 1 m in front of the container and RBR2, RBR3 and RBR4 are placed in the longshore direction inside the container, 3 m from RBR1. This cross-shore distance is determined based on the long wavelength of 12m. To get a good visualisation of the wave propagation 3 or 4 measurements per wave should be taken. 12/4 = 3 m between each sensor. With this in mind, setup 2 is created on Tuesday morning. All sensors are placed behind each other inside the container.

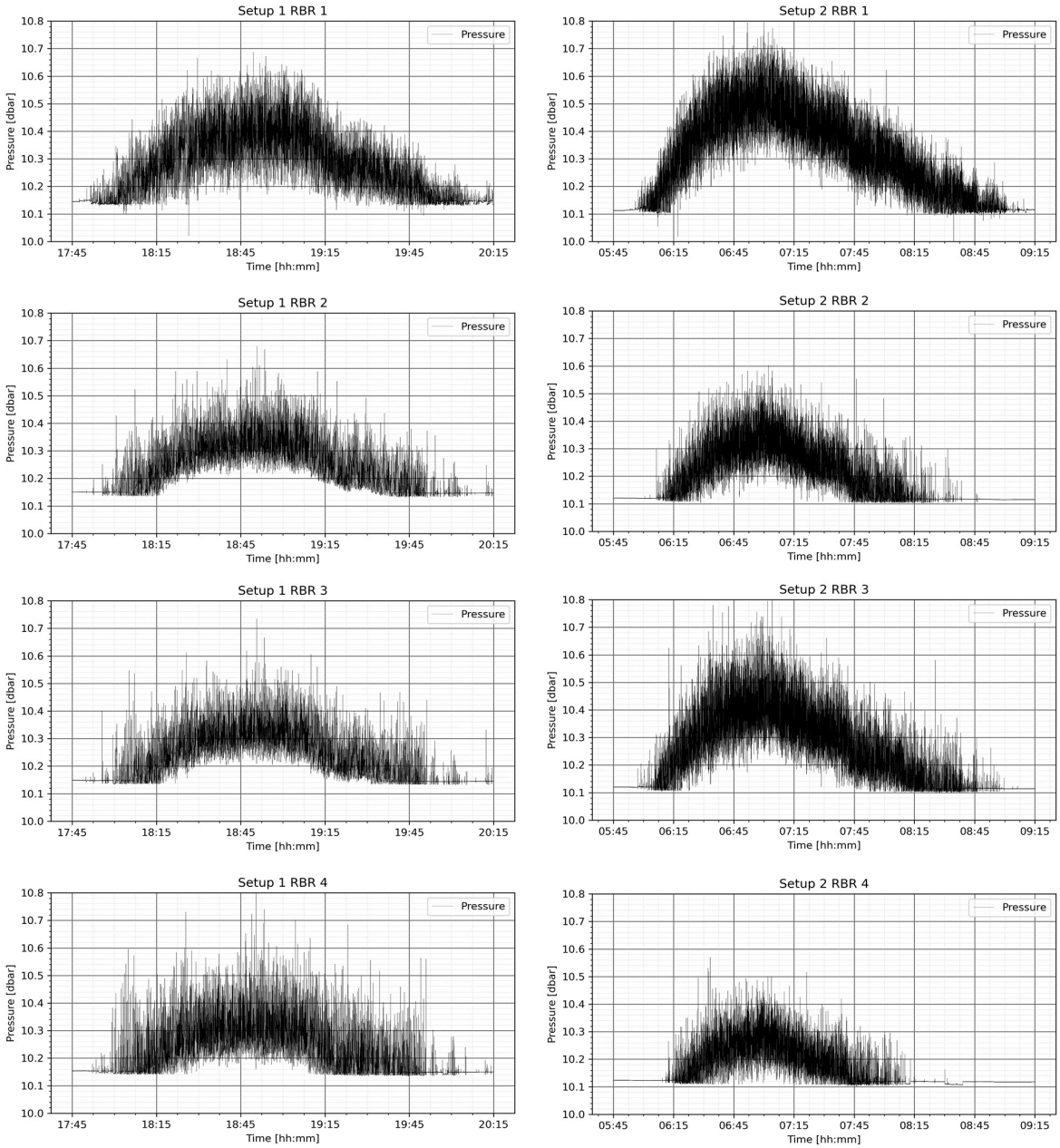

Figure C.1: Overview of the RBR raw pressure data of setup 1 and setup 2. The left four pictures describe the pressure of the four RBR's during setup 1 (Long-shore setup), shown in figure 2.13a . The right four pictures describe the pressure of the four RBR's during setup 2 (cross-shore setup) in order as shown in figure 2.13b.

Here the difference in pressure due to waves is visible. The trend in all 8 graphs is caused by tidal motion. The height of the pressure varies per instrument as the instruments are placed in different locations.

The raw absolute pressure outputs of the 4 different RBR's in setup 3 from Tuesday 22-09-2020 afternoon 17:30 until Thursday 24-09-2020 13:30 are shown in figure C.2. Here the different tides, the decreasing atmospheric pressure in between the tides, and the increased grassiness during high tides is visible. This is because of increasing wind and weather conditions during the week, causing bigger waves and therefore bigger variations in pressure. Also, not all RBRs were underwater the whole time. Only RBR3, the most offshore RBR in setup 3, remained underwater, even during low tide.

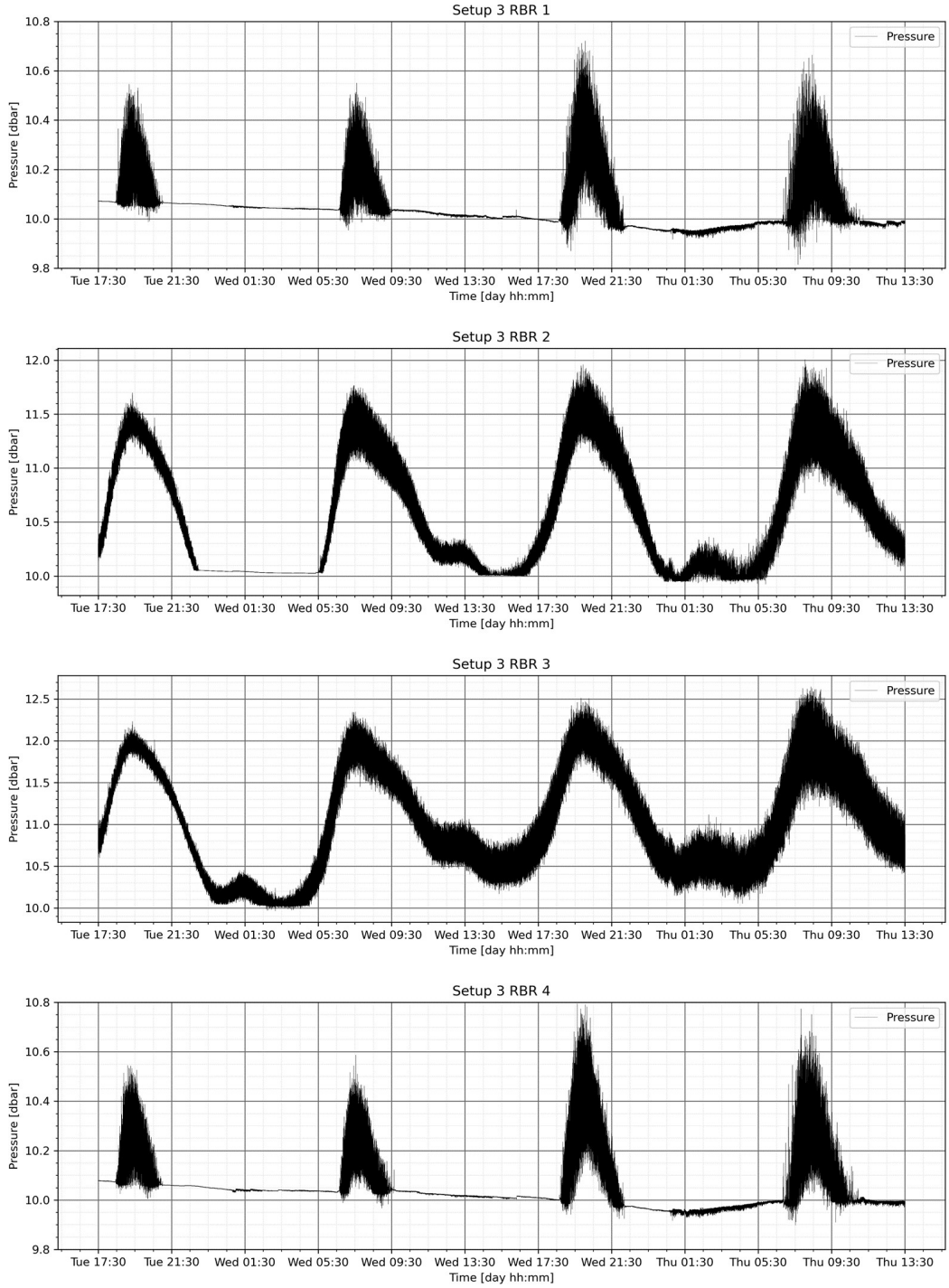

Figure C.2: Overview of raw pressure data of the four RBR's in the third RBR setup, setup 3 from Tuesday 17:30 until Thursday 13:30. The figures are shown from offshore to the onshore location of the RBR's, as shown in figure 2.14.

C.2. GPS

An overview of the GPS output without extending the transects is shown in figure C.3. These transects are taken by the two GPS systems in the two different containers. Some post-processing of the raw GPS output was done. In these data sets, faulty transects are taken out. Rotation of the coordinate system is conducted and a colour scheme is added to indicate the time of each taken transect. Blue is at the start of the experiment and red is at the end of the experiment.

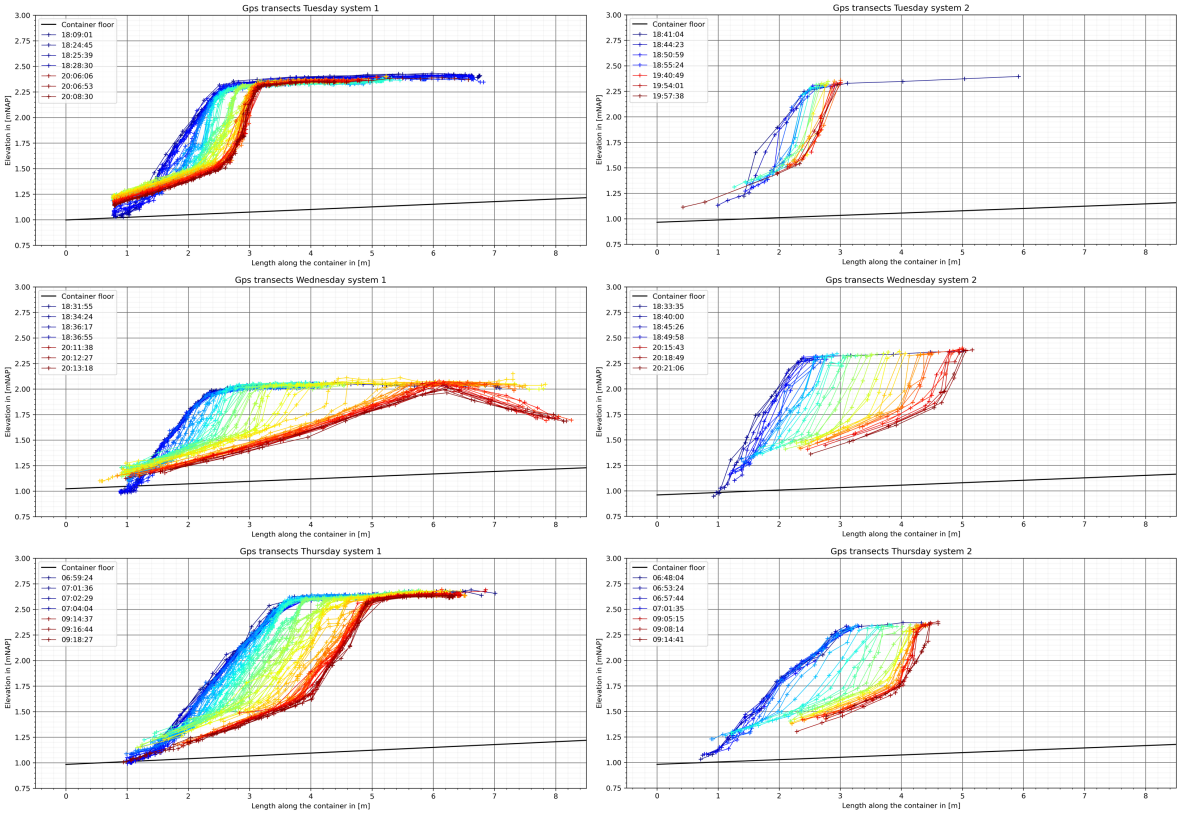

Figure C.3: Overview of the raw transects per experiment per container. Container 1 on the left and container two on the right.

From top to bottom, experiment 2, 3 and 4 are shown. The left 3 pictures show container 1 and the right 3 pictures show container 2.

D

Data processing

In this appendix, more info on the processing of the data is given. An overview of the pressure to surface elevation is given. Also, the computed wave spectra are shown.

D.1. Pressure to surface elevation

Figure D.1 is an example of pressure data from Tuesday until Thursday (RBR setup 3). On Monday (RBR setup 1 and 2), the same method is used to get the surface elevation. For the data from Tuesday until Thursday the spectra of different RBR's are added to one plot, resulting in figure D.2.

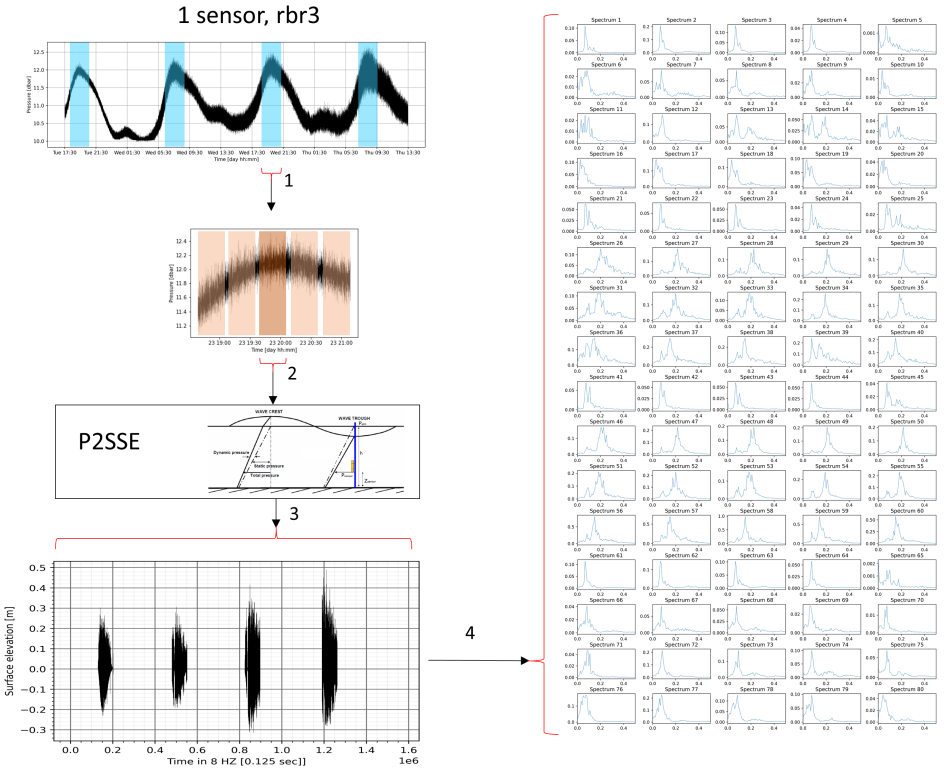

Figure D.1: An overview of the process of transforming pressure into surface elevation. From top to bottom: 4 blue blocks of 2.5 hours at high tides are taken from the full pressure data (1). These are divided into 5 red blocks of 30 min. Every blue block has its own mean wave height and antenna height. Every red block is evaluated in a python script that detrends the data (p2sse = Pressure to surface elevation) (2). Then a Fourier transformation is applied, the wavenumber (k) per frequency (f) is defined. A dynamic factor is determined and added to the data. An inverse Fourier transformation is applied and the surface elevation for this particular block is determined. This results in the bottom figure (3). From every red block (20 blocks) an energy/frequency spectrum is plotted. This is done for all 4 RBRs, resulting in 80 spectra (right)

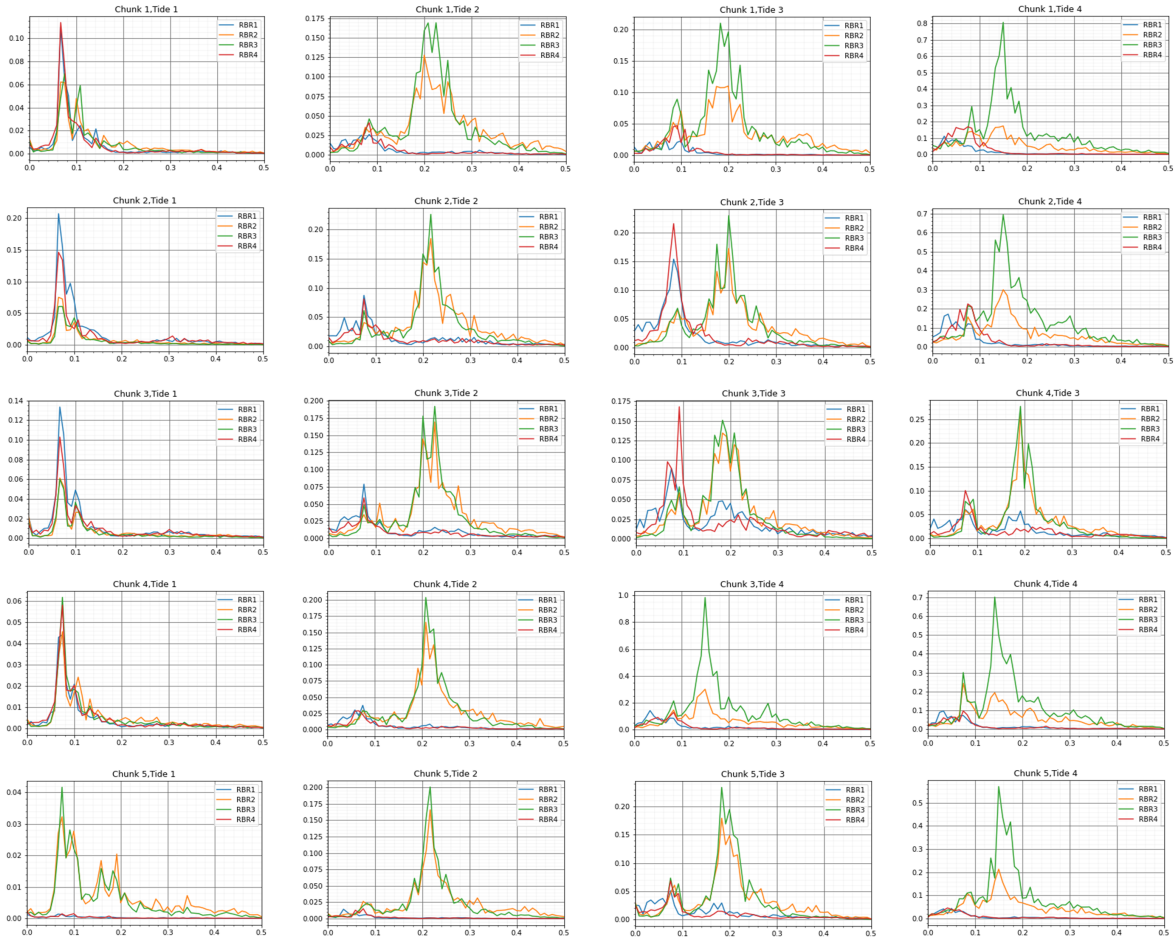

Figure D.2: Overview the energy density spectra of RBR setup 3. Tides of 2.5 hours are cut into 'chunks' of 30 min. Each with its own energy density spectrum. Each row is a different 'chunk' and each column is a different tide.

D.2. Wave analysis

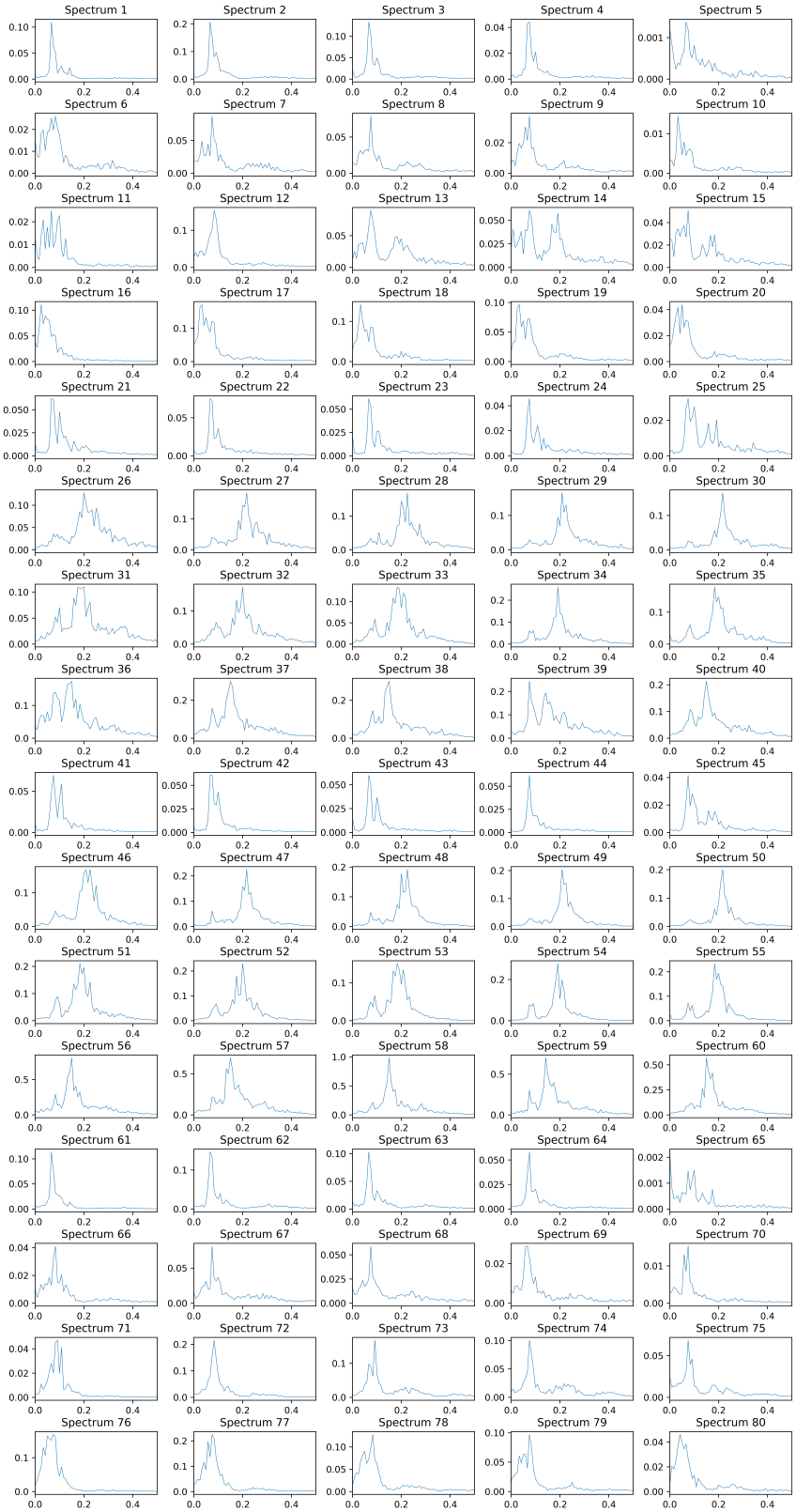

Figure D.3: Overview of the 80 spectra that are computed for the wave by wave analysis of the 4 tides of the erosion measurements in the container.

D.3. GPS Transect extension

For the evaluation of the eroded volumes of the dunes, the raw GPS data must be made usable. All transect must have the same length to investigate the amount of erosion per transect. Therefore, boundaries are determined. These boundaries vary per experiment and per container. An overview of the boundaries can be found in table D.1.

Table D.1: Overview of the transect extension parameters.

Experiment	**(toe_x , toe_y)**	**(top_x , top_y)**	**Amount of transects**	**Amount of transects extend to toe boundary**	**Amount of transects extend to top boundary**
Tue. with cart	(0.75 ; 1.03)	(6.0 ; 2.4)	95	95	78
Tue. no cart	(1.0 ; 1.0)	(4.0 ; 2.37)	21	21	20
Wed. with cart	(1.0 ; 1.0)	(6.0 ; 2.08)	82	82	52
Wed. no cart	(1.0 ; 1.0)	(5 ; 2.4)	44	44	39
Thu. with cart	(1.0 ; 1.0)	(7 ; 2.65)	118	118	117
Thu. no cart	(0.75 ; 1.0)	(4.7 ; 2.38)	42	42	42

A transect can be extended to the bottom and to the top of the transect is not long enough. A transect is not long enough if it does not reach the boundaries. These boundaries are the predefined toe and top points as shown in table D.1. Almost all transect are extended. The bottom of a transect is extended in a particular way. A linear polynomial is drawn through the two values of the transect closest to the entrance of the container. An x-value of the toe, toe_x, and a y-value of the toe, toe_y, are introduced. These are predefined values and differ per experiment and are shown in table D.1. A transect is extended at the bottom if a polynomial at toe_x, is bigger than the intersection point of the polynomial and the container floor **and** if that y-value (the polynomial at toe_x) is smaller than 1.3. This 1.3 coefficient is found iteratively and prevents the extension of transects above 1.3m. The extension of this transect if it follows this condition is done by adding a point (toe_x , polynomial at toe_x). If this condition is not followed meaning that the polynomial at toe_x is smaller than the intersection point **or** if the polynomial at toe_x is bigger than 1.3 then the transect is extended with a point of two predetermined values (toe_x, toe_y).

For the top the condition is as follows: The transect is extended with the predefined point (top_x , top_y) if top_x is larger than the first point in the transect. Transects are taken from the top until bottom so the first point is at the top. If this condition does not apply, meaning that the transect is long enough, the point will not be added.

E

Visual observations

Above the doors of the container, two Go Pro's Hero 7 are attached. These Go Pro's made a time-lapse observation of container 1 during all experiments. Due to scoping of the project, it was chosen not to evaluate the Go Pro images. However, an overview of the crest and slope of the dunes at the beginning and the end of experiment 2, 3 and 4 is evaluated. From these pictures, the straightness of the dune crest is measured.

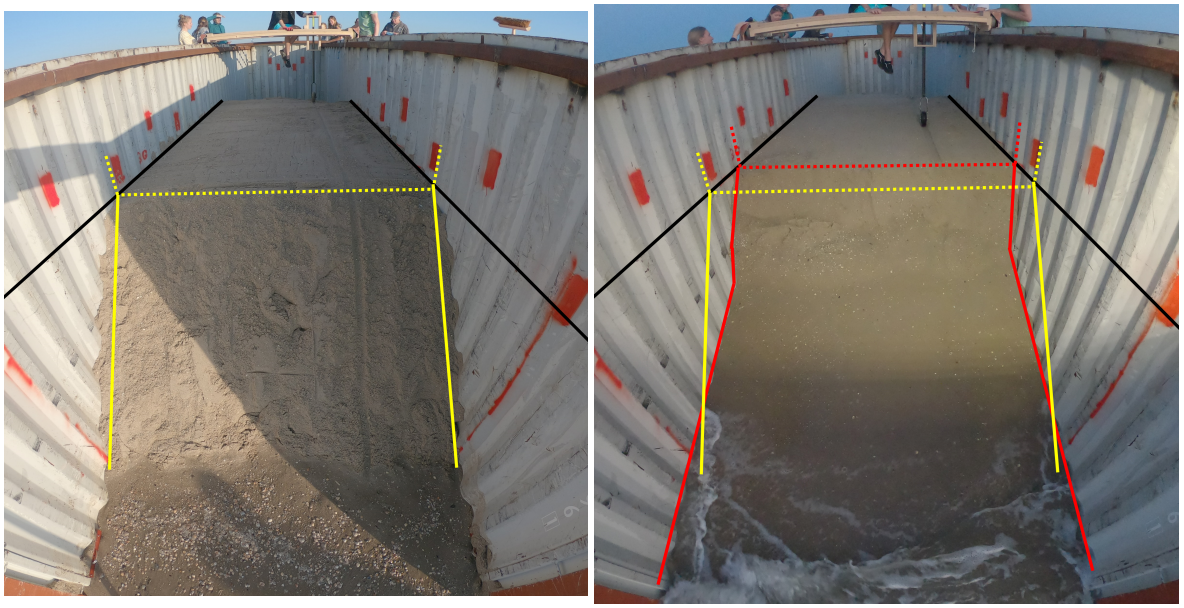

(a) Starting position of the dune face 22-09-2020 18:24.

(b) Ending position of the dune face 22-09-2020 19:54.

Figure E.1: Two go pro pictures of the dune face of experiment 2 compared to each other. In black the sides of the dune. In yellow the start position of the dune. In red the end position after +-1.5 hours.

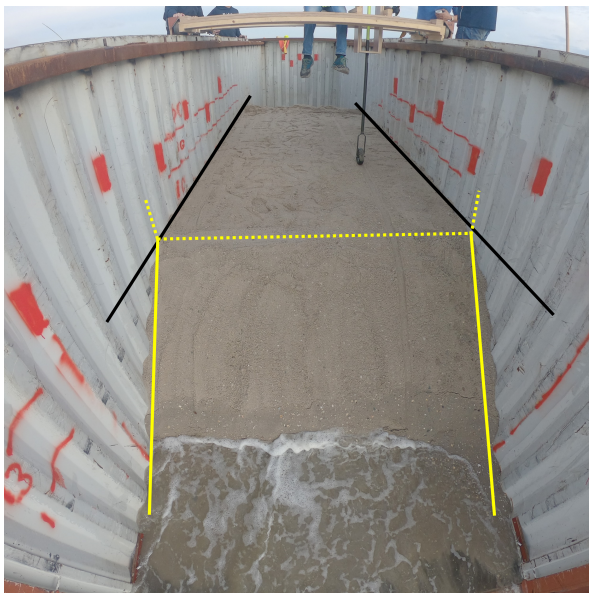

(a) Starting position of the dune face 23-09-2020 18:43.

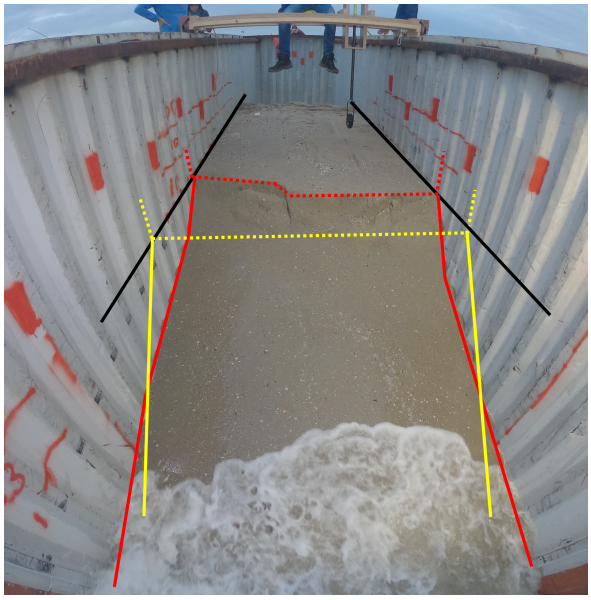

(b) Half way position of the dune face 23-09-2020 19:27.

Figure E.2: Two go pro pictures of the dune face of experiment 3 compared to each other. In black the sides of the dune. In yellow the start position of the dune. In red the halfway position after +-1.5 hours.

It is chosen to review the halfway position of the dune crest of experiment 3. At the end of the experiment, the storm regime changed from the collision phase to the overwash phase. At the end the dune crest was not visible anymore, therefore the halfway photo was reviewed.

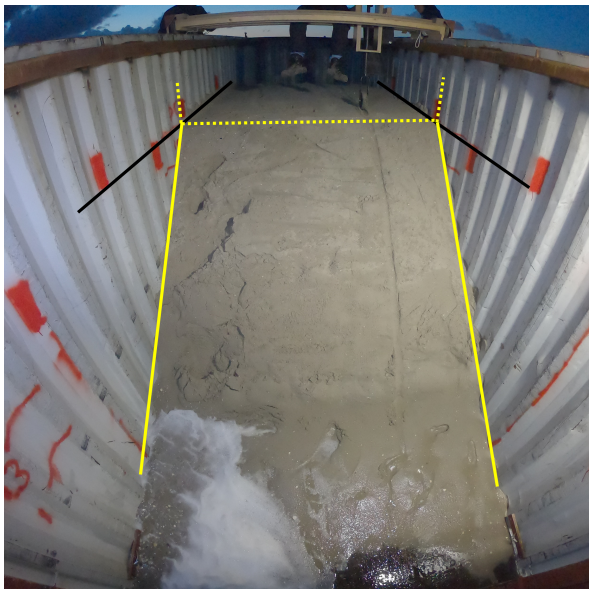

(a) Starting position of the dune face 24-09-2020 07:05

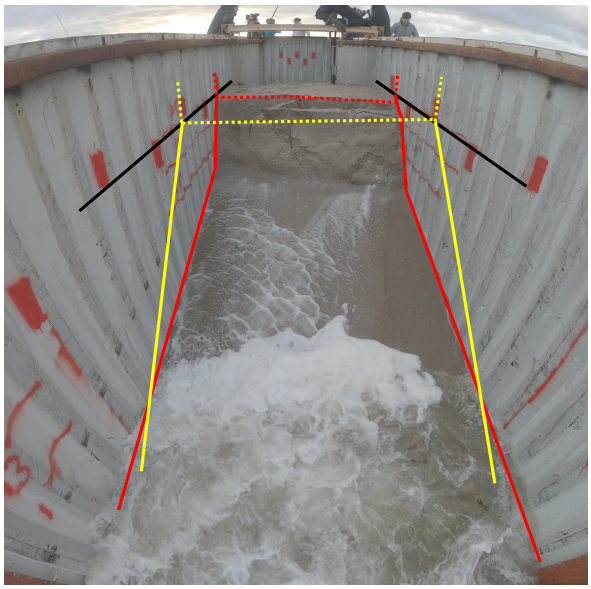

(b) Ending position of the dune face 24-09-2020 08:39

Figure E.3: Two go pro pictures of the dune face of experiment 4 compared to each other. In black the sides of the dune. In yellow the start position of the dune. In red the end position after +-1.5 hours

F

Measurement errors

F.1. Stationary GPS error

Stationary GPS measurements give an x,y spread and a z-deviation. The x,y spread is shown in the left figures and the z-deviation is shown in the right figures. GS14 is used in system 1 in container 1 and GS15 is used in system 2 in container 2.

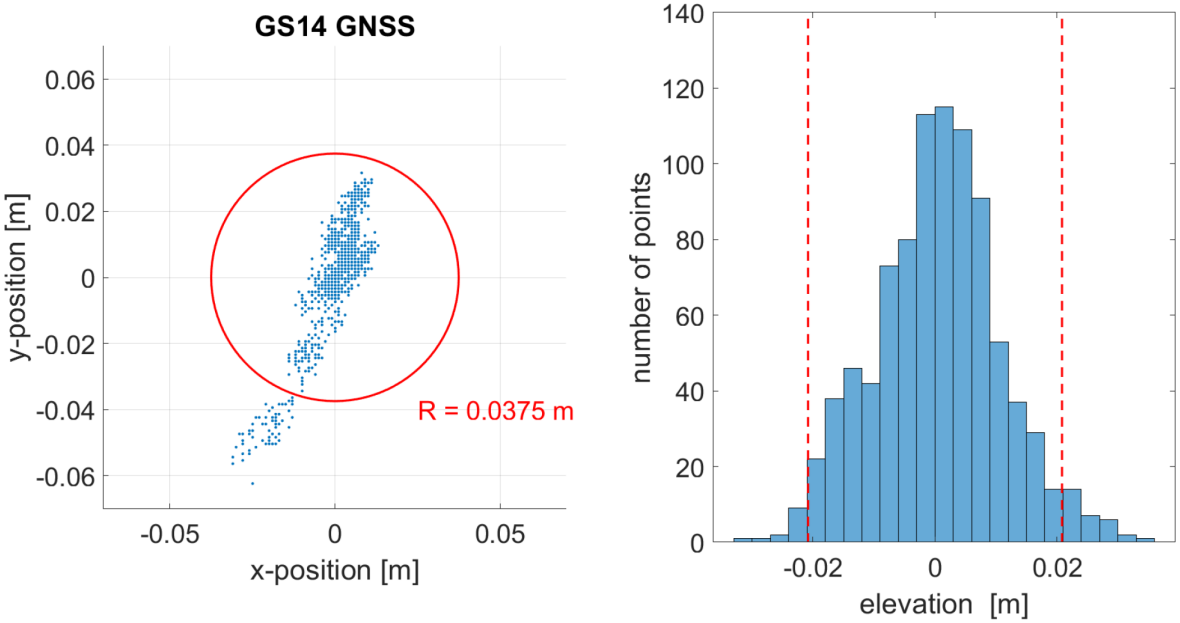

Figure F.1: Results of the stationary test for the GS14 GPS. This GPS device is used in container 1 and has a remote controller. On the left is the distribution of the horizontal position coordinates depicted. The blue dots represent the measurements and the red circle is the 95% confidence interval based on these results. The right figure shows the distribution of the measured elevation. Here the 95% interval is highlighted y the red dashed lines.

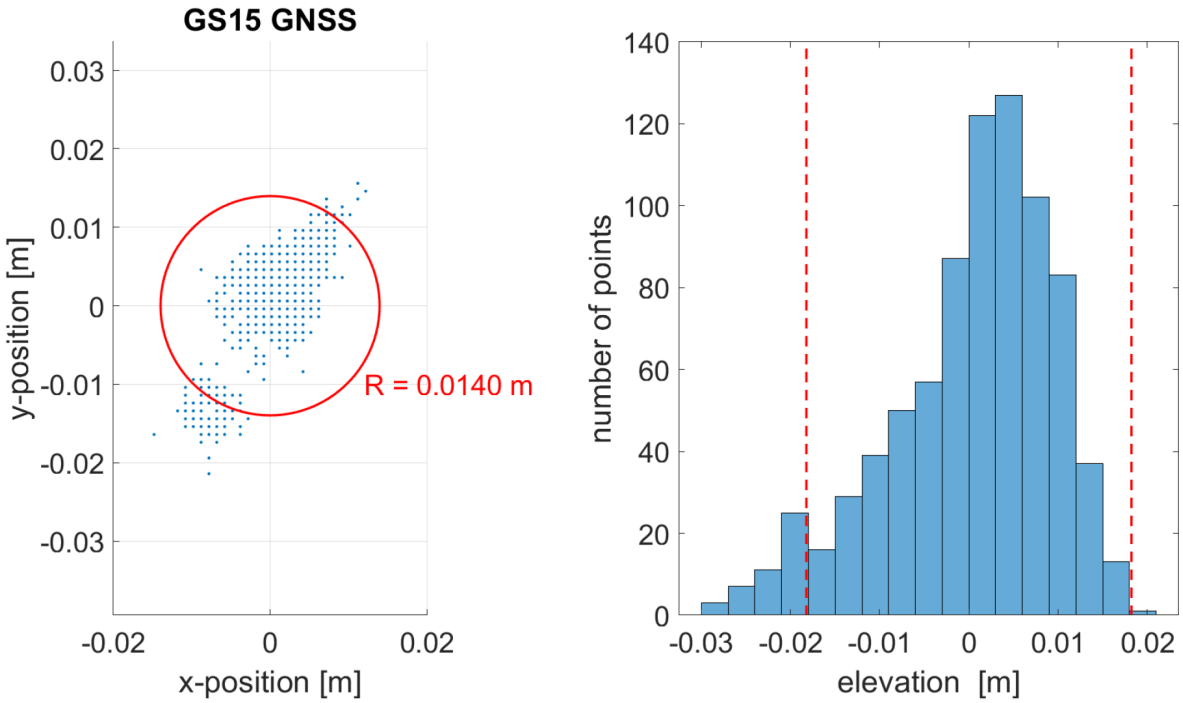

Figure F.2: Results of the stationary test for the GS15 GPS. This GPS device is used in container 2 and has a connected controller. On the left is the distribution of the horizontal position coordinates depicted. The blue dots represent the measurements and the red circle is the 95% confidence interval based on these results. The right figure shows the distribution of the measured elevation. Here the 95% interval is highlighted y the red dashed lines.

F.2. Lateral deviation

In this appendix, the lateral deviation of the GPS measurements inside the container is shown per experiment, per container. This deviation could be caused by errors in the measurement systems, but also by the movement of the cart itself. Measurement system 1, which includes the cart, was not on rails but had wheels that rode on the top of the container. The car had wooden planks mounted close to the inside of the container wall. As there was a couple of centimeters clearance between these planks the cart could move a bit from side to side. This was still more accurate than the use of system 2.

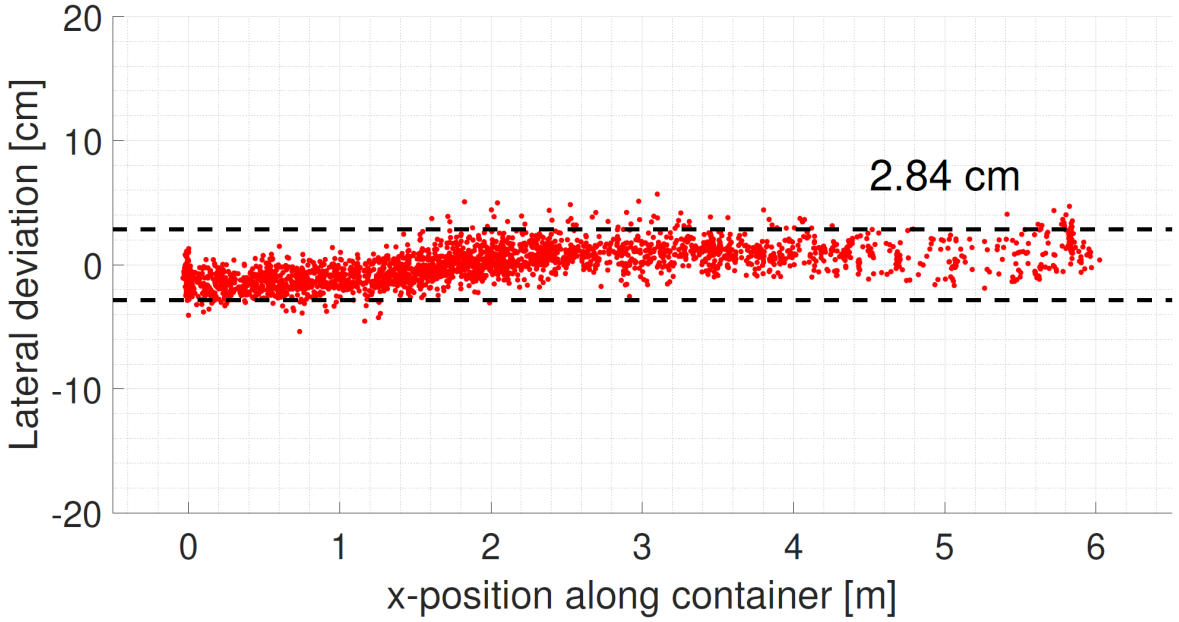

Figure F.3: Top view of the positional coordinates of each measurement point for experiment 2 on Tuesday 22-09 in Container 1. The y-axis shows the lateral deviation from a straight line.

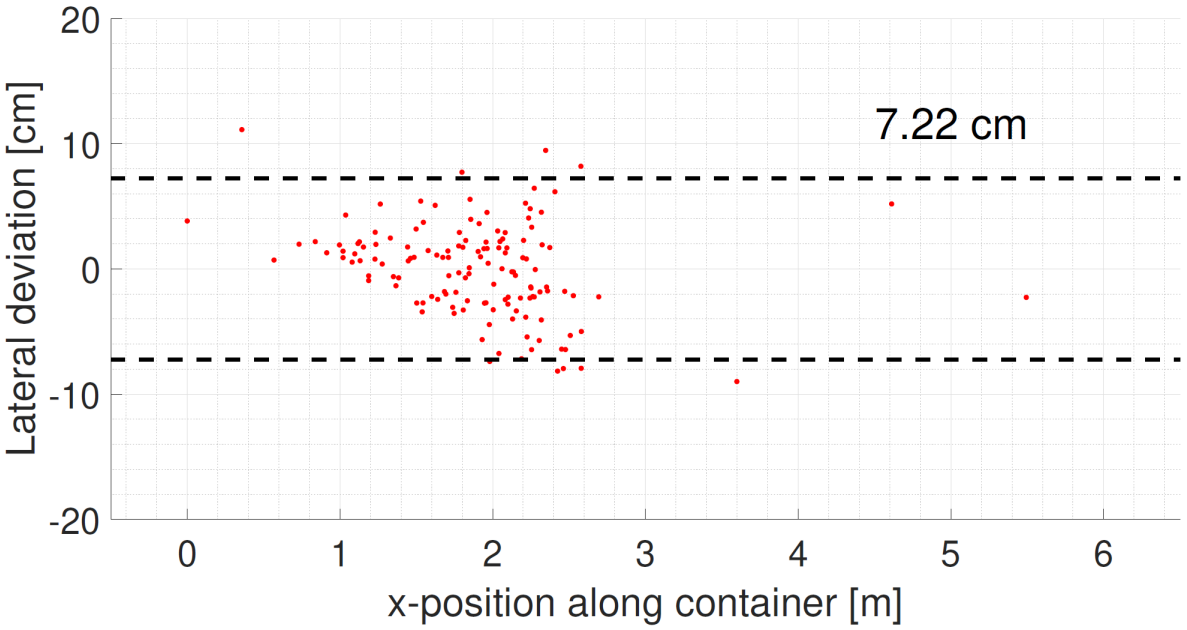

Figure F.4: Top view of the positional coordinates of each measurement point for experiment 2 on Tuesday 22-09 in Container 2. The y-axis shows the lateral deviation from a straight line.

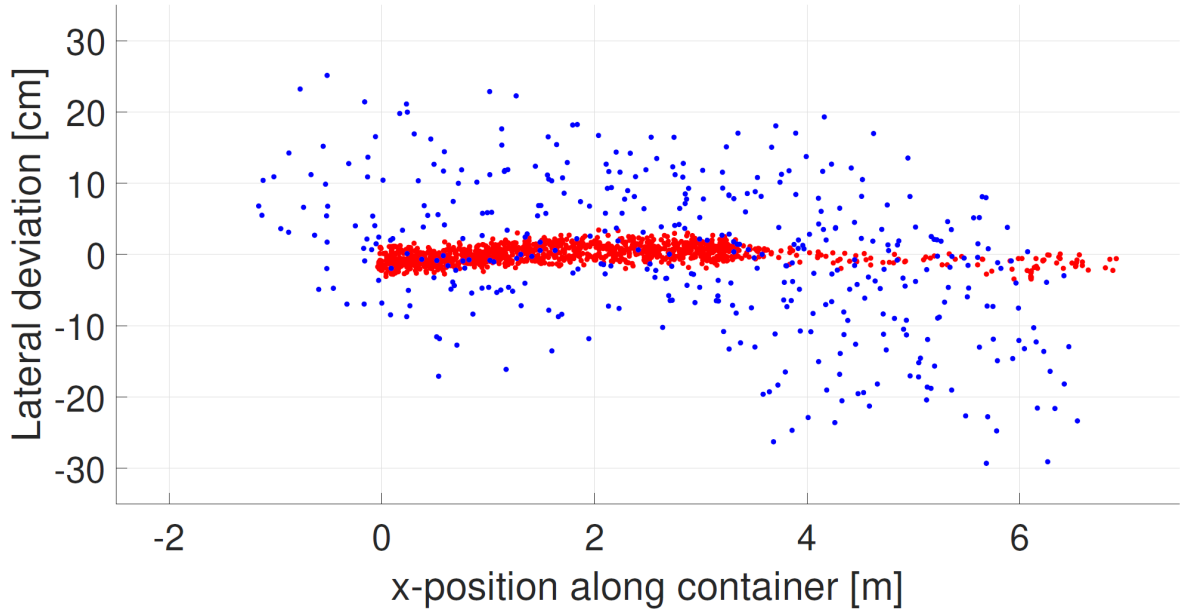

Figure F.5: Top view of the positional coordinates of each measurement point for Wednesday 23-09 in Container 1. The y-axis shows the lateral deviation from a straight line. During the experiment one of the extension poles broke. After this event measurements were done by foot, walking over the dune. Red dots show the measurements when using the cart and blue dots show the measurements on foot. A clear increase in lateral error can be seen when doing the measurements on foot compared to the measurement done with the cart.

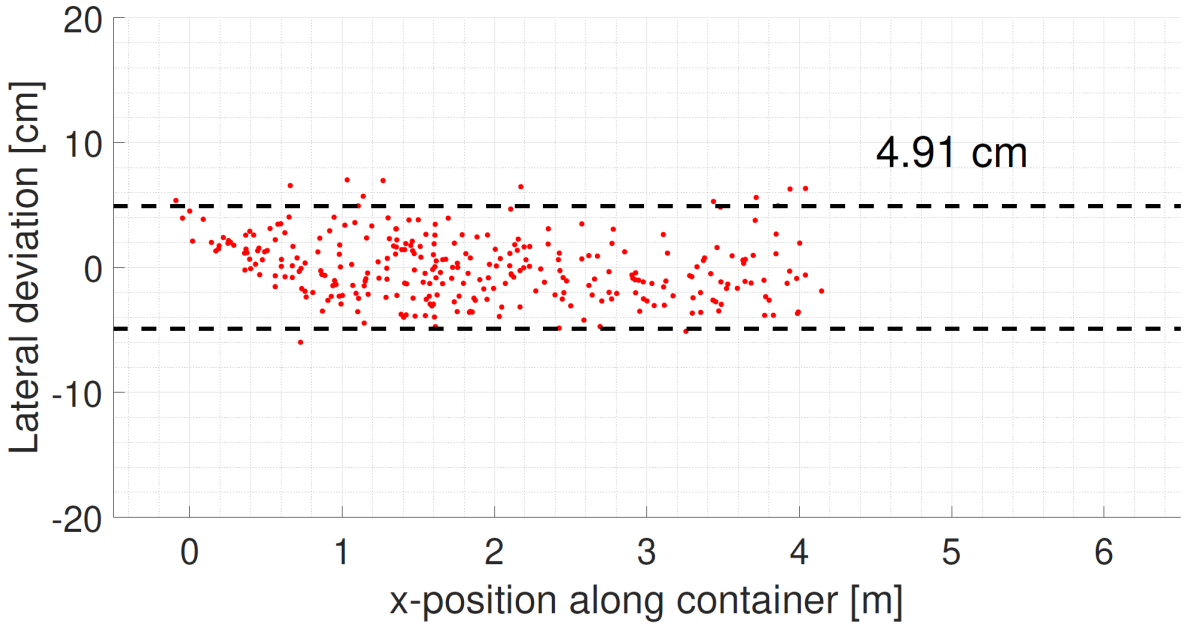

Figure F.6: Top view of the positional coordinates of each measurement point for experiment 3 on Wednesday 23-09 in Container 2. The y-axis shows the lateral deviation from a straight line.

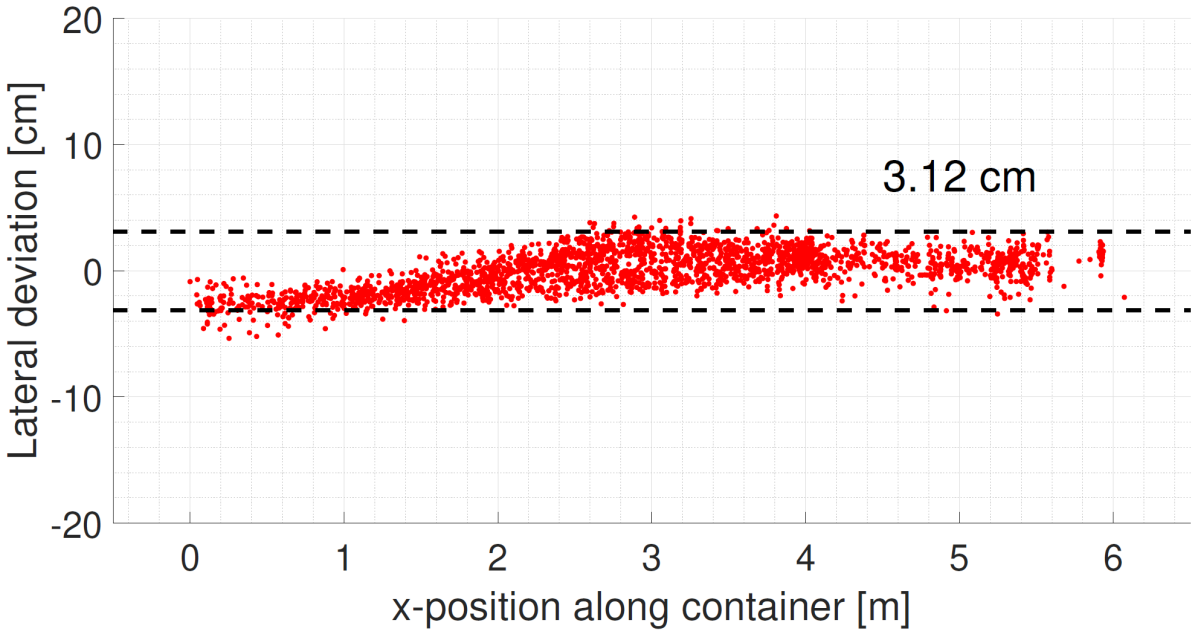

Figure F.7: Top view of the positional coordinates of each measurement point for experiment 4 on Thursday 24-09 in Container 1. The y-axis shows the lateral deviation from a straight line.

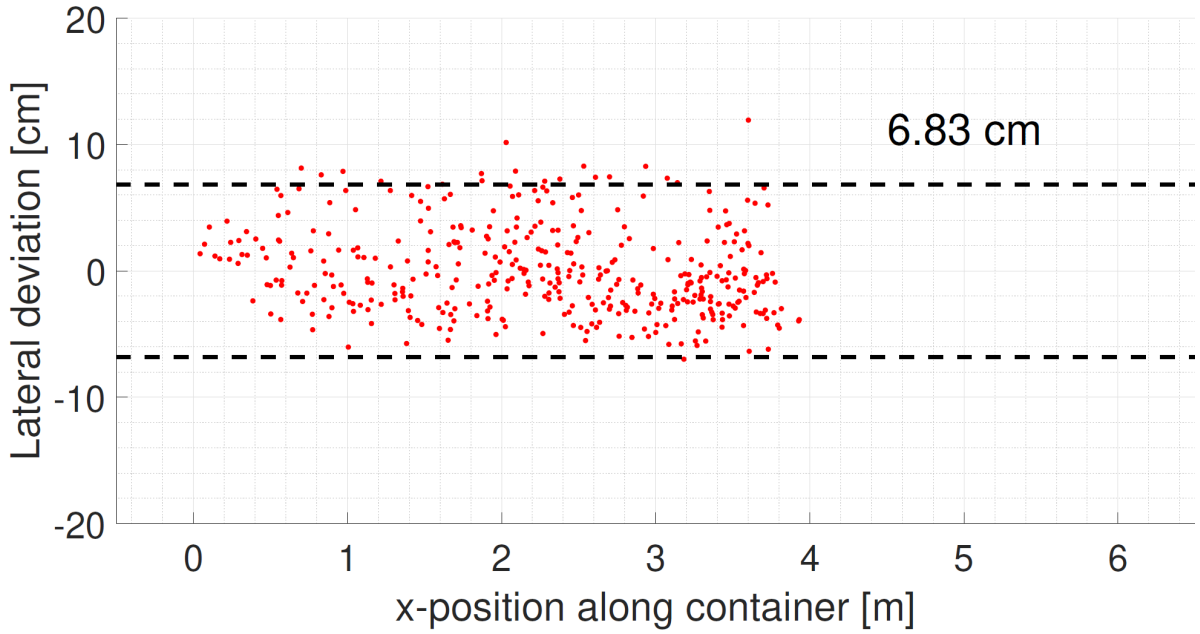

Figure F.8: Top view of the positional coordinates of each measurement point for experiment 4 on Thursday 24-09 in Container 2. The y-axis shows the lateral deviation from a straight line.

Bibliography

Anish, A. (2019). How are shipping containers made? Retrieved from https://www.marineinsight.com/tech/how-are-shipping-containers-made/.

Bonte, Y. and Levoy, F. (2015). Field experiments of beach scarp erosion during oblique wave, stormy conditions (normandy, france). *Geomorphology*, 236:132–147.

Bosboom, J., Stive, M. M. J., of Hydraulic, D., and Section., G. E. D. H. E. (2015). *Coastal dynamics I*.

Bruun, P. (1962). Sea-level rise as a cause of shore erosion. *American Society of Civil Engineers Journal of the Waterways and Harbours Division*, 88:117 – 130.

Burger, L. (2010). Complexities in the estimation of emissions and impacts of wind generated fugitive dust.

de Winter, R., Gongriep, F., and Ruessink, B. (2015). Observations and modeling of alongshore variability in dune erosion at egmond aan zee, the netherlands. *Coastal Engineering*, 99:167–175.

Erikson, L. H., Larson, M., and Hanson, H. (2007). Laboratory investigation of beach scarp and dune recession due to notching and subsequent failure. *Marine Geology*, 245(1):1 – 19.

Fisher, J. S., Overton, M. F., and Chisholm, T. (1986). Field measurements of dune erosion. pages 1107–1115.

Hapag-Lloyd (2020). 40' open top. Retrieved from https://www.hapag-lloyd.com/en/products/fleet/container/40-open-top.html.

Huang, C. H. (2020). Wind erosion. Retrieved from https://milford.nserl.purdue.edu/weppdocs/overview/wndersn.html. Accessed: 2020/06/24.

Larson, M., Erikson, L., and Hanson, H. (2004). An analytical model to predict dune erosion due to wave impact. *Coastal Engineering*, 51(8):675 – 696. Coastal Morphodynamic Modeling.

Leonardi, N., Ganju, N. K., and Fagherazzi, S. (2016). A linear relationship between wave power and erosion determines salt-marsh resilience to violent storms and hurricanes. *Proceedings of the National Academy of Sciences*, 113(1):64–68.

Lepage, G. (2020). What is an open top container? Retrieved from https://www.dsv.com/en/our-solutions/modes-of-transport/sea-freight/shipping-container-dimensions/open-top-container.

Martínez, M. and Psuty, N. (2004). *Coastal Dunes: Ecology and Conservation. Ecological Studies*, volume 171.

Maun, A. and Maun, M. (2009). *The Biology of Coastal Sand Dunes*. Biology of Habitats Series. OUP Oxford.

Morelle, R. (2015). The world's biggest manmade wave.

Okin, G. and Gillette, D. (2001). Distribution of vegetation in wind-dominated landscapes: Implications for wind erosion modeling and landscape processes. *Journal of Geophysical Research Atmospheres*, 106:9673–9683.

Okin, G., Gillette, D., and Herrick, J. (2006). Multi-scale controls on and consequences of aeolian processes in landscape change in arid and semi-arid environments. *Journal of Arid Environments*, 65(2):253 – 275. Special Issue Landscape linkages and cross scale interactions in arid and semiarid ecosystems.

Paris, A., Peytavie, A., Guérin, E., Argudo, O., and Galin, E. (2019). Desertscape simulation. *Computer Graphics Forum*, 38.

Postma, R. (2015). Ons water in nederland, nieuw nationaal waterplan 2016-2021. *Ministerie van Infrastructuur en Milieu, Met Andere Woorden*.

Roelvink, D., Reniers, A., van Dongeren, A., van Thiel de Vries, J., McCall, R., and Lescinski, J. (2009). Modelling storm impacts on beaches, dunes and barrier islands. *Coastal Engineering*, 56:1133–1152.

Roelvink, D., van Dongeren, A., McCall, R., Hoonhout, B., van Rooijen, A., van Geer, P., de Vet, L., and Nederhoff, K. (2015). Xbeach manual. Retrieved from `https://oss.deltares.nl/web/xbeach/source-code-and-exe`.

Sallenger, A. (2000). Storm impact scale for barrier islands. *Journal of Coastal Research*, 16:890–895.

Schwartz, M. (2006). *Encyclopedia of Coastal Science*. Encyclopedia of Coastal Science. Springer Netherlands.

Splinter, K. D., Kearney, E. T., and Turner, I. L. (2018). Drivers of alongshore variable dune erosion during a storm event: Observations and modelling. *Coastal Engineering*, 131:31–41.

Steetzel, H. (1993). Cross-shore transport during storm surges. *Delft Hydraulics Communications*, 476.

Stive, M. J., de Schipper, M. A., Luijendijk, A. P., Aarninkhof, S. G., van Gelder-Maas, C., van Thiel de Vries, J. S., de Vries, S., Henriquez, M., Marx, S., and Ranasinghe, R. (2013). A New Alternative to Saving Our Beaches from Sea-Level Rise: The Sand Engine. *Journal of Coastal Research*, 29(5):1001–1008.

Thiel de Vries, J. v., Dongeren, A. v., McCall, R., and Reniers, A. (2011). The effect of the longshore dimension on dune erosion. *Coastal Engineering Proceedings*, 1(32):sediment.49.

USGC (2019). Storm impact regime image. Retrieved from `https://www.usgs.gov/media/images/storm-impact-regimes`. Accessed: 2020/06/26.

van Bemmelen, C. (2018). Beach scarp morphodynamics: Formation, migration, and destruction.

van de Graaff; Job Dronkers, J. (2021). Dune erosion.

van Gent, M. (2008). Large-scale tests to analyse the influence of collapsed dune revetments on dune erosion. pages 2583–2595.

van Gent, M., Coeveld, E., de Vroeg, H., and van de Graaff, J. (2007). Dune erosion prediction methods incorporating effects of wave periods. page 14.

van Gent, M., Coeveld, E., Walstra, D., van de Graaff, J., Steetzel, H., and Boers, M. (2006). Dune erosion tests to study the influence of wave periods. pages 2779–2791.

van Haegen-Maas Geesteranus, M. S. (2016). kst-34436-d. Retrieved from `https://zoek.officielebekendmakingen.nl/stb-2016-431.html`. Accessed: 2020/06/23.

van Rijn, L. (1993). *Principles of sediment transport in Rivers, estuaries and coastal seas*, pages 85–86. Aqua productions, Amsterdam.

van Rijn, L. (2009). Prediction of dune erosion due to storms. *Coastal Engineering*, 56(4):441 – 457.

van Thiel de Vries, J., van Gent, M., Coeveld, E., de Vroeg, J., and van de Graaff, J. (2008a). Large-scale dune erosion tests to study the influence of wave periods. *Coastal Engineering*, 55:1041–1051.

van Thiel de Vries, J., van Gent, M., Walstra, D., and Reniers, A. (2008b). Analysis of dune erosion processes in large-scale flume experiments. *Coastal Engineering*, 55(12):1028 – 1040.

Vellinga, P. (1982). Beach and dune erosion during storm surges. *Coastal Engineering*, 6(4):361 – 387.

Wenneker, I., Hoffmann, R., and Hofland, B. (2016). Wave generation and wave measurements in the new delta flume. In *Proceedings of the 6th International Conference on the Application of Physical Modelling in Coastal and Port Engineering and Science*.